

**Evolutionary Relationships and Flight Capacity of Late Cretaceous Pterosaurs Elucidated by New Azhdarchoid Pterosaur Remains From Afro-Arabia**

by

Kierstin L. Rosenbach

A dissertation submitted in partial fulfillment  
of the requirements for the degree of  
Doctor of Philosophy  
(Earth and Environmental Sciences)  
in the University of Michigan  
2022

Doctoral Committee:

Professor Jeffrey Wilson Mantilla, Chair  
Professor Emeritus Tomasz Baumiller  
Associate Professor Matt Friedman  
Associate Professor Michael Habib  
Professor Laura MacLatchy

Kierstin L. Rosenbach

klrose@umich.edu

ORCID iD: 0000-0002-0616-2217

© Kierstin L. Rosenbach 2022

## **Dedication**

To my father, who wrote his own dissertation while caring for me, a 6-month-old child, while  
my mother was away working to support us.

He taught me to dance badly to 90s rock between spoonful's of baby food.

## Acknowledgements

I am grateful to A. Sawarieh (Natural Resources Authority, Jordan) and J. Nazzal (Yarmouk University, Jordan), A. Jamman, Jason Head, and Monica Wilson for field assistance and A. Khammash (Pella Museum) for logistical and technical support. I also thank William Sanders for preparation of fossils; Adam Rountrey, Katie Grosh, and Melissa Wood for photogrammetry; Carol Abraczinskas for artistic input; Matt Friedman, Joseph El Adli, and Kelly Matsunaga for assistance with  $\mu$ CT scanning; Alessio Capobianco, James Saulsbury, Kara Feilich, and Ethan Shirley for guidance with 3D imaging software; Danielle Goodvin, Monique Perez, and Stacy Kaneko for segmenting  $\mu$ CT scans.

I am thankful to the students, faculty, and staff at the University of Texas Austin Vertebrate Paleontology Laboratory and Jackson School of Geosciences including Matthew Brown, Christopher Sagebiel, Deborah Wagner, Earnest Lundelius, Timothy Rowe, Julia Clarke, Christopher Bell, Christopher Torres, Sarah Davis, Sarah Hood, Nicholas Crouch, Ingrid Lundeen for access to collections, intellectual discussion, guidance, and moral support.

For further access to collections and data from the US, I thank David Steadman at the Florida Museum of Natural History; Carl Mehling at the American Museum of Natural History; and Paul Sereno at the University of Chicago.

For access to collections and data internationally I thank Roger Benson at the University of Oxford in Oxford, England; Clair Sagne and Nour-Eddine Jalil at Muséum National d'Histoire Naturelle in Paris, France; Oliver Rauhut at Bayerische Staatssammlung für Paläontologie und

Geologie, in Munich, Germany; Atilla Ósi at Magyar Természettudományi Múzeum in Budapest, Hungary; Mátyás Vremir and Gareth Dyke at Babeş-Bolyai University Museums in Cluj-Napoca, Romania; Zoltán Csiki-Sava and Dan Grigorescu at the University of Bucharest in Bucharest, Romania; and Alexander Averianov at the Zoological Institute of the Russian Academy of Sciences in St. Petersburg, Russia.

I thank my committee for their valuable input, including Jeff Wilson and Matt Friedman for their guidance and mentorship over the past six years. Tom Baumiller and Laura MacLatchy for their expertise on biomechanics. And Mike Habib for his expertise on pterosaurs and his relentless positivity. And finally, I am grateful to my friends and colleagues at the University of Michigan, Ann Arbor, including Aaron Kurz, Kelly Matsunaga, Alessio Capobianco, James Saulsbury, Kara Feilich, Joseph El Adli, Ethan Shirley, Rodrigo Figueroa, James Andrews for their help with learning methods, troubleshooting, discussion of ideas, and invaluable moral support.

The American Chemical Society Petroleum Research Fund (PRF 46006-E8 to JAW) supported this field work; the Scott Turner Award and Rackham precandidacy grant supported this research.

## Table of Contents

Dedication.....	ii
Acknowledgements.....	iii
List of Tables .....	viii
List of Figures.....	ix
List of Appendices .....	xi
Abstract.....	xii
1 Introduction .....	1
2 New Pterosaur Remains From the Late Cretaceous of Afro-Arabia.....	6
2.1 Introduction .....	6
2.1.1 Institutional Abbreviations.....	7
2.2 Systematic Paleontology .....	8
2.2.1 Holotype.....	8
2.2.2 Horizon and Locality .....	8
2.2.3 Diagnosis.....	9
2.2.4 Etymology.....	9
2.3 Description .....	10
2.3.1 Cranial Bones.....	11
2.3.2 Cervical Vertebrae .....	13
2.3.3 Scapulocoracoid.....	18
2.3.4 Humerus.....	19
2.3.5 Radius .....	22

2.3.6	Ulna.....	24
2.3.7	Metacarpal IV .....	27
2.3.8	First Wing Phalanx .....	28
2.4	Systematic Paleontology .....	31
2.4.1	Holotype.....	31
2.4.2	Referred Material .....	31
2.4.3	Horizon and Locality .....	31
2.5	Description .....	32
2.5.1	Humerus .....	32
2.6	Pterosaurs of the Late Cretaceous .....	33
2.6.1	<i>Inabtanin alarabia</i> .....	33
2.6.2	<i>Arambourgiania philadelphiae</i> .....	34
2.6.3	Global Context .....	35
2.7	Conclusion.....	36
2.8	Tables .....	37
2.9	Figures.....	42
3	Evolutionary Relationships of Late Cretaceous Pterosaurs (Archosauria: Pterosauria) .....	55
3.1	Introduction .....	55
3.2	Methods.....	58
3.3	Results .....	60
3.4	Discussion .....	62
3.4.1	Azhdarchiformes as the major group of Late Cretaceous pterosaurs .....	62
3.4.2	The significance of elongated cervical vertebrae.....	64
3.4.3	Distribution of long wingspan .....	66
3.5	Conclusion.....	68

3.6	Tables .....	69
3.7	Figures .....	79
4	Analyzing Pneumatic Bones for Volumetric Airspace Proportion and Internal Trabecular Structures to Infer Flight Behavior .....	83
4.1	Introduction .....	83
4.2	Methods .....	84
4.2.1	Micro-computed tomography scanning .....	85
4.2.2	Reconstructing three-dimensional models .....	86
4.2.3	Analyzing 3D models and measuring volumetric airspace proportion.....	86
4.3	Results and Discussion.....	88
4.3.1	Inferring air space proportion .....	88
4.3.2	Inferring flight performance .....	90
4.4	Conclusion.....	94
4.5	Figures .....	95
5	Conclusion.....	99
	Appendices.....	103
	Bibliography .....	134



## List of Tables

Table 2.1 Measurements (mm) of <i>Inabtanin alarabia</i> .....	37
Table 2.2 Measurements (mm) of <i>Arambourgia philadelphiae</i> compared to <i>Quetzalcoatlus northropi</i> . ....	39
Table 2.3 Measurements of the angle of intersection of the internal bone structure in the humeri of the Jordan specimens. ....	41
Table 3.1 The 24 papers with phylogenetic analyses included in our character critique process compared to this analysis and analyses published since 2018 that were not included (starred item). ....	69
Table 3.2 Organizational categories for the database of pterosaur character statements in published literature through 2018 (available upon request) .....	70
Table 3.3 Late Cretaceous pterosaurs studied in this analysis based on their status as putative azhdarchids. ....	71
Table 3.4 Phylogenetic nomenclature relevant to this analysis with original citations and definitions. ....	75
Table C Database of specimen information and vASP values .....	131

## List of Figures

Figure 2.1 Map of Jordan showing pterosaur-bearing fossil localities, the Ruseifa Phosphate Mines and Tal Inab 6, and the stratigraphic section for the Inab site. ....	42
Figure 2.2 Photograph of in situ skeletal remains of <i>Inabtanin alarabia</i> including cranial material, one cervical vertebra, and a nearly complete wing .....	43
Figure 2.3 Generalized pterosaur body plan in flight position with arms and legs extended, labeled with the directional terms used in this description .....	43
Figure 2.4 <i>Inabtanin alarabia</i> cranial material (YUPC-INAB6-001, -002).....	44
Figure 2.5 <i>Inabtanin alarabia</i> cervical vertebrae (YUPC-INAB6-003, -004, -005) .....	45
Figure 2.6 <i>Inabtanin alarabia</i> left scapulocoracoid (YUPC-INAB6-006) .....	46
Figure 2.7 <i>Inabtanin alarabia</i> humerus (YUPC-INAB6-007, -008). ....	47
Figure 2.8 <i>Inabtanin alarabia</i> right radius (YUPC-INAB6-009) .....	48
Figure 2.9 <i>Inabtanin alarabia</i> right ulna (YUPC-INAB6-010). ....	49
Figure 2.10 <i>Inabtanin alarabia</i> right fourth metacarpal (YUPC-INAB6-011).....	50
Figure 2.11 <i>Inabtanin alarabia</i> right first wing phalanx (YUPC-INAB6-012).....	51
Figure 2.12 <i>Arambourgiania philadelphiae</i> right humerus (YUPC-RUSEIFA-001). ....	52
Figure 2.13 . Comparison of humeri of giant azhdarchid pterosaurs.....	53
Figure 2.14 Paleomap of the Earth (modified from Scotese, 2016) during the Late Cretaceous highlighting locations where putative azhdarchid pterosaur remains have been recovered .....	54
Figure 3.1 Workflow diagram summarizing the methods used to collect and filter through thousands of character statements and to organize and standardize characters prior to creating new characters and adding new OTUs or rescoring existing taxa .....	80
Figure 3.2 Phylogenetic relationships of Late Cretaceous pterosaurs. Strict consensus tree highlighting relationships within Ornithocheiroidea .....	82

Figure 4.1 Summary of workflow to produce and analyze 3D models of pneumatic bone structure along with examples of results.....	96
Figure 4.2 Comparison of the internal structure of pterosaur and bird wing bones .....	98
Figure B1 Strict consensus tree.....	129
Figure B2 Majority rule 50% tree.....	130

## List of Appendices



Appendix A. TNT code used to obtain the results of the phylogenetic analysis in Chapter 3 ....	103
Appendix B. Additional trees from the results of the phylogenetic analysis in Chapter 3.....	129
Figures.....	129
Appendix C. vASP results of the analysis in Chapter 4 .....	131
Tables.....	131

## Abstract

Pterosaurs were the earliest and largest vertebrates to evolve powered flight, but they are the only major volant group that has gone extinct. Attempts to understand pterosaur flight mechanics have relied on aerodynamic principles and analogy with extant birds and bats. Both of these lines of inquiry rely on the size, three-dimensional shape, and internal structure of flight bones, which in pterosaurs are surprisingly rare. Remarkably, two new large-bodied pterosaur individuals with three-dimensionally preserved wing elements were recently recovered from the Late Cretaceous (Maastrichtian) of Jordan. Both specimens represent azhdarchoid pterosaurs and are described in this study; one is referable to the giant species *Arambourgiania philadelphiae* (ca. 10 m wingspan) and the second to a new, smaller species *Inabtanin alarabia* gen. et sp. nov. (ca. 5 m wingspan).

The pterosaur fossil record is highly variable, which confounds attempts to understand pterosaur diversity and relationships particularly for the groups that lasted to the latest Cretaceous, like the azhdarchids and their closest relatives. Recent studies challenge the traditional understanding that the azhdarchids were the only pterosaur lineage surviving into the Maastrichtian. This complicates our ability to identify new remains and to understand changes in diversity leading up to the Cretaceous-Paleogene extinction. Here, we address this problem by systematically assessing existing character matrices and taxon sampling to be more inclusive of the latest Cretaceous pterosaur fossil record. A parsimony analysis conducted in TNT results in a topology that recovers *Inabtanin alarabia* as a member of the clade Azhdarchidae. Our topology

implies a narrower membership for that group than recovered by previous analyses, with some previously suggested azhdarchids falling outside the phylogenetic definition of the group. In contrast, Azhdarchiformes includes all taxa previously included within that group.

Traditional characters defining Azhdarchidae, such as elongation of cervical vertebrae and long wingspan, appear to be gained independently in multiple groups; the structure of the humerus is recovered as a synapomorphy of Azhdarchiformes. With this updated understanding of the evolutionary relationships of pterosaurs, we will have a stronger framework for the identification of new latest Cretaceous pterosaur remains.

Finally, we use high-resolution micro-computed tomography scans to reconstruct and compare the internal osteology of the humeri of these two differently sized species to that of extant birds, for which internal bone structure correlates with flight behavior. The humerus of *Arambourgiania* exhibits a series of helical ridges formed along the cortical bone, whereas *Inabtanin* exhibits a denser pattern of hollow struts. Variation in internal structure for these individuals likely reflects responses to mechanical forces applied on the wings of pterosaurs. Results indicate that *Inabtanin* has internal bone morphology similar to that of continuously flapping birds, whereas the internal morphology of *Arambourgiania* is most similar to that of flapping-soaring birds.

## 1 Introduction

“The history of life on the earth during the epochs of geological time unfolds no more wonderful discovery among types of animals which have become extinct than the family of fossils known as flying reptiles. Its coming into existence, its structure, and passing away from the living world are among the great mysteries of nature.

The animals are astonishing in their plan of construction. In aspect they are unlike birds and beasts which, in this age, hover over land and sea.

They gather themselves in the body of a single individual, structures which, at present day, are among the most distinctive characters of certain mammals, birds, and reptiles.”

– H. G. Seeley 1901  
Dragons of the Air

Pterosaurs are a group of flying reptiles that span the fossil record from the Late Triassic to the end of the Cretaceous. They are often mistaken as aerial counterparts to dinosaurs, or precursors to modern birds, but pterosaurs are a unique and independent group that coexisted with the large reptiles of the Mesozoic. The first pterosaur was described in 1784 (*Pterodactylus antiquus*: Collini, 1784) and although its highly unusual anatomy was improperly interpreted at the time, it was clear to the scientific community that it was distinct from living vertebrates, making it valuable for the early conceptualization of extinction and evolution (Wellnhofer, 2008).

The unusual anatomy, which perplexed 18<sup>th</sup> century anatomists and inspired H.G. Seeley’s *Dragons of the Air* has been studied and debated for almost 250 years. We now know of over 170 species across their 160-million-year history encompassing a variety of forms, ecological niches, feeding ecologies, and geographic distribution. Pterosaurs generally share

certain features, including skulls that are elongate compared to the torso, extreme hollowing and pneumatization of the skeleton, broad sternal plates and deltopectoral crests, pteroid bones, which are present only within this group, and forelimbs that are elongate and highly modified for flight (Sereno, 1991). The earliest forms of pterosaurs belong to a paraphyletic assemblage called “rhamphorhynchoids,” which can be distinguished from later forms by the absence of synapomorphies: maintaining distinct nasal and antorbital fenestrae, relatively short wing metacarpals, and relatively long fifth pedal digits associated with wing support (Wellnhofer, 1991). Overall, rhamphorhynchoids were small, flying predators with many teeth and distinctive long tails. As rhamphorhynchoid diversity waned with the end of the Jurassic, pterodactyloid diversity increased (Barrett, 2008). Pterodactyloids are a monophyletic group united by a confluent nasoantorbital fenestra, reduced or absent cervical ribs, elongate metacarpals, and reduced pedal digits and tails (Wellnhofer, 1991). This includes the most well-known pterosaurs like *Pterodactylus*, *Pteranodon*, and *Quetzalcoatlus*.

For this dissertation we turn our focus to the pterosaurs of the latest Cretaceous (Maastrichtian), a time just before the lineage would reach extinction alongside the other large reptiles of the Mesozoic. During the Maastrichtian, pterosaurs possessed long wingspans with multiple species achieving ca. 10 m wingspans. The largest individuals were so impressively large that it is often overlooked that the typical pterosaur of the time would have a 5–6 m wingspan. These species may be half the size of some of their contemporaries, but it is notable that the average pterosaur wingspans in the latest Cretaceous is the same range as the upper limits for the estimated wingspans of volant birds across their entire evolutionary history. No other volant vertebrates have achieved such extreme wingspans.



Today, fossils of these giants are found in Upper Cretaceous deposits on every continent. The paleoenvironments range from large shallow seas to lacustrine habitats to inland continental landscapes (Averianov, 2014). Here, I focus on the paleocontinent of Afro-Arabia, which contains modern day Africa and the Arabian peninsula as a continuous landmass recently split from Madagascar and India. In the northeast corner, partially submerged in the Neo-Tethys ocean, a shallow marine environment was home to a variety of marine invertebrates, fishes, marine reptiles, and pterosaurs in what is now Jordan (Bardet & Pereda-Suberbiola, 2002). Here my colleagues uncovered the remains of the famous *Arambourgiana* (Arambourg, 1959) and a new pterosaur species described in Chapter 2. The *Arambourgiana* material is fragmentary but represents skeletal elements not previously known. The new species is represented by cranial and postcranial elements preserved in three dimensions, which are exceedingly rare in pterosaurs. This dissertation describes the new material and explores its contribution to our understanding of the evolutionary relationships of pterosaurs in the Late Cretaceous and their capacity for flight at extremely long wingspans.

The broad taxonomic divisions described above are well established, but the more detailed taxonomy and phylogenetics of pterosaurs are still being actively investigated and our understanding of pterosaur relationships grows with each new discovery. The phylogenetic analysis of Chapter 3 was inspired by the description of the new material from Jordan. As I explored possible affinities for the new specimen, it became evident that the relationships of Late Cretaceous pterosaurs needed further clarification before I could assign it to a group. This led me to begin an extensive process of collecting all the phylogenetic literature on pterosaurs and developing a technique for documenting and evaluating existing character matrices. I created a database of pterosaur characters that was filtered down to a core group of heritable, variable, and

independent character statements. This process allowed us to create a character matrix that was balanced between cranial and postcranial information to guide my extensive in person study of pterosaur remains from the latest Cretaceous. I sought to maximize my independent, hands-on interpretation of these fossils to avoid recycling characters and scores without critical thought. The results of this analysis indicate that the broader assemblage of latest Cretaceous pterosaurs with long edentulous beaks, unique humeral structure, and large body sizes (5–10 m wingspans) form a monophyletic group called Azhdarchiformes. This group contains the Jordanian specimens as well as all the putative azhdarchids that have been inconsistently associated with Azhdarchidae or more basal groups like ornithocheiroids or tapejarids (Vidovic and Martill, 2017; Longrich et al., 2018; Andres, 2021). This analysis is accompanied by discussions of pterosaur taxonomy and nomenclature, as well as the prevalence of morphogroups based on neck elongation and wingspan.

The anatomical and descriptive work of Chapter 2 also inspired our investigation of internal bone structure in large pterosaurs in Chapter 4. Recent analyses of bone structure in pterosaurs using new non-destructive methods to measure air space proportion and quantify the extreme level of hollowing in pterosaur wings compared to other archosaurs (Martin and Palmer 2014a, 2014b). The three-dimensional preservation of the Jordanian pterosaurs offered us a rare opportunity to look closely at the trabecular bone structure of these organisms. Building on the framework of using micro computed-tomography (micro-CT) scans to analyze airspace proportion in samples of two-dimensional slices, I sought to take a three-dimensional approach, but I could not predict what micro-CT scans would reveal. Scanning and reconstructing three-dimensional models of our material uncovered intricate and rarely preserved internal structures in pterosaur bones that reflect the same structures present in bird bones. Given that these

structures had been explored by materials science researchers as an adaptive remodeling of bone in response to the mechanical stresses of flight (Kiang, 2013; Novitskaya et al., 2017; Sullivan et al., 2017), I was also able to explore the relationship between these structures and flight behavior. I applied this method to pterosaur, dinosaur, and bird specimens. I found that neither pterosaur species displayed traits consistent with the loss of flight, despite their extreme size. They do, however, contain certain structures that correlate with flight behavior in birds.

In the broader context of paleontology and pterosaur research, the projects in this dissertation contribute new specimens to the literature and novel approaches to phylogenetic analyses and biomechanical questions. The importance of descriptive work is often overlooked, yet the citations used here date back to 1784, highlighting that comprehensive descriptive anatomy has the power to be useful for centuries. Interpretations of phylogeny and biomechanics reflect the best knowledge available at the time, but I expect that the information provided here will continue be relevant to the future generations of paleontologists who share an interest in flying reptiles.

## 2 New Pterosaur Remains From the Late Cretaceous of Afro-Arabia

**Authors:** Kierstin L. Rosenbach, Danielle M. Goodvin, Mohammed G. Albshysh, Hassan A. Azzam, Ahmad A. Smadi, Hakam A. Mustafa, Iyad S.A. Zalmout, and Jeffrey A. Wilson  
Mantilla

### 2.1 Introduction

Pterosaurs are a group of extinct flying reptiles that existed from the Late Triassic to the Cretaceous-Paleogene extinction event. Across their 150-million-year history, the diversity of pterosaur forms varies greatly. The highest peak of pterosaur morphological and phylogenetic diversity occurs during the middle Cretaceous (Butler et al., 2013). During the Cretaceous, pterosaur wing spans ranged from 0.35–10 meters, far outstretching the range of wingspan estimates birds achieved across their entire evolutionary history. Cretaceous pterosaurs also displayed an impressive variety of cranial crests and dentition styles ranging from standard piscivorous-style teeth to baleen-like filaments to completely edentulous beaks. Approaching the Cretaceous-Paleogene (K-Pg) extinction, pterosaur diversity was historically thought to decline until it was represented by a single group, Azhdarchidae, containing 5–7 species. But discoveries in the past decade suggest that both Pterosauria and Azhdarchidae were more diverse at this time than previously thought. New evidence suggests that the Maastrichtian azhdarchids were contemporaneous with pteranodontids and nyctosaurids (Longrich et al., 2018), as well as potentially more basal forms (Dalla Vecchia, 2017).

Recent field work conducted by University of Michigan (UM) and the Natural Resources Authority of Jordan (NRA) in Upper Cretaceous deposits of Jordan uncovered two new pterosaur specimens buried in an environment that allowed for infilling of bone by limestone matrix and preservation of detailed three-dimensional structure. Prior to these discoveries, the Maastrichtian pterosaur fossil record of Jordan consisted of only ten isolated specimens attributed to *Arambourgiania philadelphiae* (Arambourg, 1959; Frey and Martill, 1996; Martill and Moser, 2017), one of the largest known azhdarchid species. These specimens were recovered from the phosphate mines of Ruseifa, near the Jordanian capital of Amman. Prospection in the area uncovered the shaft of an exceptionally large humerus attributed to *Arambourgiania* (estimated wingspan 10 m). In addition, exposures of the Muwaqqar Formation in south-central Jordan yielded a partial pterosaur skeleton (estimated wingspan 5 m) from a site near Tal Inab. Its distinct spatiotemporal context, long wingspan, and long, edentulous beak suggest that it represents a new azhdarchiform species, which we refer to as *Inabtanin alarabia* gen. et sp. nov.

Interpretation of pterosaur diversity changes across the Mesozoic depends largely on continued sampling of the fossil record and division of groups based on our best understanding of evolutionary relationships. For any taxon, interpretation of taxonomy will change over time and so establishing detailed descriptions and accessible visual representation of well-preserved material remains an important aspect of paleontological research. Here we discuss the impact of these specimens on Late Cretaceous pterosaur diversity and most importantly, we provide detailed anatomical descriptions and photogrammetric models to be made publicly accessible through the University of Michigan Online Repository of Fossils (UMORF).

### **2.1.1 Institutional Abbreviations**

**NRA**, Natural Resources Authority of Jordan, Amman; **UMMP**, University of Michigan

Museum of Paleontology, Ann Arbor, U.S.A.; **YUPC**, Yarmouk University Paleontological Collection in the Department of Earth and Environmental Sciences, Irbid, Jordan.

## **2.2 Systematic Paleontology**

Pterosauria Kaup, 1834

Pterodactyloidea Plieninger, 1901

Azhdarchoidea Nesov, 1984

*Inabtanin* gen. nov.

*Inabtanin alarabia* sp. nov.

### **2.2.1 Holotype**

YUPC-INAB-6-001–010, a partial skeleton of an adult individual consisting of an upper and lower jaw, atlantoaxis, cervical vertebrae 3–4, a scapulocoracoid, a left humerus, and a nearly complete right wing consisting of a humerus, radius, ulna, metacarpal IV, and first wing phalanx.

### **2.2.2 Horizon and Locality**

The specimen was collected at locality Inab-6, located 34 km north of the current border with Saudi Arabia (Fig. 1). Stratigraphic information was collected by the authors in collaboration with the NRA (Fig. 1b). Field reports record 12 units fining upwards. These units consist of alternating clays, limestones, chalks, and phosphates. *Inabtanin* was found in situ from Unit 11, a layer of maroon-colored clay with a sugary texture and thick gypsum. Unit 11 varies in thickness from 5–20 cm. The Inab section is consistent with the paleoenvironments inferred for the Muwaqqar Formation, deposited during the Maastrichtian through the early Paleocene. The Muwaqqar Formation ranges in thickness from 60 m (Zalmout and Mustafa, 2001) to 780 m

(Powell, 1989) and consists of chalk interbedded with chert, marl, and limestone, indicating an open marine condition during the Maastrichtian. The exceptional preservation of fossil taxa suggests low oxygen content at the seafloor (Kaddumi, 2009). The predominance of chalk, combined with the lack of benthic macrofauna, lack of erosional surfaces, and the abundance of plankton indicates a moderately deep pelagic environment (Powell, 1989). This is also supported by macrofossils indicating a paleowater depth of less than 100 m (Kaddumi, 2009).

### **2.2.3 *Diagnosis***

*Inabtanin alarabia* is identified as an azhdarchiform pterosaur based on a long, edentulous beak and a humerus with a deltopectoral crest that originates from a distally placed position on the shaft and is rectangular, flat, and elongate in shape. *Inabtanin alarabia* differs from azhdarchids based on the presence of a deep laterally compressed lower jaw, short cervical vertebrae (length-to-width ratio that is less than 5), and gracile distal wing bones (length-to-width ratios of at least 10).

### **2.2.4 *Etymology***

*Inabtanin* is named for the geomorphological structure near the locality where the specimen was collected, which is called Tal Inab (“grape hill”) owing to its prominent coloration. The generic name combines the Arabic words *inab*, for grape, and *tanin* for dragon. Allusions to dragons are common in pterosaur etymology and so *tanin* was chosen to reflect the Arabic language of Jordan, and because of its similarity to the English word *tannin*, derived from the French *tanin* which relates to coloration. The generic name translates to both grape-dragon and grape-colored. The specific name *alarabia* was chosen in reference to the Arabian Peninsula.

### 2.3 Description

*Inabtanin alarabia* was discovered partially in situ (Fig. 2), with additional material recovered by sieving from the scree slope directly below. The in situ material included the upper and lower jaws, a cervical vertebra, the right radius, distal fourth metacarpal, and first wing phalanx. The upper and lower jaw were preserved in occlusion, and the upper jaw was subject to a higher degree of erosion than the dentary and limb bones, especially on the dorsal and posterior surfaces. The scree contained additional cervical vertebrae, the left scapulocoracoid, both humeri, the right ulna, and the proximal right fourth metacarpal. These elements collected from the scree are missing cortical bone, leaving behind a matrix-based natural cast of the bones that contain many surface details and preserve complex morphology. Individual pieces collected from the scree could be fit to one another to form complete elements (e.g, humerus). Measurements are summarized in Table 1.

We have determined that *Inabtanin* represents a single adult individual based size-independent criteria for the maturity of large pterodactyloids (Bennett, 1993). These include the presence of a fully fused scapulocoracoid and epiphyses of the appendicular bones. This is particularly evident in the fusion of the extensor process on the proximal end of the first wing phalanx, which is one of the last fusions to occur before an individual reaches skeletal maturity. Additionally, the articulations are smooth as opposed to pitted, indicating the bones are fully ossified.

This description uses the directional terms outlined in Figure 3. We avoid the use of terms such as “cranial,” “caudal,” and “rostral,” in favor of terms that are consistent across all bones and body regions (Wilson, 2006). Features of the skull will be described as “anterior” and “posterior.” The default posture assumes wings outstretched in flight position, so that surfaces of



the wing bones facing the leading edge of the wing are called “anterior,” and those facing the trailing edge of the wing are called “posterior.”

### **2.3.1 Cranial Bones**

The skull is represented by the upper and lower jaw preserved anterior to the nasoantorbital fenestra (Fig. 4). Based on comparisons with other edentulous pterosaurs, this represents at least 80% of the skull length. We identify the upper jaw by the presence of the ventral margin of the nasoantorbital fenestra preserved on the left side; the lower jaw is identified by the presence of the symphysis and mandibular rami. The jaws show evidence of pneumaticity, revealed in CT images (see below) as well as fortuitous breaks in the cortical bone (ca. 2 mm thick) that reveal underlying trabecular bone (average >1 mm thick) and irregularly shaped, variably sized alveoli. The alveoli are variable in shape; some are circular (2 mm diameter) or ovular (5–10 mm x 2 mm), and others are highly irregular (maximum 10 mm).

The jaws are elongate, edentulous structures that in occlusion form an elongate pyramid that is broadest at the preserved proximal end and tapers to a fine point at its terminus. Near the preserved base, the lower jaw is twice as deep as the upper jaw. At the jaw tip, they are subequal in dimensions. The occlusal margin, as seen in lateral view, is sharp and straight. As discussed below, medially both the upper and lower jaw are recessed from this margin.

#### **2.3.1.1 Upper Jaw**

The preserved portion of upper jaw is nearly half a meter long by 50 mm wide and tall. It consists of a premaxilla and maxilla (Fig. 4). The dorsal margin is nearly completely preserved, but its apex is missing, which we estimate to measure a few additional millimeters. What remains of the dorsal margin is a 12 mm wide ridge that tapers to 6 mm at the anterior break. The upper jaw maintains a subtriangular cross-section throughout its length. The upper jaw tapers to

a point that is broken off, leaving a triangular cross section (12 mm x 10 mm). We estimate only 4 mm is missing distally.

In cross-sectional view, the occlusal surface is highly concave at the anterior end, with sharp occlusal margins defined by ventrally directed ridges that are 1 mm wide. This curvature flattens entirely at the posterior end. There are no nutrient foramina on the occlusal surface. The posterolateral surfaces of the upper jaw have no mediolateral curvature, and no nutrient foramina are identifiable, but this may be because the cortical bone has been eroded. At the preserved posterior margin of the upper jaw, a small (45 mm) portion of the left nasoantorbital fenestra is represented by a thin margin of bone (23 mm x 9 mm) with a laterally compressed, triangular cross-section.

#### *2.3.1.2 Lower Jaw*

The preserved portion of the lower jaw consists of the dentary, including the symphysis and rami, but not the articulations. The maximum dimensions of the lower jaw are located posterior to the symphysis, where it is nearly twice as deep as it is wide (99 mm x 58 mm). The anterior end of the dentary tapers to a point that is interrupted by sharp break that is 36 cm from the symphysis. There, the terminal cross section is V-shaped and measures 8 mm high by 12 mm wide. The lower jaw retains this cross-sectional shape throughout its preserved length.

In dorsal view, left and right occlusal margins are parallel to one another at the anterior end of the lower jaw and bend away from one another to become medially concave near their midlength. The occlusal margins are sharp and oriented dorsally at the anterior end. Towards the posterior end they rotate to slightly lateral orientation. In cross-sectional view, the occlusal surface is gently concave at the anterior end, where the occlusal margins flare out laterally. This creates a trough along the entire occlusal surface that is deepest near the midpoint and shallowest

at the posterior occlusal surface. There is a shallow median ridge along the midline of the trough extending from the symphysis to the anteroposterior midpoint. There are no pits or foramina on the occlusal surface.

The ventral ridge of the dentary is 1–2 mm wide and is 99 mm deep at the posterior end, just anterior to the symphysis. The lateral surfaces of the dentary are finely textured due to underlying trabecular structure revealed by the eroded cortical bone. Several small (2 mm) nutrient foramina punctuating the lateral surfaces of the lower jaw are concentrated near the posterior occlusal margin. These do not exhibit any pairing or alternating arrangement.

The dentary symphysis creates a U-shape in dorsal view, with a maximum lateral width of 61 mm. The rami are preserved for 91 mm on the left side and 138 mm on the right side. The rami are thin, laterally compressed and slightly laterally convex. They measure 8 mm wide by ca. 36 mm high, and so the rami have a maximum height that is about one-third of the maximum height of the dentary.

### **2.3.2 *Cervical Vertebrae***

The atlantoaxis and two middle cervical vertebrae were collected (Fig. 5). The best-preserved vertebra is interpreted to be cervical vertebra 4, which was found in situ with the cranial material and wing bones. The atlantoaxis and incomplete middle cervical vertebra were collected from the scree immediately adjacent to the in situ material.

The atlantoaxis is identified by its relatively high neural arch and spine, lack of elongation, pentagonal cross section, tab-shaped posterior condyle, and posterior end that is transversely narrower than the anterior end. The incomplete middle cervical vertebra preserves its right posterior quarter. It can be identified as cervical vertebra 3 based on its articulation with the element we identify as cervical vertebra 4, to which serially comparable features are nearly

identical. Cervical vertebra 4 is well preserved and is identified by its moderate elongation, reduced neural spine, absent cervical ribs, paired pneumatic foramina flanking the neural canal, paired lateral pneumatic foramina on the centrum, and procoelous central articulations. Cervical vertebra 4 has a neural arch that is low and compressed (=confluent, sensu Unwin, 2003) onto the centrum, which extends further posteriorly and has prominent exapophyses. Exapophyses are an additional pair of intervertebral articulations unique to pterosaur cervical vertebrae. They are located beneath the posterior condyle to provide additional support and restrict torsion and lateral bending between vertebrae. All three vertebrae lack fused cervical ribs, which is characteristic of mid-series cervical vertebrae in azhdarchiform pterosaurs.

#### 2.3.2.1 *Atlantoaxis*

The atlantoaxis is well preserved and includes most of the neural spine, neural arch and canal, most of the centrum and posterior articulation. The atlantoaxis is pentagonal in anterior and posterior views and hourglass shaped in dorsal and ventral views.

The neural spine is damaged, but we estimate that when complete, it would have been a low ridge that was slightly taller at its posterior end. We estimate that the spine was more than 7 mm tall, less than 8 mm wide, and 20 mm long. The neural arch is medially concave, and the maximum length is at least 32 mm. The neural arch is transversely widest at the anterior end (estimated to be at least 34 mm) and narrowest at the midpoint (28 mm). The pedicles are each 6 mm thick and together correspond to the medially pinched minimum transverse width of 20 mm. The pedicles are laterally concave and contain no pneumatic foramina. The posterior end is dorsally elevated, where the pedicles are 12 mm high. The postzygapophyses are not preserved, but their bases provide a maximum posterior width of at least 31 mm.

The neural canal of the atlantoaxis is circular. It measures 7 mm in diameter at the anterior opening and expands slightly to 9 mm at the posterior opening. A small (4 mm) pneumatic foramen opens dorsal to the posterior opening of neural canal. There are no paired pneumatic foramina flanking the neural canal.

The centrum is damaged at its anterior end, and so the shape of the articular surface is unknown. The preserved portion of the centrum is elliptical in cross-section, measuring roughly 30 mm wide by 13 mm tall. The centrum is pinched at the midpoint (22 mm) relative to the ends (ca. 29 mm), which results in a nearly symmetrical hourglass shape. The centrum lacks lateral pneumatic foramina. The ventral surface of the centrum is smooth and slightly transversely convex. Towards the anterior third of the ventral centrum is a break that may represent a broken hypopophysis. The bases of paired exapophyses are situated dorsal to the posterior condyle and extend ventrally and posteriorly. The posterior condyle is a well-preserved articular surface on a dorsoventrally compressed tab (25 x 9 mm) extending posteriorly with a dorsal inclination.

#### *2.3.2.2 Cervical Vertebra 3*

A small (46 mm long) fragment preserving part of the neural arch and neural spine, neural canal, and centrum represents the posterior right quarter of cervical vertebra 3. The centrum preserves a lateral pneumatic foramen, the base of a postzygapophysis, an exapophysis, and half of the posterior condyle. Its complete dimensions are estimated to be slightly smaller than that of cervical vertebra 4 (see below).

The neural spine is represented by a low ridge that is narrowly pinched (2 mm wide) at the posterior end. The spine terminates above a 15 mm deep pneumatic cavity that is partially framed by a thin lamina that leads to the base of the right postzygapophysis.

A fragment of the neural arch remains on the right side, where it is low and compressed onto the centrum. As in cervical vertebra 4, the neural arch does not extend as far posteriorly as the centrum. The dorsal surface of the neural arch is concave on either side of the spine. The lateral extent of the neural arch is defined by a lamina connecting the prezygapophysis to the postzygapophysis, which has been referred to as the “postzygoprezygapophyseal” lamina (Tschopp, 2016). The breadth of the vertebra across this lamina exceeds that of the centrum. The right half of the neural canal is preserved and suggests a circular cross section whose diameter changes little along the length of the vertebra. Owing to preservation, it is not known whether there are paired pneumatic foramen flanking the neural canal.

The preserved centrum is 7 mm long by 2 mm wide, and if it were complete it would form a compressed oval in cross section. The centrum has a medially concave lateral surface. It contains one lateral pneumatic foramen, located at its midlength. The ventral surface of the centrum contains the posterior concavity, which is defined by the bases of the exapophyses. Half of the posterior articulation is preserved as a dorsoventrally compressed condyle (preserved 13 mm width x 8 mm height). The right lateral end of the condyle is confluent with a saddle-shaped articular surface on the dorsal side of the exapophysis (10 mm long x 4 mm wide). Here it articulates with the presumed cervical vertebra 4.

#### 2.3.2.3 *Cervical Vertebra 4*

Cervical vertebra 4 includes a portion of neural spine, a compressed neural arch and centrum that preserves a neural canal, pneumatic structures, the right prezygapophysis, the anterior articulation, the base of the right postzygapophysis, the posterior condyle, and both exapophyses. The vertebra is 67 mm long, with a minimum transverse width of 23 mm. Its elongation index (length/transverse width) is 2.9, and it is roughly hourglass shaped.

The dorsal surface of the neural arch is eroded but retains the base of a neural spine. The spine is low. The base of the spine is broad anteriorly (10 mm) and posteriorly (11 mm) and narrow near the midpoint (8 mm). The neural arch has a minimum transverse width of 39 mm. This point corresponds to the minimum width of the laminae connecting the prezygapophyses and postzygapophyses, which compose the lateralmost margins of the vertebra. The neural arch is consistently wider than the centrum, and it terminates slightly anterior to the condyle.

The anterior opening of the neural canal is circular, measuring 6 mm in diameter. On either side of the neural canal are paired pneumatic foramina (8 mm x 4 mm). The posterior opening of the canal it is slightly larger and laterally compressed (7 mm x 5 mm).

The anterior end of cervical vertebra 4 is slightly eroded, presenting a rhomboidal cross section that is at least 51 mm wide and 37 mm tall. The anterior articulation (i.e., the cotyle) is shallow, concave, and dorsoventrally compressed (>15 mm wide x 7 mm tall). The right prezygapophysis is preserved except for its articular surface. It is a small, round nub (8 mm diameter) that extends anteriorly beyond the cotyle and laterally much further than the centrum. The prezygapophyseal articular surface would have been oriented slightly ventrally. The damage at the anterior end exposes a large hollow cavity surrounding the neural canal with many alveoli (air pockets) that are ovoid, ranging from 4 mm to 9 mm in length. The most prominent foramen is on the left of the neural canal, where it hollows out the left prezygapophysis. Here, the trabecular bone is well-preserved as smooth white webbing that is less than 1 mm thick.

The centrum is dorsoventrally compressed and confluent with the arch. The anterior end preserves smooth, white cortical bone and a small (1 mm) nutrient foramen. Posteriorly, the centrum expands dorsally to a height of 17 mm. Overall the centrum is hourglass shaped with an anterior width greater than 30 mm, a minimum width of 23 mm, and a posterior width of 47 mm.

The centrum contains paired lateral pneumatic foramina that are dorsoventrally compressed ovals (6 mm long x 4 mm tall) extending at least 2 mm deep.

The ventral surface of the centrum varies along its length. Anteriorly it is transversely convex and contains a small median ridge that likely bore a hypopophysis, which are common in pterosaurs with elongate necks. The ventral surface of the centrum is missing cortical bone and reveals fine (1 mm) trabecular bone exhibiting a crosshatch pattern. There is one small (2 mm) round pneumatic foramen. The ventral surface is concave posteriorly between the bases of the exapophyses, which originate at the midpoint of the centrum and produce narrow, elongate projections that extend laterally and posteriorly beyond the condyle. The exapophyses are ca. 7 mm in diameter and are oriented slightly ventrally.

A prominent condyle extends posteriorly and slightly dorsally. It is elliptical, ca. 36 mm wide and 8 mm tall. At the lateralmost points of the condyle, it connects to small saddle-shaped articular surfaces situated on the dorsal sides of the exapophyses. The base of the right postzygapophysis is preserved. It originates from a thin (2 mm) lamina that connects the postzygapophyses and from the lamina that connects the prezygapophysis to the postzygapophysis. The postzygapophysis is oriented laterally and extends beyond the centrum.

### ***2.3.3 Scapulocoracoid***

A partial left scapulocoracoid was preserved (Fig. 6). It is missing the cortical bone and the distal ends of the scapular and coracoid processes. The scapulocoracoid is identified by the distinct laterally facing glenoid, where bears a transverse suture between the scapula and coracoid, and large pneumatic foramina. The glenoid is angled by roughly 45 degrees relative to the vertical axis of the bone. The scapula is oriented dorsally, the coracoid is oriented ventrally, and both are inclined medially.



The scapular blade is thin and supported by an anteroposteriorly compressed, elliptical base (25 x 16 mm). The scapula is smooth and flat on its anterior surface. There is a 12 mm-wide scapular ridge that leads to the anterior supraglenoid tubercle on its dorsolateral face. The scapular process on the posterior face is wide and low, and it was continuous with the posterior supraglenoid tubercle of the glenoid fossa.

The glenoid is concave with a trapezoidal articular surface, which is defined by parallel supraglenoid and infraglenoid tubercles as well as an anterior lesser tubercle that is twice as long as the posterior lesser tubercle. The maximum height and width of the glenoid are 43 mm and 27 mm. The glenoid is most deeply concave at the posterior half. The transverse suture is fused but patent and cuts across the middle of the glenoid, following a shallow sinusoidal path. The suture is not visible on the anterior surface, but it is faintly visible on the posterior surface. In the absence of cortical bone, we can see fine (1 mm) trabecular bone that is densely packed at the articular surface and sparse elsewhere. There are numerous 1–2 mm nutrient foramina covering the non-articular surface.

The coracoid is supported by a wide, compressed, irregularly shaped base. The orientation of the base of the coracoid suggests that the bone would have extended medially and twisted posteriorly in relation to the scapula. The distal coracoid is missing and the break reveals a D-shaped cross section (40 x 19 mm). The base of the coracoid is predominated by a prominent, laterally pointing coracoid flange ventral to the glenoid. On the posterior surface of the coracoid there is a large, ovoid pneumatic foramen (21 mm x 9 mm).

#### **2.3.4 Humerus**

Partial right and left humeri are preserved. The left humerus is preserved in three pieces, missing two small portions of bone. The proximal third of the right humerus includes the neck of

the proximal articular head, the proximal articular tuberosity, proximal shaft, and the deltopectoral base. Pterosaurs are characterized by a complex proximal humerus with an articular surface formed by the confluence of the articular head and tuberosity and a prominent deltopectoral crest. Neither humerus is complete, but together they provide enough information to provide a complete description of the humerus and to reconstruct its anatomy in three dimensions (Fig. 7).

The left humerus is incomplete and weathered externally such that its surface is smoothed. Shaft pieces that pertain to this element do not have a snap-fit, but comparison with the other humerus suggests that only a few millimeters are missing. The total length is estimated to be 241 mm with a maximum proximal width of 74 mm, a minimum diameter of 27 mm, and a distal width at least 52 mm.

The proximal articulation is crescentic in outline, with the proximal articular tuberosity oriented dorsoventrally and the proximal articular head oriented anteroposteriorly. The proximal articular head is wide and round with a smooth convex surface. The posterior margin of the articular head flares further posteriorly than the shaft, and the anterior margin is smoothly confluent with the shaft.

The proximal articular tuberosity is an hourglass-shaped tab facing the midline of the body. It has a smooth convex surface and when viewed from the midline, it is pinched at the middle (11 mm). It has a maximum width of 17 mm at the dorsal break, which corresponds roughly to the ventral margin of the proximal articular head. The ventral margin of the proximal articular tuberosity has a maximum width of 23 mm. This point corresponds to the ventral-most extent of the humerus, and it produces an ulnar crest that descends along the shaft. The anterior and posterior surfaces of the proximal articular tuberosity are concave, smooth, and pneumatic,

although no foramina are preserved here. The anterior surface is confluent with the concave surface of the shaft adjacent to the deltopectoral base. The posterior surface of the humerus becomes flat 18 mm from the proximal articular tuberosity. The ventral surface of the humerus is predominated by the ulnar crest that descends from the ventral margin of the proximal articular tuberosity.

The deltopectoral base extends anteriorly from the anterodorsal side of the shaft. Its long axis is oriented perpendicular to the long axis of the shaft. Relative to other pterosaurs, the base of the deltopectoral crest is transversally narrow (37 mm) and distally displaced, leaving it entirely disconnected from the proximal articular head by at least 25 mm. On the right humerus, the deltopectoral crest is interrupted by a sharp break 51 mm from the posterior margin of the shaft and leaves behind an elliptical cross section (37 mm x 16 mm). The left deltopectoral crest is identified by its squared distal margin. The distal margin teardrop shaped in anterior view (Fig. 7a). We estimate the deltopectoral crest is two times longer than its transverse width based on the dimensions of the preserved sections on both humeri.

The shaft of the left humerus has a variable cross section. The shaft near the deltopectoral crest base is slightly D-shaped in cross section where the anterior shaft surface is slightly flattened and the dorsal, posterior and ventral surfaces are rounded into an arc. The shaft tapers to the minimum dimensions (27 x 30 mm) proximal to the midpoint, where the cross section is subcircular. The shaft is interrupted by a sharp break near the midpoint. Here the shaft is 30 mm in diameter, the same dimensions as corresponding break on the distal half. The subcircular cross section continues along the shaft until the entepicondyle and ectepicondyle expand dorsally and ventrally from the shaft returning to a D-shape cross section again at the distal end. The distal end is so highly eroded that it is entirely formed of the matrix infilled natural cast and is not

reflective of the true anatomy. There it reaches maximum dimensions of 52 mm in dorsoventral height and 36 mm in anteroposterior width. It does not preserve the morphology of the epicondyles, capitulum, or trochlea.

The majority of the left humerus preserves the internal anatomy well, so we can observe pneumatic structure on the exposed surface. There, a seemingly unorganized network of trabecular bone is visible. Some trabecular bone is exposed as small hollow circles (2 mm diameter), and other areas terminate trabeculae at an oblique angle revealing 2 mm wide tubes extending across the shaft.

### **2.3.5 *Radius***

The right radius is complete except for most of the cortical bone, patches of which remain on the shaft surface (Fig. 8). Most of the preserved bone is the matrix-filled natural cast of the interior volume. The length of the radius is 361 mm, twenty times as long as the minimum diameter of the shaft. The shaft remains thin and straight throughout its length. The articulations expand dorsoventrally from the shaft, and the proximal end is dorsally inflected from the long axis of the bone.

The proximal end of the radius is defined by the radial tubercle, proximal cotyle, and three tuberosities referred to as anterior, posterior, and ventral. The radial tubercle is a dorsally pointing projection that ends in a small, anteriorly oriented plateau. The articular surface of the radial tubercle is convex and oriented perpendicular to the long axis of the shaft. The articular surface of the cotyle is concave and tear-drop shaped, tapering dorsally at the radial tubercle. Its anterior margin is high and rounded compared to the posterior margin, which is short with a sharp, pinched edge. The three tuberosities are located on the ventral side of the proximal radius. The posterior tuberosity is low and rounded, whereas the anterior tuberosity is smaller and

sharper. The trough formed between them continues distally to connect with a low, smooth ventral tuberosity. The ventral tuberosity peaks 35 mm distally, creating a sharp angle that emphasizes the dorsal inflection of the proximal radius.

The radial shaft has an elliptical cross section that is flattened anteroposteriorly. It bows slightly dorsally and has no anteroposterior curvature. The shaft margins are parallel from near the proximal end to the midshaft before expanding through the distal two-fifths produce the distal articulation.

The distal end of the radius is defined by the styloid process, ulnar notch, distal condyle, and a prominent flange. The styloid process and ulnar notch form an hourglass-shaped distal articular surface. Between these features, the anterior articular surface is a shallow concavity and the posterior articular surface is slightly convex. The dorsal and ventral shaft surfaces are narrow ridges contributing to the styloid process and ulnar notch. The styloid process expands dorsally to a convex distal condyle with an articular surface that is oriented posteriorly. The articular surface of the styloid condyle is triangular with a curved base and an apex pointing ventrally. The ulnar notch expands ventrally from the shaft to form a prominent flange that curves sigmoidally from the ventral surface to the anterior surface and to the distal articular surface. The ulnar notch forms a distinct J-shape in ventral view. The flange occurs on the anterior surface and continues to form the ventral margin of the dorsal articular surface where it is convex anteriorly and concave posteriorly. The maximum width of the distal articular surface is 22 mm.

Although no foramina are preserved, the structure of the cortical and trabecular bone indicates the element was pneumatized. Some cortical bone is preserved along the shaft where it is 2 mm thick, white in color, and chalky in texture. Below the cortical bone, the trabecular bone is visible. The trabeculae are denser at the articulations and enclose alveoli that are elongate or

tubular in shape and 1–3 mm in length. Where they are visible in the shaft, the trabeculae are 1 mm thick and do not enclose alveoli but rather extend as struts throughout. The struts are hollow, which is visible where some struts terminate in circular or oblique cross-section (0.5 mm diameter) at the exposed shaft.

### **2.3.6 *Ulna***

The right ulna is nearly complete, consisting of two pieces separated by a small gap located towards the proximal end of the shaft (Fig. 9). The ulna would have been approximately 369 mm long, based on interpolation of the gap separating the two preserved shaft pieces, using the articulation with the radius as a constraint on length. The ulna is a gracile element with a shaft diameter that is less than one-tenth its length. Both the proximal and distal ends expand dorsoventrally from the shaft, but the proximal end is more robust than the distal.

The proximal end of the ulna forms a crescent shape composed of a dorsal tuberosity, a convex olecranon, a ventral process, and a flat to gently concave anterior surface. The proximal articular surface contains dorsal and ventral cotyles that are separated by an intercotylar crest.

The dorsal cotyle of the proximal ulna is triangular and defined by the dorsal tuberosity, the intercotylar crest, and the olecranon. The dorsal cotyle is oriented anteriorly, thus limiting extension at the elbow. A low ridge dorsoventrally bisects the articular surface of the dorsal cotyle. This emphasizes the concave, anterior-facing surface on the anterior half of the dorsal cotyle. The posterior half of the dorsal cotyle has a flatter, medial-facing surface. The anterior margin of the dorsal cotyle (33 mm) is low, smooth, and curved in a very slight distal arc until the ventral margin at the intercotylar crest. The posterior margin of the dorsal cotyle (30 mm) is sharp and terminates in a low, rounded bulb. The ventral margin of the dorsal cotyle is punctuated by a ridge that protrudes dorsally, forming the margin of a small depression (11 mm

x 7 mm). The intercotylar crest is 17 mm long and is oriented anterodorsally to proximovertrally. The rugose texture of the intercotylar crest indicates a high degree of abrasion, but it appears to have connected with the olecranon process.

The ventral cotyle (27 x 16 mm) is rhomboidal in shape and defined by the intercotylar crest, the biceps tubercle, and the ventral process. The cotylar surface is concave and oriented anteriorly. The concavity is deepest dorsally and becomes shallower ventrally. The dorsal and posterior margins of the ventral cotyle are shaped by the intercotylar crest connecting to the olecranon at an obtuse angle. The ventral and anterior margins are shaped by the peaks of the ventral process and biceps tubercle. The intercotylar crest and the biceps tubercle are separated by a smooth slope that connects the ventral cotyle to the concave anterior surface.

The dorsal tuberosity is a pinched tab that is tilted proximally. The anterior margin of the dorsal tuberosity extends distally to form a ridge that grades into the shaft. The posterior margin of the dorsal tuberosity is contiguous with the olecranon. The olecranon is damaged, as indicated by a sharp break in its posterior margin. The arced surface of the posterior portion of the ulnar shaft is low and smooth, indicating that the olecranon did not project far proximally or posteriorly. The ventral process (16 mm wide) is low and tapers gradually from the ventral cotyle along the shaft for at least 50 mm before a large break interrupts it. The anterior surface of the proximal ulna articulates with the radius and is gently concave except for the presence of the biceps tubercle, which is narrow (4–13 mm) and descends from the ventral cotyle to the anterior shaft.

The shaft of the ulna is oval in cross section throughout its length and elongated in the dorsoventral plane. It bows anteriorly, reaching the peak of its arc proximal to the mid-point, where the shaft narrows to its minimum diameter (22 mm x 17 mm). From this point, the shaft

height increases gradually in the dorsoventral plane, where the cross section is increasingly elliptical at the distal end.

The distal articular surface is peanut-shaped, consisting of two bulbous condyles constricted in the middle by a trough and a large foramen. There are three tuberosities connecting to the condyles. The dorsal tuberosity is broad and shallow (16 mm wide) and terminates in a flat, rounded peak connected to the dorsal condyle. A ventral tuberosity forms a flange that is inflected anteriorly, with a concave anterior surface and a convex posterior surface. The ventral tuberosity extends for 50 mm and reaches a maximum width of 14 mm proximal to the ventral condyle. A median tuberculum extends from the dorsal condyle and grades into the anterior shaft. There is a small depression between the tuberculum and the dorsal tuberosity, and the anterior shaft is gently concave between the tuberculum and ventral tuberosity.

The dorsal condyle is sigmoidal (19 x 33 mm), and its articular surface is oriented so far posteriorly that it is not visible in anterior view. This indicates that the wrist joint would have had very limited mobility in the anterior direction. The dorsal tuberosity provides the posterodorsal peak of the sigmoid curve, and the tuberculum provides the anterior peak pointing ventrally toward the trough. The ventral condyle is a small round bulb (15 mm diameter) that points distally and is distinct from the ventral tuberosity by a small indentation that contains a 2 mm ventral fovea. The trough between the two condyles is smooth and narrows to 10 mm anteroposteriorly. The posterior surface of the distal end contains a large (21 x 16 mm) pneumatic foramen between the two condyles and connects to the trough between them.

The ulna is highly pneumatic. The cortical bone is entirely abraded away, exposing the trabecular bone underneath. The visible trabecular bone indicates a much greater density of bone tissue at the articulations than in the shaft. There are some visible struts (1 mm) in the midshaft.



The trabeculae enclose elongated alveoli in the proximal and distal ends of the ulna. The alveoli decrease in length towards the articulations, becoming rounder at the articular surfaces.

### **2.3.7 *Metacarpal IV***

A right metacarpal IV consists of three pieces separated by two gaps in the proximal shaft (Fig. 10). The proximal end and a portion of the shaft were collected from scree on the slope below the in situ material. Cortical bone is preserved on the distal end and in small amounts along the shaft. The high degree of abrasion on the proximal end of metacarpal IV obscures the anatomy, but the distal end preserves more complex morphology.

Metacarpal IV is at least 545 mm long, accounting for the gaps of missing material that are interpolated based on a continuous angle of taper of the shaft dimensions flanking the gaps. The bone is extremely elongate, with a length that is almost 50 times its minimum shaft diameter. The shaft is anteroposteriorly compressed and the articulations expand both dorsoventrally and anteroposteriorly.

The proximal articulation is a triangular surface composed of the dorsal articular surface, the proximal tuberculum, and the ventral articular surface. The dorsal articular surface is a ventrally pointing triangle (19 x 14 mm); it is concave and angled anteriorly. The proximal tuberculum is small and round (15 mm diameter), pointing proximally. The ventral articular surface is also a ventrally pointing triangle, its convex articular surface is the broadest of the proximal articular features (26 x 23 mm). Between the three articular features is a crescentic sulcus that is deepest at the dorsal half. From this point it arcs around the proximal tuberculum and dips into the shaft dorsal to the ventral articular surface.

The posterior surface of the proximal end is flat where it forms the base of the triangular shaped proximal articular surface and becomes convex for the remainder of the shaft. The

proximal tuberculum connects to a median tuberosity on the anterior surface, which extends distally and twists to the ventral margin of the shaft leaving the rest of the anterior shaft flat. The shaft has a distinct D-shaped cross section. The anterior surface is flat or concave to accommodate the smaller metacarpals, which are not preserved. There is no discernable curvature to the shaft. The shaft narrows gradually to its minimum diameter (13 x 19 mm), which is positioned distal to the midlength, before it expands dorsoventrally towards the distal end. After the minimum diameter, the cross section becomes elliptical and the ventral surface contains a V-shaped tubercle for attachment of soft tissue associated with the complex joint of metacarpal IV and the first wing phalanx.

The distal articular surface is inverse saddle shaped, with dorsal and ventral condyles that expand anteroposteriorly. They are angular, rather than round or bulbous, and separated by an intercondylar sulcus that varies in dorsoventral width as it arcs from anterior to posterior. Anteriorly, the intercondylar sulcus is broad and deeply concave to accommodate the extensor process of the first wing phalanx. As the intercondylar sulcus arcs posteriorly, it grades into the shaft. The dorsal condyle measures at least 30 mm anteroposteriorly, but it likely expanded further distally. The distal and posterior margins of the dorsal condyle are expanded to accommodate the dorsal cotyle of the first wing phalanx. The posterior margin of the dorsal condyle is damaged but preserves a slight dorsal inflection. Both the anterior and dorsal faces of the dorsal condyle are flat and continuous with the margins of the shaft. The ventral condyle expands further than the dorsal condyle, forming a more circular surface. The margin of the ventral condyle extends further anteriorly than it does posteriorly. This anterior margin grades into the shaft, whereas the posterior margin ends in a sharp protrusion that intersects the shaft.

### **2.3.8 *First Wing Phalanx***

A right first wing phalanx is preserved in two pieces, with a distal break in the shaft representing a small amount of missing bone (Fig. 11). The proximal and distal portions have identical cross-sectional shape and size on either side of the gap, indicating that the missing portion of shaft is a few millimeters.

The first wing phalanx is highly elongated and dorsoventrally compressed; it is estimated to be greater than 680 mm long. This uncertainty is due to the small break in the distal shaft and the high degree of abrasion on the distal articulation. The proximal articulation is the most robust feature of the bone. The shaft is comparatively narrow and expands slightly at the distal articulation. The proximal articulation is exceptionally well preserved with no discernable distortion and much of the cortical bone intact. Cortical bone is also preserved along the shaft until the distal break. The distal end contains no cortical bone and is represented by a matrix-filled natural cast.

The proximal end is saddle shaped with two cotyles defined by the extensor tendon process, dorsal tuberculum, flexor tendon process, and ventral tuberosity. The extensor process is fully fused to the dorsal tuberculum, indicating that this is a skeletally mature individual. It is subtriangular with a strong indentation on the anterior side for the attachment of the extensor tendon. The dorsal tuberculum is prominent and extends the full length of the shaft. The apex of the extensor process curves posteriorly to limit extension and brace the leading edge of the wing. The flexor tendon process is rounded and dorsoventrally compressed. It is placed further dorsally than the extensor process and further posteriorly than the ventral tuberosity. The dorsal cotyle is a 29 x 14 mm concave crescent that extends from the base of the extensor tendon process to the apex of the flexor tendon process. The articular surface is teardrop-shaped with sharp margins oriented slightly dorsally. The ventral tuberosity is low and smooth and grades into the shaft just

after the pneumatic foramen. Its posterior extent is limited, supporting the folding of the wing. The ventral tuberosity contributes a sharp margin to the ventral cotyle. The ventral cotyle is crescent shaped and extends from the ventral tuberosity to the apex of the extensor tendon process. It is wider and longer than its dorsal counterpart (35 x 15 mm). The concave articular surface of the ventral cotyle is also oriented posteriorly. A 7 mm-thin ridge separates the cotyles. A prominent pneumatic foramen is situated between the flexor tendon process and the ventral tuberosity. It is large, elliptical, and elongated proximodistally (16 x 8 mm). Trabecular bone is visible within the foramen and between the cotyles.

The shaft has an ovoid cross section that is compressed dorsoventrally. The anterior edge is narrower than the posterior edge and defined by the prominent dorsal tuberculum. The length of the shaft arcs anteriorly, suggesting resistance to bending in the anteroposterior plane during flight. The shaft reaches a minimum diameter (11 x 19 mm) distal to the midpoint. On both the dorsal and ventral surfaces, there is a thin longitudinal trough indicating some crushing of the shaft during preservation. Near the distal end, the cross section becomes sub-triangular in shape with a flat ventral surface and a low dorsal ridge. The distal end expands anteroposteriorly from the shaft reaching a maximum diameter (28 x 19 mm) before becoming rounded and dorsoventrally compressed. This rounded end indicates that the distal articulation was not much longer than what is preserved despite the high degree of abrasion.

The wing phalanx preserves more cortical bone than any other element. The cortical bone is less than 1 mm thick at the proximal articulation, where it is supported by trabecular bone, and it averages 2 mm thick throughout the shaft. Trabecular bone is visible at the proximal and distal ends of the wing phalanx but appears far less dense than the trabecular tissue of other wing bones, particularly at the distal end. No struts are visible on the surface of the midshaft.

## 2.4 Systematic Paleontology

Family AZHDARCHIDAE Nesov, 1984

*ARAMBOURGIANIA PHILADELPHIAE* (Arambourg, 1959) Nesov et al., 1987

### 2.4.1 *Holotype*

UJA VF1, a mid-series cervical vertebra recovered from the Ruseifa Phosphate Mines (Arambourg, 1959).

### 2.4.2 *Referred Material*

YUPC-RUSEIFA-1, a partial right humerus shaft. Previously referred material includes two phalanges, a cervical vertebra (Frey and Martill, 1996); SNSB-BSPG 1966 XXV 501, 503, 506, 507, 508, 512, a proximal metacarpal IV, three probable fragments of cervical vertebrae, a partial femur, and a possible distal radius (Martill and Moser, 2017). We suspect that a fragmentary appendicular bone previously described as a possible ornithopod tibia (Martill et al., 1996) might also pertain to *Arambourgiania*, based on similarity in dimensions, surface details, and spatiotemporal context.

### 2.4.3 *Horizon and Locality*

The Ruseifa phosphate mine section is located 7 km NE of Amman. It is composed of the Phosphorite Unit and the overlying Muwaqqar Formation (Fig. 1c). Ruseifa contains four levels of phosphorite that fine upwards and are separated by thinner layers of limestone, marl, dolomite, and chert. Each horizon begins with a cemented and silicified base and becomes well-laminated upwards. Units 3 and 4 display lamination, cross bedding, and erosional surfaces (Zalmout and Mustafa, 2001). All four units yield vertebrate fossils (Bardet and Suberbiola, 2002). The remainder of the section consists of the Muwaqqar Formation represented by chalk,

marl, limestone, and chert (Zalmout and Mustafa, 2001). The Ruseifa pterosaur was surface collected, and so the stratigraphic origin of this isolated element is not certain. Other giant pterosaur fossils from Ruseifa have been linked to Unit 1 (Frey and Martill, 1996), which has been interpreted as a deep marine environment owing to the lack of near shore sedimentary structures present in Units 3 and 4.

## **2.5 Description**

### **2.5.1 *Humerus***

The right humerus shaft is 185 mm long and has the shape of a flattened cylinder that expands distally. The shaft is broken just distal to the deltopectoral crest, where the preserved minimum diameter is found. The cross section of the proximal end is an anteroposteriorly compressed oval (80 x 60 mm). As it expands distally, the cross-sectional shape changes. A posteroventral ridge begins 75 mm from the preserved distal end of the humerus, giving it a subtle D-shaped cross section. As the ridge extends distally, it becomes more prominent and would have been contiguous with the ectepicondyle. The preserved maximum diameter is located at the distal break (119 x 73 mm).

The broken ends of the shaft reveal thin (2 mm) cortical bone. The cortical bone is abraded away on some of the surface of the shaft revealing thin (1 mm) trabecular bone. The trabecular bone forms a crosshatch pattern infilled with matrix. The ratio of matrix to trabecular bone indicates a high proportion of air space, approximately 90% air by volume. Where the structure of the trabeculae is visible, the thin bony walls separate alveoli that range from 1–3 mm in length.

## 2.6 Pterosaurs of the Late Cretaceous

During the Maastrichtian, Jordan occupied a position on the northern margin of Afro-Arabia, partially ringed by the Neo-Tethys Ocean. The Maastrichtian vertebrate fossil record of Jordan is represented by fishes, turtles, mosasaurs, plesiosaurs, and crocodylians (Bardet & Pereda-Superbiola, 2002) in addition to the ten isolated fragments attributed to *Arambourgiania philadelphiae* (Arambourg, 1959; Frey and Martill, 1996; Martill and Moser, 2017). The results of this field work contribute a new limb element to the collection of *Arambourgiania* fossils as well as the previously unknown species, *Inabtanin*.

### 2.6.1 *Inabtanin alarabia*

*Inabtanin alarabia* possesses features typically associated with azhdarchids, such as long wingspan, an edentulous beak, and the structure of the deltopectoral crest of the humerus. Additionally, the trabecular walls of the wing bones enclose elongated alveoli as reported in azhdarchids (Buffetaut et al., 2002, 2003). However, *Inabtanin* lacks other features typically associated with azhdarchids. It retains lateral pneumatic foramina on the cervical vertebrae, its vertebrae do not have an elongation ratio greater than 5, and it lacks paired nutrient foramina on the mandible (Martill and Moser, 2017). Due to this mix of azhdarchid and non-azhdarchid traits, it is likely that *Inabtanin* is an azhdarchiform that falls outside of Azhdarchidae.

The cranial material of *Inabtanin* overlaps with pterosaurs like *Aerotitan*, *Alanqa*, *Bakonydraco*, *Mistralazhdarcho*, which are represented largely by jaw remains. Most notably, the lower jaw at the symphysis is approximately twice as deep as the height of the upper jaw. This is unique among Azhdarchiformes which have relatively thin dentaries. *Inabtanin* lacks a median eminence on the dorsal surface of the lower jaw, which differs from the

contemporaneous pterosaurs *Alanqa* and *Mistralazhdarcho*. The distinctive eminence of the anterior jaw of the azhdarchoid *Bakonydraco* also varies significantly from *Inabtanin*.

The lack of elongate mid-series cervical vertebrae also argues against close affinities to *Albadraco*, *Azhdarcho*, *Cryodrakon*, *Eurazhdarcho*, *Mistralazhdarcho*, *Phosphatodraco*, *Quetzalcoatlus lawsoni*., and *Zhejiangopterus*. Although its spatiotemporal context draws the closest comparisons with *Arambourgiania*, its cervical vertebrae differ greatly from the holotypic vertebra of *Arambourgiania philadelphiae*, which has an elongation ratio of 11 (compared to 2.8 in the *Inabtanin* holotype). The cervical vertebrae of *Inabtanin* bear the closest resemblance to those of *Hatzegopteryx thambema*. *Inabtanin* is an adult, so it is unlikely that it represents a juvenile of the giant pterosaurs *Arambourgiania*, *Hatzegopteryx*, or *Quetzalcoatlus northropi*.

The appendicular material of *Inabtanin* overlaps with *Arambourgiania*, *Azhdarcho*, *Hatzegopteryx*, *Montanazhdarcho*, *Q. northropi*, and *Q. lawsoni*. The humerus is one-third of the size and has a different cross-sectional shape than the *Arambourgiania* specimen described here. The proximal cotyle of the radius is teardrop shaped as in *Azhdarcho lancicollis* (Averianov 2010), but the dorsally projecting tubercle is relatively less extended. Most notably, the wing bones of *Inabtanin* appear very gracile in comparison to the more robust wing bones of any azhdarchid with overlapping appendicular material.

### **2.6.2 *Arambourgiania philadelphiae***

This specimen is identified as pterosaurian based on the distinct internal bone structure comprised of thin cortical bone and thinner trabecular bone. This indicates that it possesses an extremely high air space proportion (ASP) that is only found pterosaurs. Previous studies utilizing  $\mu$ CT scans have exhibited ASPs ranging from 70% to 90% air in the pneumatized long bones of the largest taxa (Martin and Palmer, 2014a, 2014b). The thin bony walls separate



numerous, elongated alveoli similar to the condition described in the giant azhdarchid from Romania, *Hatzegopteryx* (Buffetaut et al., 2002, 2003). The cross-sectional shape and measurements of this specimen compare favorably with the humerus of *Q. northropi* (89 x 69 mm at minimum shaft diameter) (Fig. 13). We attribute this humerus to *Arambourgiania* because it comes from the holotypic quarry, is of comparable size, and is very similar in shape to that of the closely related species *Q. northropi* (Table 2).

### 2.6.3 Global Context

Today, Late Cretaceous pterosaur fossils can be found on every continent, indicating a worldwide distribution leading up to the K-Pg extinction. During this time, the paleocontinent of Afro-Arabia was also home to other medium-sized pterosaurs including the pteranodontid *Tethydraco regalis*, the nyctosaurids *Alcione elainus*, *Simurghia robusta*, *Barbaridactylus grandis*, and the azhdarchids *Phosphatodraco mauritanicus* and other unnamed attributed taxa (Pereda-Superbiola et al., 2003; Longrich et al., 2018). With the addition of these Azhdarchiformes from Jordan, Afro-Arabia retains the highest diversity of pterosaur remains from uppermost Cretaceous deposits. It is also notable that the productivity of localities yielding azhdarchiform fossils has grown since it was first posited that the largest azhdarchid pterosaurs often overlapped with smaller species (Vremir et al., 2013). At the time, authors were aware of this occurrence at four regions globally. With the discovery of *Inabtanin* fossils in Jordan, we are now aware that all seven regions where giant pterosaurs occur, there are also remains of smaller species. Furthermore, of the twelve regions where azhdarchiform remains have been recovered, two-thirds of them contain multiple species (Fig. 14). We expect that continued field work in any pterosaur-yielding Late Cretaceous localities will continue to support this pattern. These discoveries, along with other recent evidence of diverse assemblages of flying vertebrates in

Afro-Arabia (Longrich et al., 2018), provide valuable information for future investigation of the paleobiogeography of the continent. Additionally, these findings support the notion of catastrophic mass extinction as opposed to a slow decline in pterosaur diversity at the end of the Mesozoic.

## 2.7 Conclusion

The remains of *Inabtanin* and *Arambourgiania* are remarkable for their 3D preservation and for *Inabtanin* being one of the most complete individual pterosaurs to be recovered from Afro-Arabia. These fossils provide us with an opportunity to establish the detailed anatomy of azhdarchiform pterosaurs in the Late Cretaceous. The 3D structure of these wing elements contains rarely preserved information about the bone structure of the largest flying vertebrates. Their geological context provides valuable information about the paleobiogeography of Afro-Arabia and the state of pterosaur diversity at the end of the Cretaceous. With this new information we are conducting further study on the evolutionary relationships of Late Cretaceous pterosaurs as well as examining the relationship of internal bone structure with flight behavior and capacity.

## 2.8 Tables

Table 2.1 Measurements (mm) of *Inabtanin alarabia*.

Element	Side	Measurements	mm
Upper Jaw		Preserved length	495
		Length anterior to nasoantorbital fenestra	425
		Maximum preserved width	50
		Maximum preserved depth	49
Lower Jaw		Preserved length	499
		Length anterior to the symphysis	361
		Maximum preserved width	58
		Maximum preserved depth	99
Atlantoaxis		Length, anteroposterior, preserved	48
		Anterior width	30
		Posterior width	26
		Minimum width	24
		Height, dorsoventral, preserved	40
		Diameter of neural canal	7
Cervical 3		Length, preserved	50
		Height, preserved	34
Cervical 4		Length, preserved	67
		Minimum width of centrum	24
		Posterior width	48
		Maximum preserved height	36

		Diameter of neural canal	7
Scapulocoracoid	Left	Maximum length, dorsoventral	82
		Width, anteroposterior	42
Humerus	Left	Minimum length	237
		Length, estimated	241 <sup>e</sup>
		Minimum diameter, anteroposterior	27
		Minimum diameter, dorsoventral	30
		Deltpectoral crest, width, mediolateral	40
	Right	Minimum diameter, anteroposterior	27
		Minimum diameter dorsoventral	31
Radius	Right	Length	361
		Proximal diameter, dorsoventral	39
		Proximal diameter, anteroposterior	19
		Minimum diameter, dorsoventral	17
		Minimum diameter, anteroposterior	10
		Distal diameter, dorsoventral	35
		Distal diameter, anteroposterior	22
Ulna	Right	Length, estimated	369 <sup>e</sup>
		Proximal diameter, dorsoventral	66
		Proximal diameter, anteroposterior	33
		Minimum diameter, dorsoventral	22
		Minimum diameter anteroposterior	17
		Distal diameter, dorsoventral	54

		Distal diameter, anteroposterior	23
Metacarpal IV	Right	Length, estimated	545 <sup>e</sup>
		Proximal diameter, dorsoventral	47
		Proximal diameter, anteroposterior	38
		Minimum diameter, dorsoventral	18
		Minimum diameter anteroposterior	12
		Distal diameter, dorsoventral	28
		Distal diameter, anteroposterior	46
Wing phalanx I	Right	Length, estimated	681 <sup>e</sup>
		Proximal diameter, dorsoventral	84
		Proximal diameter, anteroposterior	67
		Minimum diameter, dorsoventral	10
		Minimum diameter anteroposterior	18
		Distal diameter, dorsoventral	18

Table 2.2 Measurements (mm) of *Arambourgiana philadelphiae* compared to *Quetzalcoatlus northropi*.

Specimen	Element	Measurement	mm
<i>Arambourgiana</i>	Humerus shaft	Preserved length	185
		Preserved minimum diameter, dorsoventral	80
		Preserved minimum diameter, anteroposterior	60
		Preserved maximum diameter, dorsoventral	119
		Preserved maximum diameter, anteroposterior	73
<i>Q. northropi</i>	Humerus	Length	535

Minimum diameter, dorsoventral 89

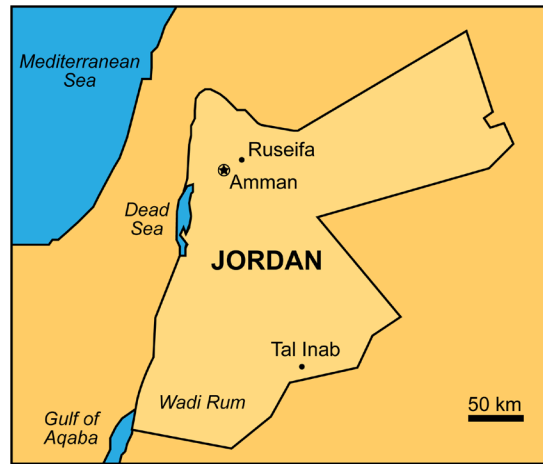
Minimum diameter, anteroposterior 69

---

Table 2.3 Measurements of the angle of intersection of the internal bone structure in the humeri of the Jordan specimens.

<b>Specimen</b>	<b>Element</b>	<b>Measurement</b>	<b>Degrees</b>
<i>Inabtanin</i>	Humerus	Average angle of diaphyseal struts intersection	83
		Standard deviation	31
		Average angle of epiphyseal struts intersection	87
		Standard deviation	24
<i>Arambourgiana</i>	Humerus	Average angle of ridge intersection	92
		Standard deviation	8
		Average angle of ridges to long axis	45
		Standard deviation	6

## 2.9 Figures



Tal Inab 6

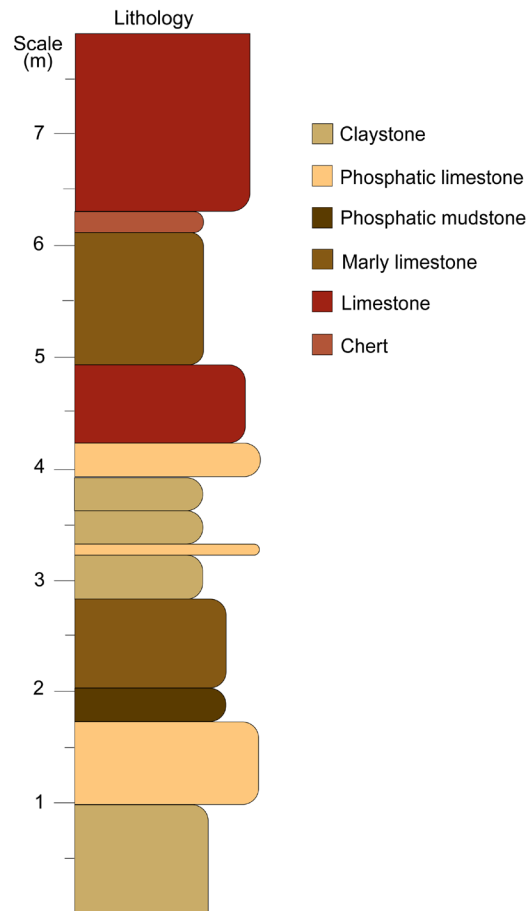


Figure 2.1 Map of Jordan showing pterosaur-bearing fossil localities, the Ruseifa Phosphate Mines and Tal Inab 6, and the stratigraphic section for the Inab site.





Figure 2.2 Photograph of in situ skeletal remains of *Inabtanin alarabia* including cranial material, one cervical vertebra, and a nearly complete wing.

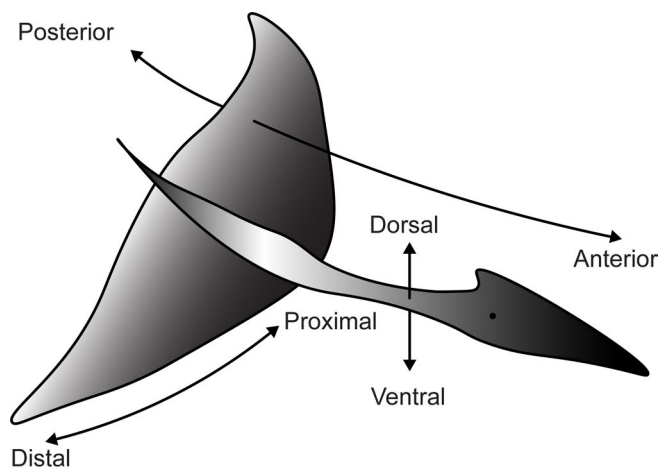


Figure 2.3 Generalized pterosaur body plan in flight position with arms and legs extended, labeled with the directional terms used in this description. Here we use “anterior” and “posterior” in place of “cranial” and “caudal” so that directional terms are consistent throughout cranial and postcranial bones.

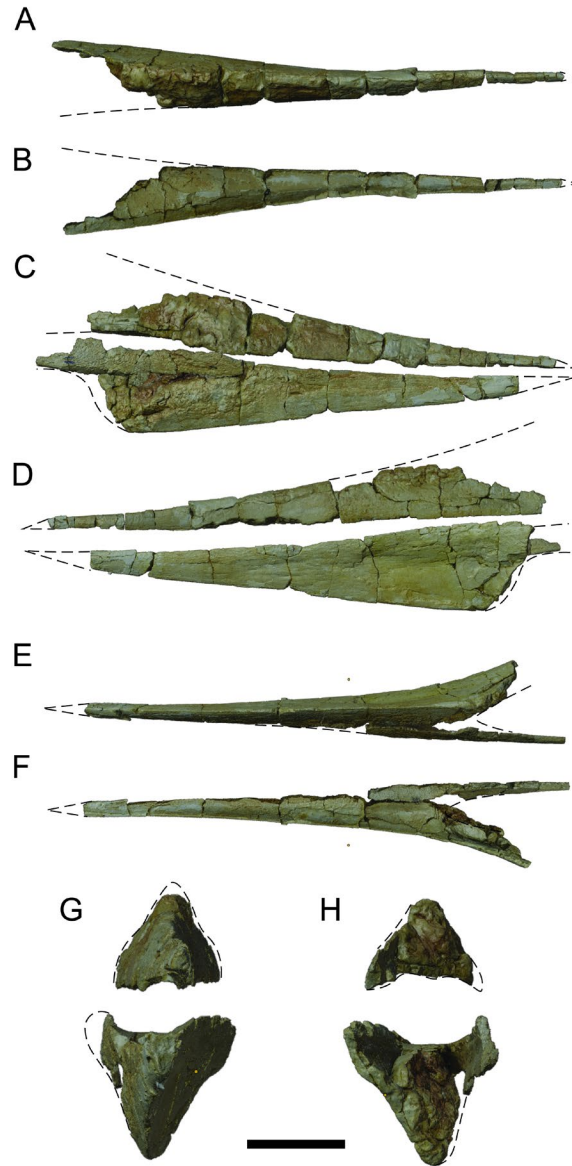


Figure 2.4 *Inabtanin alarabia* cranial material (YUPC-INAB6-001, -002). Photogrammetric reconstruction of the upper jaw in **A**, dorsal view; and **B**, ventral view. Photogrammetric reconstruction of the paired upper and lower jaws in **C**, right lateral view; and **D**, left lateral view. Photogrammetric reconstruction of the lower jaw in **E**, ventral view; and **F**, dorsal view. Photogrammetric reconstruction of the paired upper and lower jaw in **G**, anterior view; and **H**, posterior view. Dashed lines indicate reconstructed outline of bone. Scale bar equals 5 cm for **A–F**; 3 cm for **G–H**.

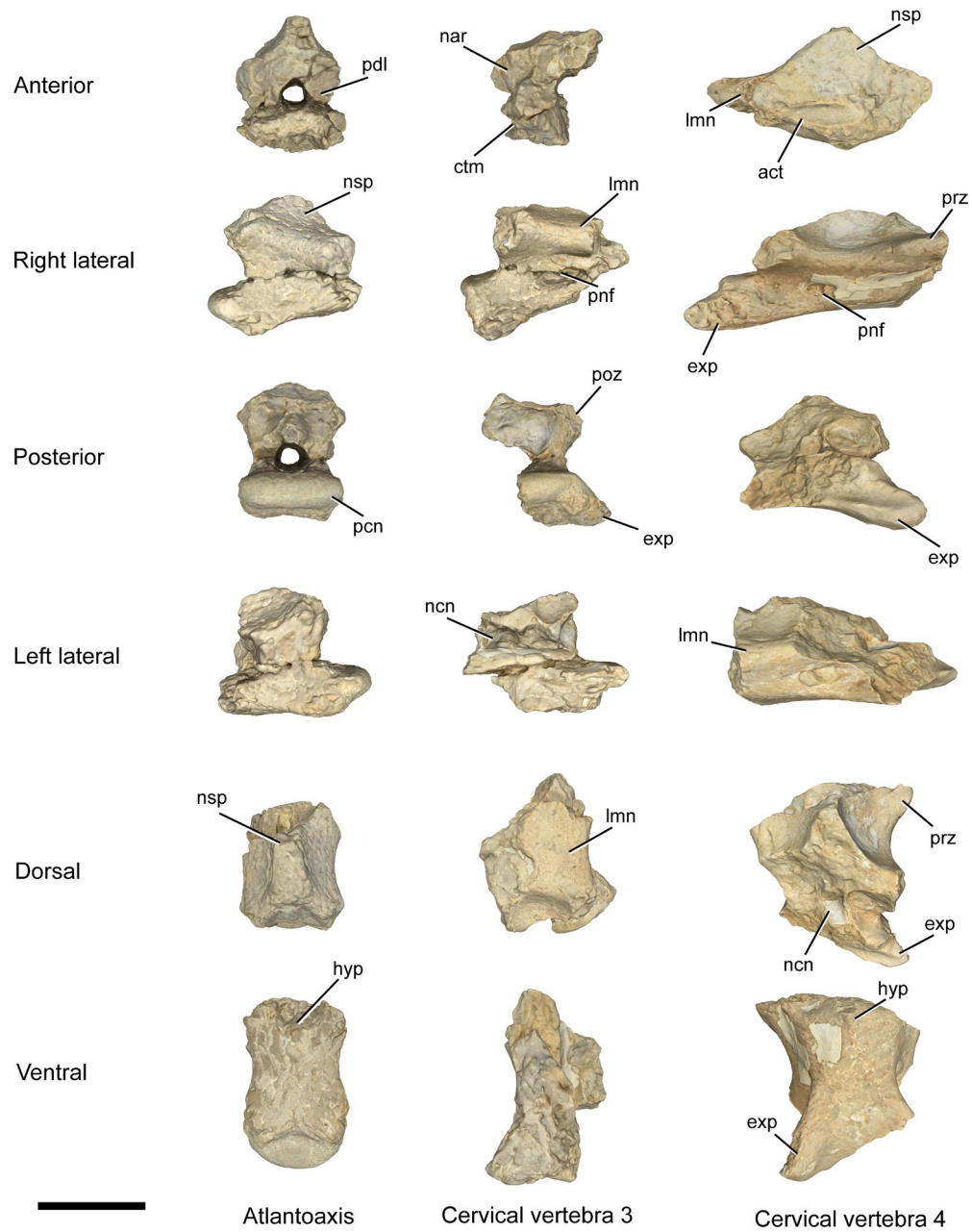


Figure 2.5 *Inabtanin alarabia* cervical vertebrae (YUPC-INAB6-003, -004, -005).

Photogrammetric reconstruction of the atlantoaxis in the left column, cervical vertebrae 3 in the center column, cervical vertebra 4 in the right column. **Abbreviations:** **act**, anterior cotyle; **ctm**, centrum; **exp**, exapophysis; **hyp**, hypopophysis; **lmn**, lamina; **nar**, neural arch; **ncn**, neural canal; **nsp**, neural spine; **pcn**, posterior condyle; **pdl**, pedicle; **pnf**, pneumatic foramina; **poz**, postzygapophysis; **prz**, prezygapophysis. Scale bar equals 2.5 cm.

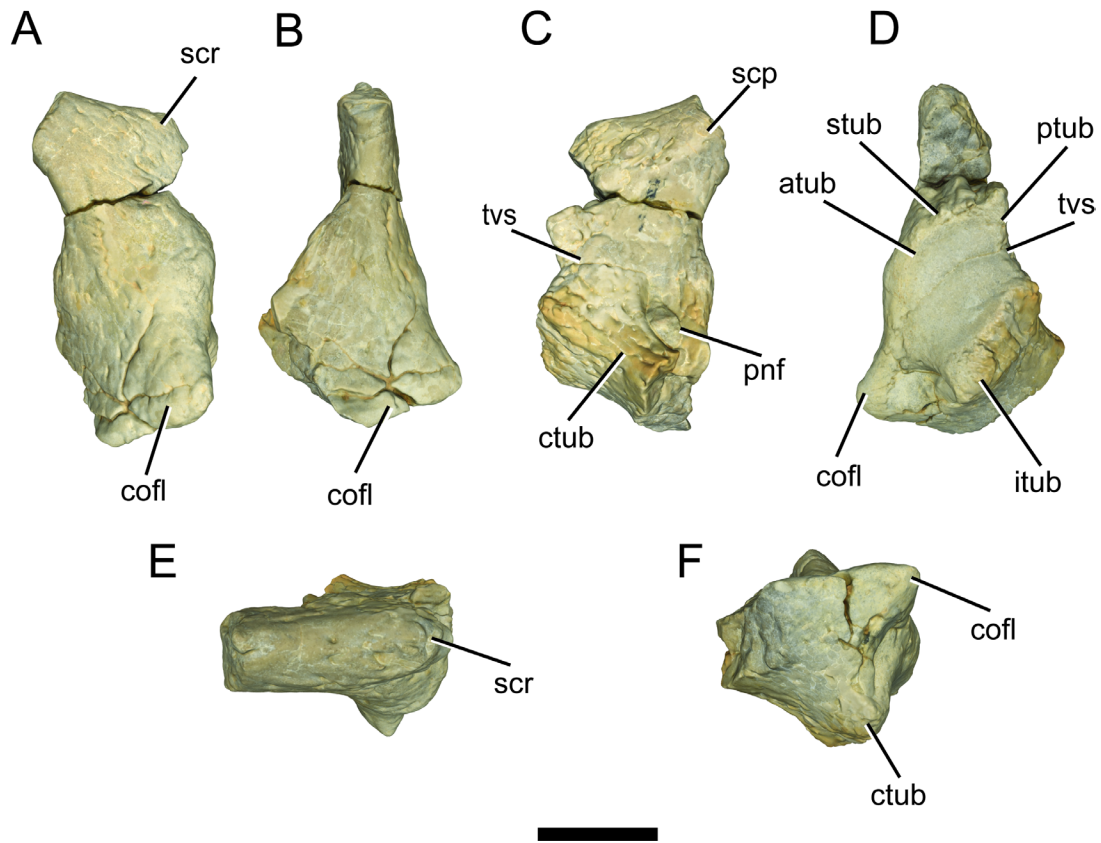


Figure 2.6 *Inabtanin alarabia* left scapulocoracoid (YUPC-INAB6-006). Photogrammetric reconstruction in **A**, anterior view; **B**, medial view; **C**, posterior view; **D**, lateral view; **E**, dorsal view; and **F**, ventral view. **Abbreviations:** **atub**, anterior lesser tubercle; **cfl**, coracoid flange; **itub**, infraglenoid tubercle; **ptub**, posterior lesser tubercle; **scp**, scapular process; **scr**, scapular ridge; **stub**, supraglenoid tubercle; **tvs**, transverse suture. Scale bar equals 2 cm.

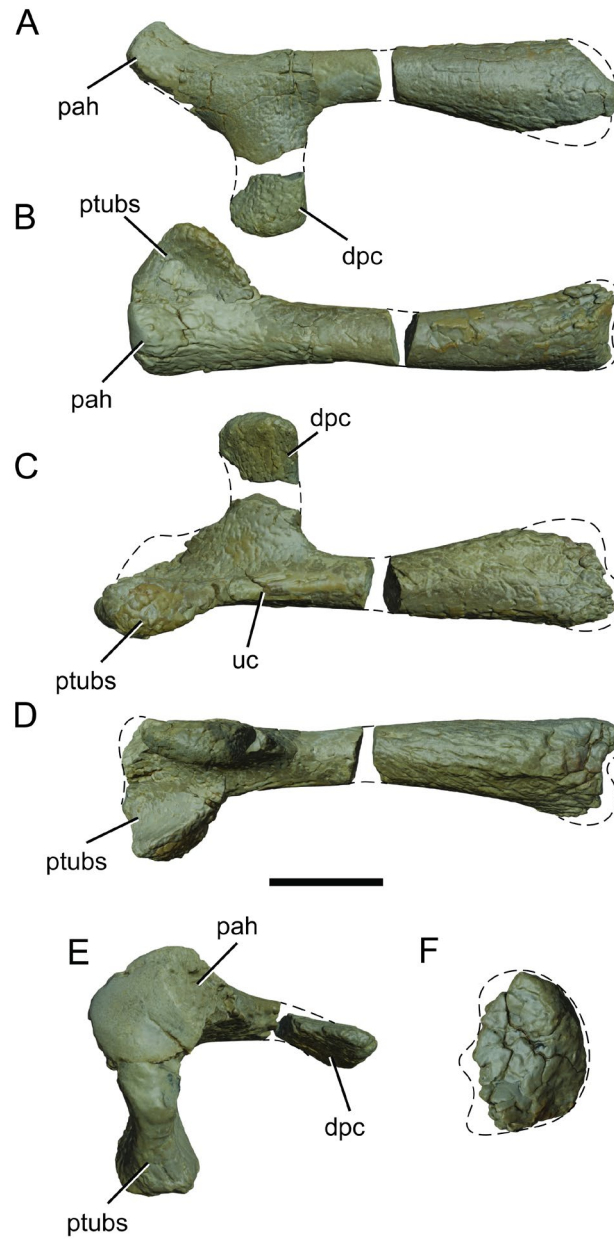


Figure 2.7 *Inabtanin alarabia* humerus (YUPC-INAB6-007, -008). Blender model combining photogrammetric reconstructions of the right and left humeri in **A**, dorsal view; **B**, anterior view; **C**, ventral view; **D**, posterior view; **E**, proximal view; and **F**, distal view. Dashed lines indicate reconstructed outline of bone. **Abbreviations:** **dpc**, deltopectoral crest; **pah**, proximal articular head; **ptubs**, proximal articular tuberosity; **uc**, ulnar crest. Scale bar equals 5 cm for **A–D**; 3 cm for **E–F**.

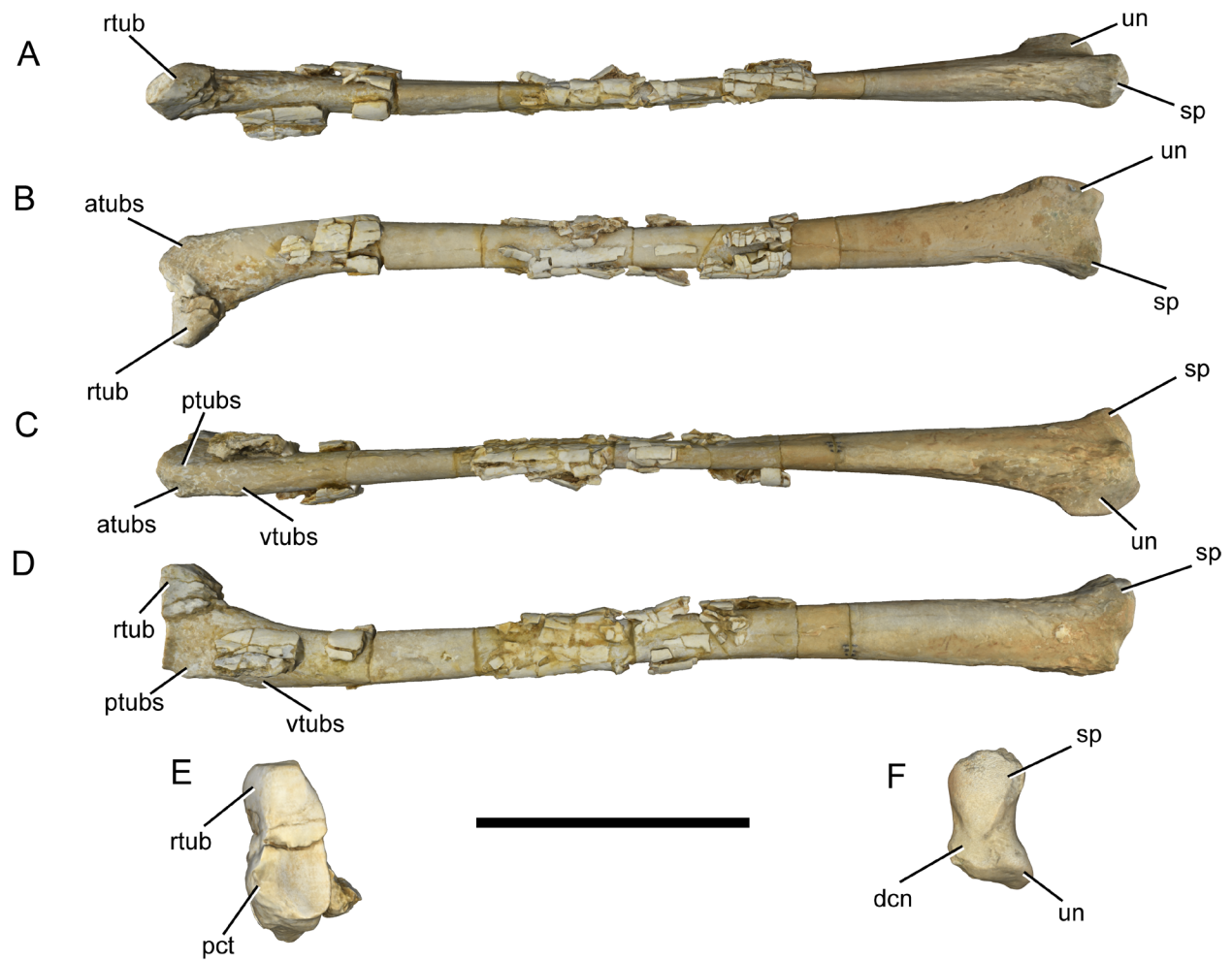


Figure 2.8 *Inabtanin alarabia* right radius (YUPC-INAB6-009). Photogrammetric reconstruction in **A**, dorsal view; **B**, anterior view; **C**, ventral view; **D**, posterior view; **E**, proximal view; and **F**, distal view. **Abbreviations:** **btub**, biceps tubercle; **dcn**, distal condyle; **pct**, proximal cotyle; **ptubs**, posteroventral tuberosity; **rtub**, radial tubercle; **sp**, styloid process; **un**, ulnar notch; **vtubs**, ventral tuberosity. Scale bar equals 10 cm for **A–D**; 7.5 cm for **E–F**.

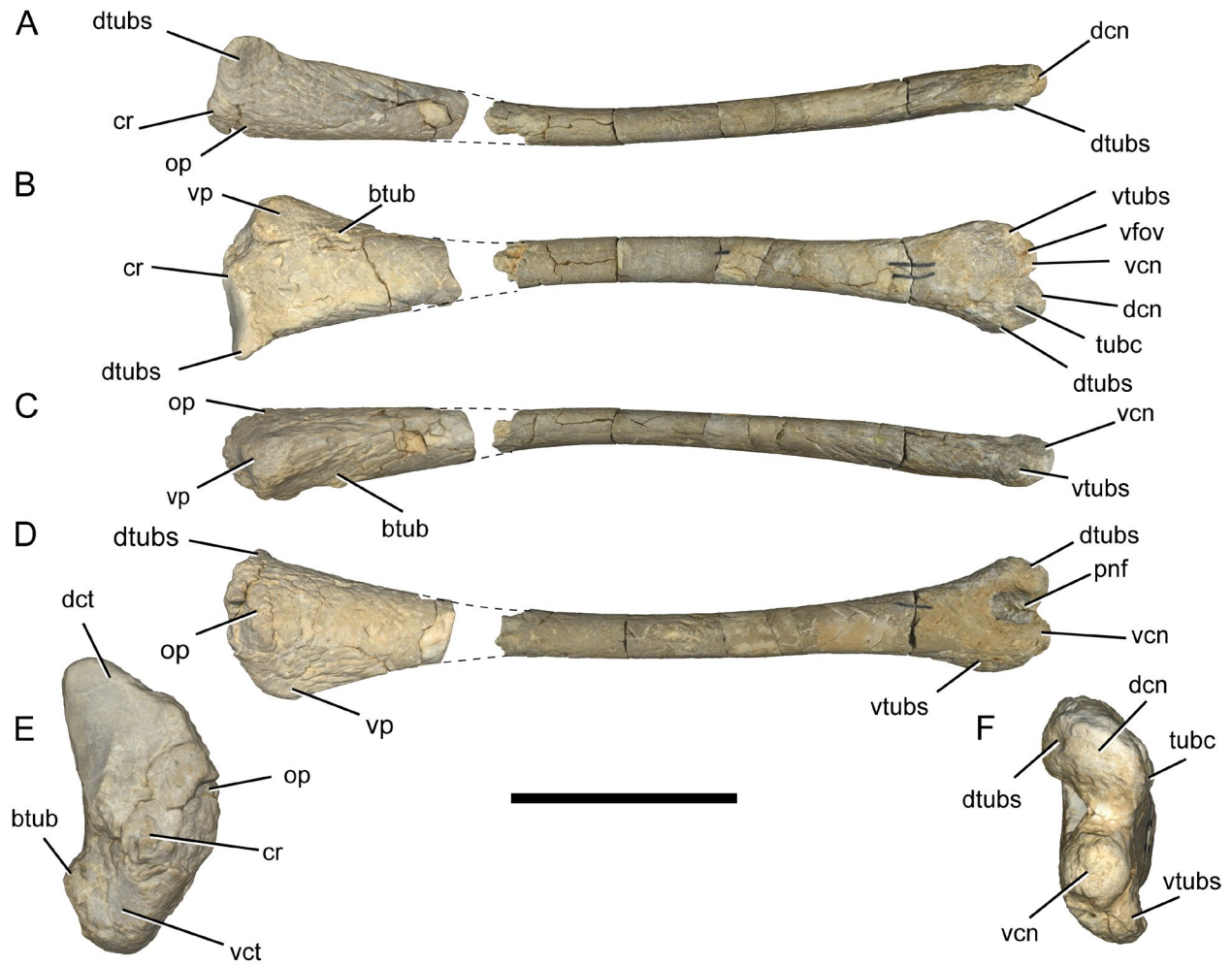


Figure 2.9 *Inabtanin alarabia* right ulna (YUPC-INAB6-010). Photogrammetric reconstruction in **A**, dorsal view; **B**, anterior view; **C**, ventral view; **D**, posterior view; **E**, proximal view; and **F**, distal view. Dashed lines indicate reconstructed outline of bone. **Abbreviations:** **btub**, biceps tubercle; **cr**, crest; **dct**, dorsal cotyle; **dcn**, dorsal condyle; **dtubs**, dorsal tuberosity; **op**, olecranon process; **pnf**, pneumatic foramen; **tubm**, tuberculum; **vcd**, ventral condyle; **vct**, ventral cotyle; **vfov**, ventral fovea; **vp**, ventral process; **vtubs**, ventral tuberosity. Scale bar equals 10 cm for **A–D**; 5 cm for **E–F**.

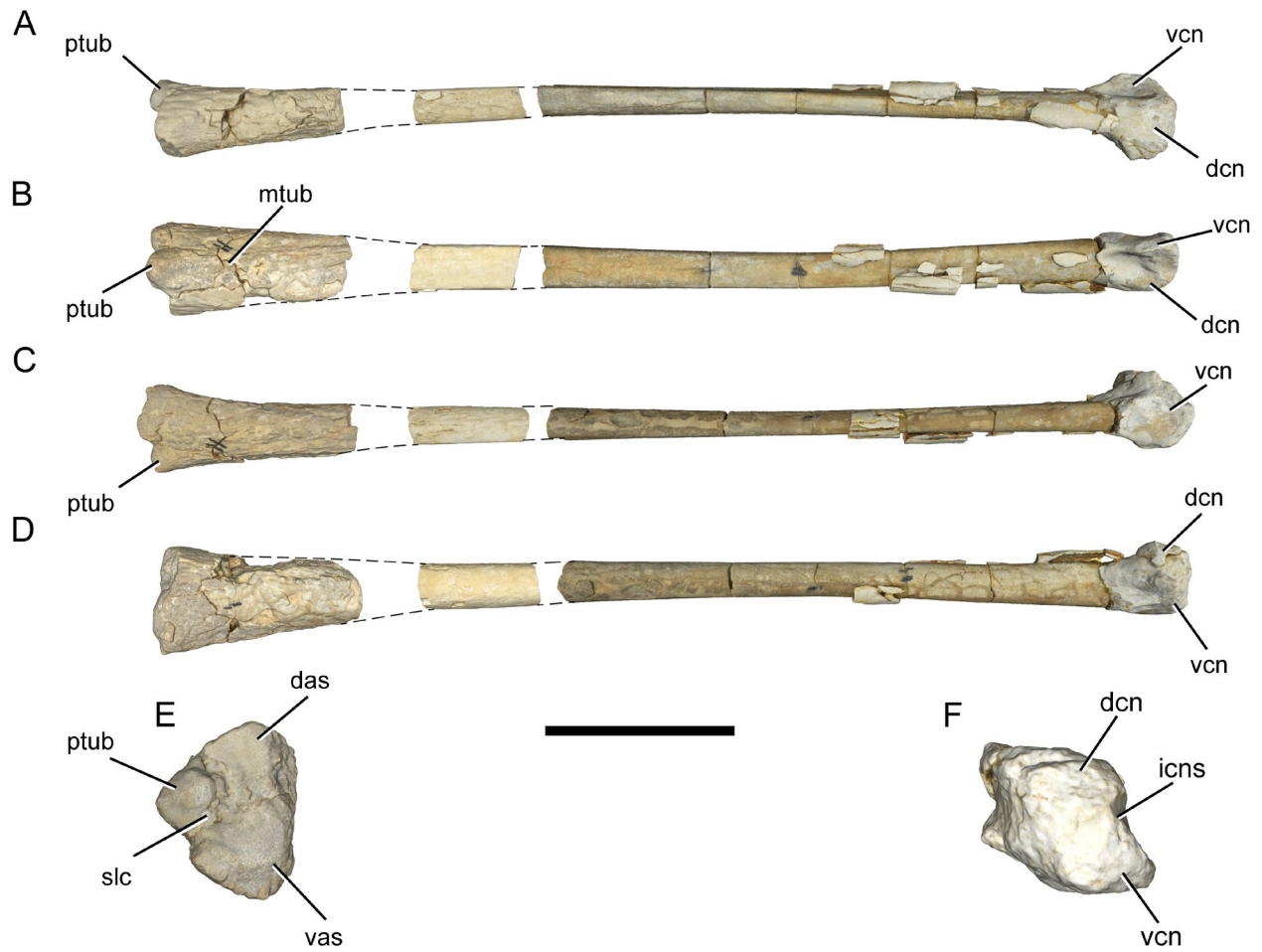


Figure 2.10 *Inabtanin alarabia* right fourth metacarpal (YUPC-INAB6-011). Photogrammetric reconstruction in **A**, dorsal view; **B**, anterior view; **C**, ventral view; **D**, posterior view; **E**, proximal view; and **F**, distal view. Dashed lines indicate reconstructed outline of bone.

**Abbreviations:** **das**, dorsal articular surface; **dcn**, dorsal condyle; **icns**, intercondylar sulcus; **mtubs**, median tuberosity; **pas**, proximal articular surface; **ptubm**, proximal tuberculum; **slc**, sulcus; **vas**, ventral articular surface; **vcn**, ventral condyle. Scale bar equals 10 cm for **A–D**; 5 cm for **E–F**.



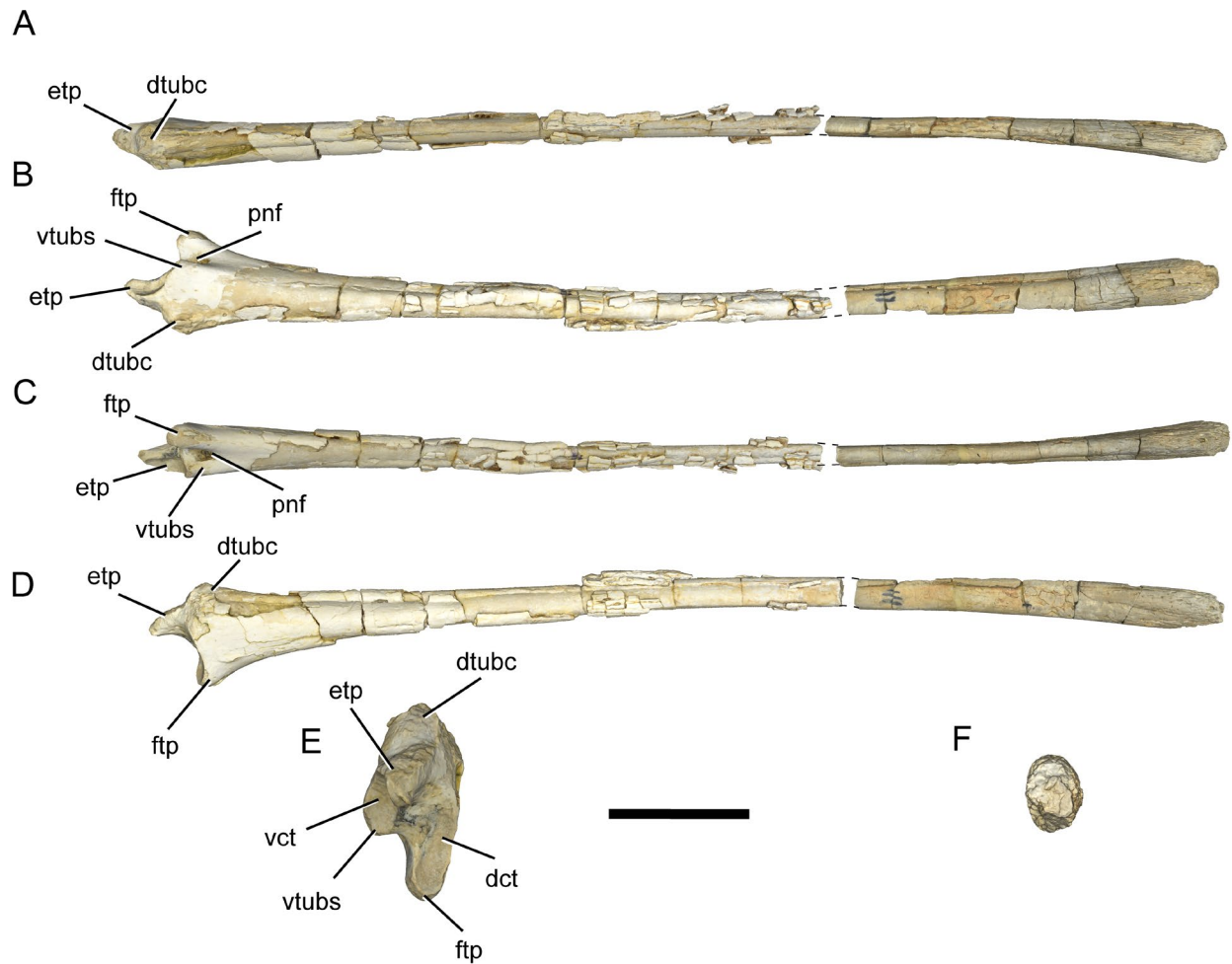


Figure 2.11 *Inabtanin alarabia* right first wing phalanx (YUPC-INAB6-012). A photogrammetric reconstruction in **A**, dorsal view; **B**, anterior view; **C**, ventral view; **D**, posterior view; **E**, proximal view; and **F**, distal view. Dashed lines indicate reconstructed outline of bone. **Abbreviations:** **dct**, dorsal cotyle; **dtubm**, dorsal tuberculum; **etp**, extensor tendon process; **ftp**, flexor tendon process; **pnf**, pneumatic foramen; **vct**, ventral cotyle; **vtubs**, ventral tuberosity. Scale bar equals 10 cm for **A–D**; 5 cm for **E–F**.



Figure 2.12 *Arambourgiania philadelphiae* right humerus (YUPC-RUSEIFA-001). Photographs in **A**, dorsal view; **B**, anterior view; **C**, ventral view; **D**, posterior view; **E**, proximal view; and **F**, distal view. Scale bar equals 5 cm.

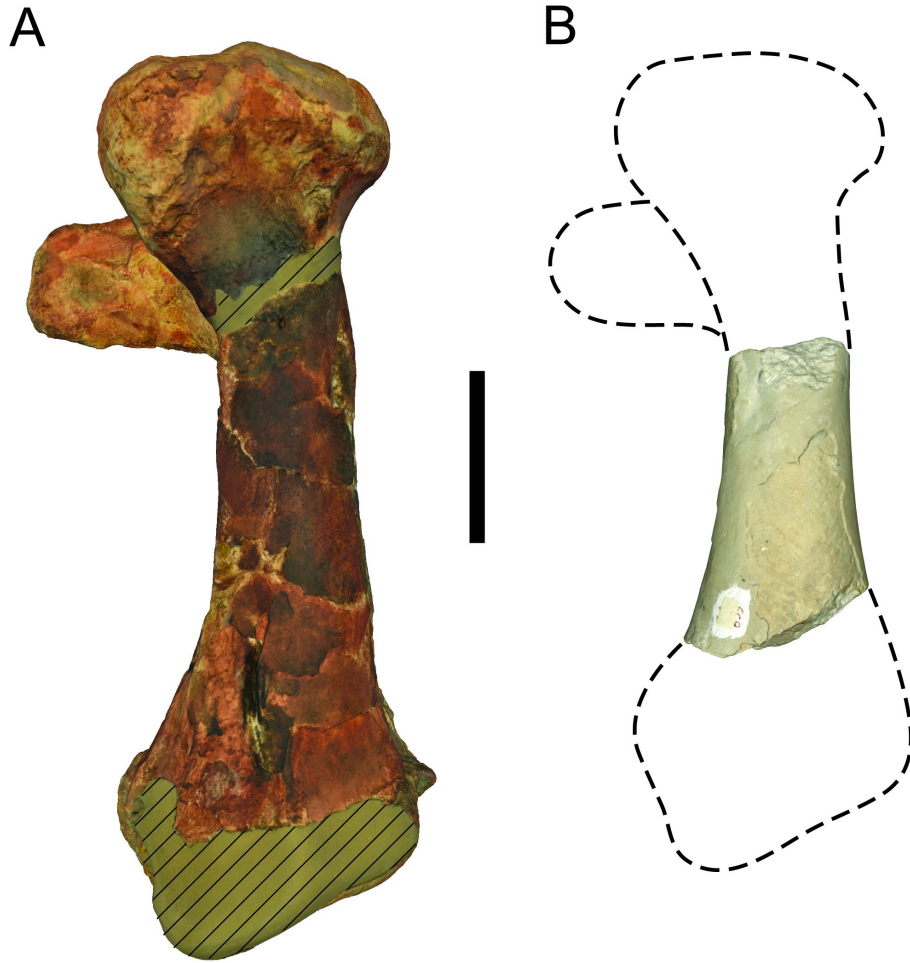


Figure 2.13 . Comparison of humeri of giant azhdarchid pterosaurs. **A**, *Quetzalcoatlus northropi* (TMM 41450-3), cast of the left humerus (reversed) in posterior view. **B**, *Arambourgia philadelphiae* (YUPC-RUSEIFA-001) right humerus in posterior view. Dashed lines indicate reconstructed outline of bone. Diagonal lines indicate broken areas. Scale bar equals 10 cm.

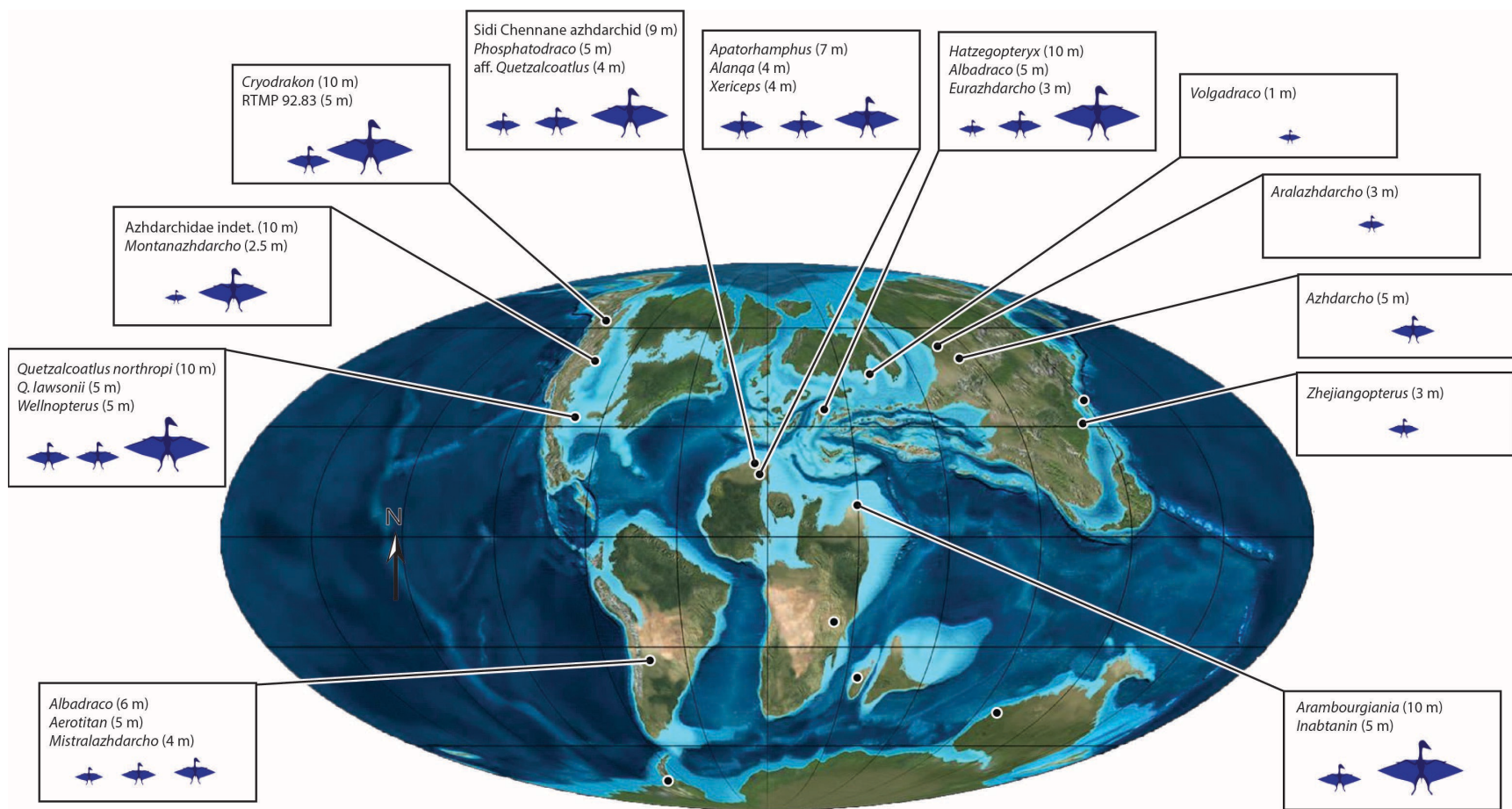


Figure 2.14 Paleomap of the Earth (modified from Scotese, 2016) during the Late Cretaceous highlighting locations where putative azhdarchid pterosaur remains have been recovered. Pinpoints without lines indicate areas where potential azhdarchid material has been reported but not formally described. Pterosaur icons are scaled to represent estimated wingspans ranging from 1-10 m.

### 3 Evolutionary Relationships of Late Cretaceous Pterosaurs (Archosauria: Pterosauria)

**Authors:** Kierstin L. Rosenbach and Jeffrey A. Wilson Mantilla

#### 3.1 Introduction

Pterosaurs span the fossil record from the Early Triassic to the end of the Cretaceous and include at least 170 species (Andres, 2021). Although the spatiotemporal context of pterosaurs is comparable to other major groups like dinosaurs, there have been less than 40 published phylogenetic analyses since their discovery in 1784. By comparison, the number of phylogenetic analyses containing dinosaurs surpassed 40 in the last three years alone. Furthermore, fewer than 30 of these pterosaur phylogenies contain publicly available methods and character matrices.

The broad taxonomic divisions of pterosaurs were established early in the 20<sup>th</sup> century and are still used today, such as the paraphyletic assemblage of “rhamphorhynchoids” and the monophyletic group, Pterodactyloidea (Plieninger, 1901). Research interest in pterosaurs was minimal for the decades following, until the 1970s when Wellnhoffer discerned reliable variation in cranial structure and defined much of the nomenclature that is foundational for current phylogenetic analyses (Wellnhofer, 1978). The first formal phylogenetic analysis of pterosaurs was published in 1986 and focused on variation in the morphology of cervical vertebrae (Howse, 1986). In the following decade, the analyses by Bennett (1989, 1991, 1994), Kellner (2003), and Unwin (2003a, 2003b) helped to define the contents of major groups including rhamphorhynchids, anhanguerids, pteranodontids, tapejarids, and azhdarchids. These analyses

produced valuable comparisons of cranial and general wing anatomy within Pterosauria that remain well supported in the present.

More recently, the work of Andres and colleagues (Andres and Ji, 2008; Andres 2010; Andres et al., 2010; Andres et al., 2014) built the current understanding of basal pterodactyloid relationships as a generally pectinate organization of groups that are defined by cranial structure. This extensive study of cranial variation produced an abundance of well-designed cranial characters. Only within the past several years have there been any phylogenetic analyses with a broad sampling of Late Cretaceous pterosaurs (Vidovic and Martill, 2017; Longrich et al., 2018; Andres, 2021). As noted in Andres (2021), even the earliest pterosaur phylogenetic analysis (Howse, 1986) contained what would be a defining azhdarchid, *Quetzalcoatlus northropi*. But 35 years later, we still have a limited understanding of the relationships of pterosaurs in the latest Cretaceous, particularly the azhdarchids and potential members of the group.

The traditional understanding of pterosaur diversity leading up to the Cretaceous-Paleogene extinction (K-Pg) is that all Upper Cretaceous pterosaurs remains are large and toothless and belong to the group Azhdarchidae. However, recent work suggests other groups survived into the Maastrichtian as well (Dalla Vecchia, 2017; Longrich et al., 2018). These include pteranodontids and nyctosaurids, both of which share features of azhdarchids (elongate edentulous beaks, wingspans reaching 6 m, etc.). Additionally, recent research suggests that many pterosaurs once attributed to Azhdarchidae (i.e., *Volgadraco bogolubovi*, *Alanqa saharica*, *Aerotitan sudamericanus*) belong to other more basal groups (Vidovic and Martill, 2017; Longrich et al., 2018; Andres et al., 2021), thus complicating the placement of newly discovered remains from the latest Cretaceous like *Inabtanin alarabia*, *Xericeps curvirostris*, and

*Argentinadraco barrealeensis*. Resolving these relationships has valuable implications for our understanding of diversity changes across the Mesozoic, especially approaching the K-Pg.

A major hurdle for overcoming this gap in the literature is that the existing matrices for pterosaur characters may not be well suited for analyzing the anatomy of fragmentary Late Cretaceous fossils. Subsequent use of these matrices is limited by the tendency to recycle existing characters without critical assessment of their value. This circumstance allows for overlapping content and poor representation of certain groups that causes low support values and leads to compounding errors over decades. For example, pterosaur phylogenies are predominated by cranial characteristics, over 60% of characters focus on cranial bones. This is common across many groups, but we question the validity of this distribution for a group whose most notable anatomy is an appendicular skeleton modified for flight. We do not question the value of cranial characteristics, rather we seek a greater proportion of characters dedicated to the anatomy of wing bones.

In this study we critically evaluate the majority of characters from pterosaur matrices published through 2018. This includes collecting, organizing, and eliminating thousands of characters to ensure that each is variable, heritable, and independent. The resulting matrix was used to study Late Cretaceous pterosaurs from across the world and to include a new taxon, *Inabtanin alarabia*. With this analysis we aim to provide a stronger representation of the relationships of Late Cretaceous pterosaurs and address the notion that Azhdarchidae might be a wastebasket taxon. The results of this analysis suggest that there is a monophyletic group of large Late Cretaceous pterosaurs that includes, but is not limited to, Azhdarchidae. We find that the monophyly of Azhdarchiformes is supported by several humeral characters. We also discuss the validity of morphogroups based on cervical elongation and extreme wingspan and provide clarity

on future use of pterosaur nomenclature to build a framework for future analyses of Late Cretaceous pterosaurs.

### **3.2 Methods**

We created a database of pterosaur characters in the literature available online and in print with the intent of critically evaluating existing pterosaur matrices (full database available upon request). We collected character lists from appendices or supplemental information of 24 papers published through 2018 (Table 1). This database contains over 2,500 characters organized according to Table 2 prior to filtering the characters (Fig. 1). Ultimately the process described here is iterative and should be repeated when additional papers are added to the database. The outcome is a character list that encompasses the full history of matrices with an organization that reflects the most current knowledge of the group of interest. Completing this process prevents the addition of new overlapping characters and highlights the body regions that may be lacking in characters to address the addition of a new species or reassessment of a group.

The filtration process began with a database organized into anatomical bins, this allows us to look at character distribution within the bins and eliminate characters by removing duplicates. We eliminated exact duplicates that were recycled from previous analyses, accounting for over 60% of the characters. We then searched for functionally overlapping characters, meaning that the characters were duplicates based on character states but not based on the vocabulary or format of the character statement. This removed 40% of the remaining characters. This part of the process essentially collapses large groups of characters, retaining the most current version of the wording along with citations for the original authors and all subsequent authors that used a version of the character. We identified 40 characters that were compound statements, combining what should be two independent characters. These characters



were separated into constituent parts and fed back into the filtration process. Finally, we scrutinized the remaining ca. 500 characters for quality based on the Rejection Criteria for Morphological Characters (Serenio, 2007: Table 10). This includes the following criteria: comparative (i.e. high variation and homoplasy); logical (i.e. overlapping or interdependent statements); and operational (i.e. ambiguous or imprecise descriptions). This left us with a core group of 303 heritable, variable, and independent characters evenly split between cranial and postcranial anatomy.

Pterosauria is composed of mostly monotypic genera and some well-established genera with multiple species, so we chose to define our operational taxonomic units (OTU) at the species level. We expanded our OTU list to be at least as inclusive as the most recent paper with broad sampling of pterosaurs (Andres et al., 2021). Our outgroups are *Euparkeria capensis* (Broom, 1913), *Ornithosuchus longidens* (Huxley, 1877), *Herrerasaurus ischigualastensis* (Reig, 1963), and *Scleromochlus taylori* (Woodward, 1907). We included non-pterodactyloids and basal pterodactyloids in the analysis to determine if our core characters produce results that are reasonably consistent with past literature. We expanded the typical species list to include a broad sampling of putative azhdarchids since our focus is on Late Cretaceous pterosaurs. We also included the newly described *Inabtanin alarabia* that has not been previously included in phylogenetic analyses.

We performed in-person collections visits for the purpose of scoring the new matrix for pterosaur fossils from the latest Cretaceous. Some taxa were scored based on published descriptions and personal communications if we could not study the fossils in person (Table 2). We rescored 17 taxa based on our examination of the anatomy of latest Cretaceous pterosaurs. Scores for the taxa outside of our group of interest were taken from the most recent published

matrix containing the character at the time of analysis (Vidovic & Martill, 2017; Longrich et al., 2018; Andres, 2021).

This parsimony analysis included 47 continuous and 256 discrete characters. The resultant matrix included 303 characters and 176 taxa. We analyzed this matrix using TNT (Tree analysis using New Technology) 1.5 (Goloboff & Catalano, 2016), with the settings outlined in Andres (2021:205) the default setting was retained where ambiguous branch support is not used thus collapsing if at least one optimization lacks support; continuous characters were automatically rescaled to unity ('nstates stand'); tree buffer was set to keep up to 130,000 trees ('hold = 130000'); the random seed is set as 0 = time ('rseed 0'); for wagner trees insertion sequence are randomized ('rseed [ '); 27 characters were ordered ('ccode'), all characters were equally weighted; basic tree searches of 2,000 random addition sequence replicates were conducted followed by branch swapping phases using tree bisection reconnection (TBR); zero-length branches were automatically collapsed, and the resultant trees were filtered for best score ('best'); when referring to terminal nodes, names are used ('taxname= '). We formatted the resulting trees in Adobe Illustrator.

### **3.3 Results**

This phylogenetic analysis of Late Cretaceous pterosaurs focusing on putative azhdarchids resulted in 3 most parsimonious trees with a tree length of 1671.910 steps. The resulting trees are generally pectinate and reflect the topology of major groups established in past literature (Table 4). A strict consensus tree of Late Cretaceous pterosaurs is reported in Figure 2, the full tree is available in Appendix B. Under strict consensus, many groups of the Jurassic collapse, but the relationships of Cretaceous pterosaur groups remain. A notable difference in our analysis and recent analyses (Andres, 2021) is that Dsungaripteridae is more basal than

Thalassodromidae, both are excluded from Azhdarchoidea, which contains tapejarid-line pterosaurs as the sister group to azhdarchimorphs. This configuration has been presented in past studies (Andres et al., 2014; Kellner et al., 2019; ).

This analysis produces a monophyletic group containing all azhdarchids as defined in the literature plus almost all of the putative azhdarchids that have been associated with the group inconsistently since their initial publications. This monophyletic group fits the nomenclature for Azhdarchiformes as defined by Andres (2021). It is the sister taxon to the chaoyangopterids, which includes *Eoazhdarcho* and *Microtuban* in our analysis. Azhdarchiformes includes those pterosaurs that have previously appeared within Tapejaridae (*Aerotitan*, *Alanqa*, *Mistralazhdarcho*) and ornithocheiromorpha (*Volgadraco*) and others (*Montanazhdarcho*). A putative azhdarchid not in this group is *Bakonydraco*, which falls into Tapejaridae here and in most recent phylogenies (Andres et al., 2014; Longrich et al., 2018; Martill et al., 2020; Andres, 2021).

When accounting for temporal ranges, we see many ornithocheiroids reach extinction during the Aptian-Albian. This is followed by a radiation of pteranodontids, nyctosauromorphs, and most notably, the Azhdarchiformes. These three groups persist until the end of the Cretaceous.

Azhdarchiformes branches into two groups, Group 1 (new) and one leading to Azhdarchidae. Group 1 includes recently published species of pterosaurs with uncertain placement (*Xericeps*, *Argentinadraco*, *Aptorhamphus*, *Ornithostoma*), although it should be noted that none of these preserve cervical vertebrae and are heavily or entirely based on cranial characters. We assign the name Group 2 to the branch leading to and including Azhdarchidae. It is explored further in the discussion.

Azhdarchidae is most commonly defined as the least inclusive clade containing *Azhdarcho lancicollis* and *Quetzalcoatlus northropi* (Unwin, 2003). In the same year, an alternative was published, defining Azhdarchidae as, “all pterosaurs closer related to *Quetzalcoatlus* than to any other pterosaur” (Kellner, 2003). This definition is not widely used because of its lack of clarity and failure to distinguish *Quetzalcoatlus* at the species level. This is problematic because both *Q. northropi* and “*Quetzalcoatlus* sp.” were known at the time but would not be described or established as two species in a genus by phylogenetic analyses until recently (Andres, 2021; Andres and Langston, 2021). Pêgas et al. (2022) proposed a new node-based definition of Azhdarchidae as, “The least inclusive clade containing *Azhdarcho lancicollis* (Nesov, 1984), *Phosphatodraco mauritanicus* (Pereda-Suberbiola et al. 2003) and *Quetzalcoatlus northropi* (Lawson, 1975).” The authors assert that this new definition allows the commonly used group name to continue to reflect its current use.

### **3.4 Discussion**

Our understanding of the relationships between Late Cretaceous pterosaurs has long been hampered by a number of factors including fragmentary fossil record, insufficient representation in character lists, limited inclusion in phylogenetic analyses, and inconsistent use of nomenclature. We cannot change the state of the fossil record, but this study contributes to the resolution of the other issues by careful review of character lists, broad sampling of the group of interest, and proposing an updated use of terminology.

#### ***3.4.1 Azhdarchiformes as the major group of Late Cretaceous pterosaurs***

Azhdarchidae has long been a contentious group with multiple definitions that often differ from the colloquial use of the name. We find that it has outgrown its definition, or that the name Azhdarchidae is no longer a useful category when describing the relationships of Late Cretaceous pterosaurs. This is due in part to highly variable understanding of what defines the group.

The notion that an updated definition of Azhdarchidae would better reflect our current understanding of the group (Pêgas et al., 2022) could also apply to our analysis, however we recognize that definitions of phylogenetic nomenclature specify content, not the other way around. For this reason, we instead propose broader use of the term Azhdarchiformes, and organize this group into two sister lineages, Group 1 and Group 2. Group 2 includes Azhdarchidae and the azhdarchid-line pterosaurs that are often referred to Azhdarchidae. Furthermore, we assert that the name Azhdarchidae should only be used in reference to its least inclusive definition (Unwin, 2003). The introduction of new node-based group names allows for better organization of Late Cretaceous pterosaur species and prevents confusion and disagreement on the use of the name Azhdarchidae as well as its use as a wastebasket taxon.

Our results suggest that the broader group name Azhdarchiformes is a better reflection of the collection of Late Cretaceous pterosaurs commonly referred to as azhdarchids. Azhdarchiformes includes the Late Cretaceous pterosaurs with elongate, edentulous beaks and long wingspans. This analysis and others (Andres, 2021; Pêgas et al., 2022) find that the most useful characters for this distinction are in the structure of the humerus. Group 2 contains all pterosaurs that preserve humeri with elongate, rectangular deltopectoral crests that are distended distally along the shaft, away from the proximal articulation. We note that the division in Azhdarchiformes categorizes those with preserved humeri in Group 2 and those missing humeral

data in Group 1. Future discovery of postcrania will likely change this division. Secondarily, the structure of the beak and cervical vertebrae contribute to the group's affinities but are not as crucial.

A strong example of this is *Inabtanin alarabia*, described in the previous chapter. It is a large, edentulous pterosaur from the Maastrichtian with an azhdarchid style humerus. By traditional assumptions, this pterosaur would be referred to as an azhdarchid simply because of its elongate edentulous beak and spatiotemporal context. By the standards of recent literature, it would fall outside of Azhdarchidae due to its gracile wing bones and short cervical vertebrae. Unexpectedly, this analysis places *Inabtanin* firmly nested within Azhdarchidae, even by its most strict definition from Unwin (2003). This supports the idea that humeral structure is more representative of the group's affinities than elongated cervical vertebrae.

### ***3.4.2 The significance of elongated cervical vertebrae***

The evolution of elongate necks is not uncommon in vertebrates, occurring numerous times in mammals and birds as well as extinct groups of marine reptiles, pterosaurs, and dinosaurs. An elongate neck can be achieved by the addition of cervical vertebrae, by the elongation of each existing vertebrae, or by the cervicalization of dorsal vertebrae, thus displacing the shoulder girdle posteriorly (Müller et al., 2021). Many groups that display this adaptation use a combination of these skeletal adaptations, such as the sauropod dinosaurs, which exhibit all of these options. By contrast, pterosaurs retain nine cervical vertebrae and display only the individual elongation trait. All pterosaurs possess nine cervical vertebrae, and the lineages with elongate necks achieve this through greatly elongating cervical vertebrae 3 through 7. Interestingly, it is always cervical vertebra 5 that is the longest, with the flanking cervical vertebra 4 and 6 being slightly shorter, and cervical vertebra 3 and 7 even more so.

Presumably, an organism could evolve elongate cervical vertebrae that are longest at the base of the skull grading posteriorly, or longest that shoulder girdle grading anteriorly. A further mystery to this configuration is that pterosaurs are the only group of long-necked vertebrates that possess procoelous vertebral connections, all other groups independently acquired opisthocoelous cervical vertebrae. It is currently unclear why a centrally placed elongation pattern or procoelous connections occur in pterosaurs, or what the biomechanical significance of these adaptations are.

Elongation of the cervical region has been associated with azhdarchid pterosaurs since before the group was formally named and is usually represented by a character for the length of a mid-series cervical vertebrae (Howse, 1986; Bennett, 1989; Bennett, 1991; Bennett, 1994; Kellner, 2003; Unwin 2003a; Wang et al., 2005; Lu and Ji 2006; Martill and Naish 2006; Andres and Ji, 2008; Wang et al., 2008; Lu 2009; Lu et al., 2009; Wang et al., 2009; Andres et al., 2010; Vidovic and Martill, 2014). This is quantified by the ratio of maximum length to minimum width of the longest mid-series cervical vertebra, here referred to as the cervical elongation ratio (CER). When coded as a discrete character, the groups are as follows: short-necked pterosaurs,  $CER < 2.5$ ; intermediate-necked pterosaurs,  $2.5 \leq CER < 5$ ; and long-necked pterosaurs,  $CER \geq 5$ . In this analysis we chose to include this character as continuous to avoid introducing human bias to data that is inherently continuous.

The majority of pterosaurs have a cervical elongation ratio of less than 4 and the traditional short-necked category of  $CER < 2.5$  has no natural gap according to the extensive data collected in Andres (2021) and used in this analysis. Both *Inabtanin* and *Volgadraco* have a  $CER < 2.5$ . Additionally, *Albadraco*, *Hatzegopteryx*, *Montanazhdarcho*, and all pterosaurs outside of Ctenochmastidae and Azhdarchiformes have a  $CER > 4$ . Pterosaurs with  $CER \geq 5$  are traditionally considered long necked, although there is no natural gap in the continuum of CER

values around this number either. These long-necked pterosaurs include *Azhdarcho*, *Eurazhdarcho*, *Phosphatodraco*. We do find that a natural group forms for extreme long-necked pterosaurs with  $CER \geq 7.5$ . This includes *Arambourgiania*, *Cryodrakon*, *Quetzalcoatlus lawsoni*, *Wellnhopterus*, and *Zhejiangopterus*.

Although our analysis finds that CER does not define any groups, we suggest that future analyses use the continuous form of the character (Longrich et al., 2018; Andres, 2021) to avoid the continued use of human-made bins that do not reflect the natural groups based on independent acquisition of an elongated cervical region. Many pterosaurs from the Late Cretaceous do not preserve cervical vertebrae, including the azhdarchiformes *Aerotitan*, *Alanqa*, *Apatarhamphus*, *Aralazhdarcho*, *Argentinadraco*, *Mistralazhdarcho*, *Q. northropi*, and *Xericeps*. Any future discovery of cervical vertebrae will contribute greatly to our understanding of the value of CERs in pterosaur relationships. We find this to be worthy of continued investigation because the unique nature of cervical elongation in pterosaurs likely hold biomechanical significance and therefore may have phylogenetic signal that we are not capturing with the information available today.

### **3.4.3 Distribution of long wingspan**

The development of extremely long wingspans is often associated with Late Cretaceous pterosaurs, which represent the uppermost limits of wingspans achieved by flying vertebrates. Across the Mesozoic, pterosaur wingspan generally increases, with greatest range in the Cretaceous. By the end of the Cretaceous, only pterosaurs of medium to long wingspan remain (5–10 m). This has led some to hypothesize about competition from the radiation of large birds that reached wingspans up to 6 m (Benson et al., 2013; Longrich et al., 2018: figure 20).



Regardless of the cause, we find limited evidence for a phylogenetic component to the acquisition of long wingspans (Fig. 2). The broad group of Azhdarchomorpha entirely contains pterosaurs with wingspan estimates greater than 1 m, and the overwhelming majority of Azhdarchiformes have wingspan estimates greater than 3 m. But from this point, large wingspan appears to have a homoplastic distribution. Group 1 contains a wide range of wingspans from 1–7 m. Group 2 does contain comparatively large pterosaurs with wingspans 5–10 m, however the “giant” pterosaurs are generally considered to be those with wingspan estimates of ~10 m. Additionally, these do not all fall within Azhdarchidae as previously assumed, or even within the broader Group 2. It is also notable that pteranodontids have wingspan estimates around 6 m, making them larger than most of the Azhdarchiformes. These large taxa do not form any groups, suggesting that an extreme long wingspan is achieved independently.

This is not unexpected given that within other groups that achieve extremely long wingspans, this can be acquired independently many times over the lineage’s evolutionary history. We can observe this in Aves, whose largest members occur in phylogenetically disparate groups such as swans (Anseriformes), albatrosses (Procellariiformes), pelicans (Pelecaniformes), vultures and condors (Accipitriformes), storks (Ciconiiformes), and extinct giants like *Argentavis* (Cathartiformes). All of these and many others achieved long wingspan independently and share no common geographical distribution, habitat, or feeding ecology. The same is likely true of pterosaurs. We do find that pterosaurs have larger average wingspans later in the Mesozoic, but we do not find evidence that the acquisition of wingspans reaching an estimated 10 m can unify a group. Ultimately, pterosaurs of the Late Cretaceous are discerned by the structure of their humeri and potentially by their cervical vertebrae.

### 3.5 Conclusion

This analysis addresses many of the root causes of a disorganized and variable understanding of the relationships of Late Cretaceous pterosaurs and more specifically, how we refer to these groups in the literature and in informal settings, including conferences, personal communications, and science communication aimed at the public. We addressed this issue by taking careful consideration of the character statements that have been reused for decades and ensured a broad sampling of the group in question. This work was inspired by the prevalent and unclear use of the group name Azhdarchidae. We found that under review, this nomenclature does not encompass the full diversity of pterosaurs to which we commonly discuss and that it is preferable to refer to Azhdarchiformes when talking about the Late Cretaceous pterosaurs united by elongate edentulous beaks, long wingspan, and particular humeral structure. Additionally, we found that the elongation of cervical vertebrae and acquisition of long wingspan are not necessarily useful indicators for the phylogenetic composition of the Azhdarchiformes. As always, an improved sampling of the Maastrichtian fossil record will help to untangle the uncertainties.

### 3.6 Tables

Table 3.1 The 24 papers with phylogenetic analyses included in our character critique process compared to this analysis and analyses published since 2018 that were not included (starred item).

<b>Citation</b>	<b>Characters</b>	<b>Terminal taxa</b>	<b>Putative azhdarchids</b>
Bennett (1989)	14	19	3
Bennett (1991)	37	24	3
Bennett (1994)	37	27	3
Unwin (2003a)	60	20	1
Unwin (2003b)	53	16	N/A
Kellner (2003)	74	42	2
Maisch et al. (2004)	10	9	N/A
Wang et al. (2005)	80	48	3
Martill and Maish (2006)	23	9	3
Lu and Ji (2006)	80	56	3
Bennett (2007)	21	7	N/A
Wang et al. (2008)	80	49	3
Lu et al. (2008b)	73	32	3
Andres and Ji (2008)	111	67	3
Wang et al. (2009)	89	60	3
Lu (2009)	80	41	N/A
Lu et al. (2009)	117	56	3
Andres (2010)	182	101	4
Andres et al. (2010)	75	22	N/A
Andres and Myers (2013)	185	109	6
Andres et al. (2014)	224	112	4

Vidovic and Martill (2014)	127	33	2
Vidovic and Martill (2017)	320	104	4
Longrich et al. (2018)	271	134	13
*Andres (2021)	275	177	21
This analysis	303	177	22

Table 3.2 Organizational categories for the database of pterosaur character statements in published literature through 2018 (available upon request). Each level of organization corresponds to a column in the database that prepared the list of over 2,500 characters to be filtered.

<b>Level of organization</b>	<b>Key words</b>
Body region	Cranial, axial, appendicular
Bone(s)	Skull bones, upper jaw bones, lower jaw bones, teeth, cervical vertebrae, dorsal vertebrae, caudal vertebrae, scapulocoracoid, synsacrum, sternum, humerus, radius, ulna, manus, femur, tibia, fibula, pes
Bone region	Including anterior, posterior, dorsal, ventral, proximal, distal; shaft; or more specific labels such as centrum, neural arch; scapula, coracoid, ilium, ischium, deltopectoral crest, etc.
Descriptor	Including presence/absence, shape, orientation, articulation, pneumatic foramina, etc.

Table 3.3 Late Cretaceous pterosaurs studied in this analysis based on their status as putative azhdarchids. Specimen numbers include only those elements that were considered in this analysis. Sources of information include location of in-person study, personal communications, and publications with detailed anatomical information that contributed to scoring the matrix in this analysis.

<b>Species</b>	<b>Specimen numbers</b>	<b>Sources</b>
<i>Aerotitan sudamericanus</i>	MPCN-PV 0054	Novas et al., 2012; Pêgas et al., 2022
<i>Alanqa saharica</i>	BSPG 1993 IX 338 BSPG 1996 I 36 FSAC-KK 26 FSAC-KK 4000	In person analyses at Bayerische Staatsammlung für Paläontologie und Geologie, in Munich, Germany. Ibrahim et al., 2010; Martill and Ibarhim, 2015
<i>Albadraco tharmisensis</i>	PSMUBB V651a, b PSMUBB V652	Solomon et al., 2020
<i>Aralazhdarcho bostobensis</i>	ZIN PH 56/43 ZIN PH 57/43 ZIN PH 47/43 ZIN PH 49/43	In person analyses at the Zoological Institute of the Russian Academy of Sciences in St. Petersburg, Russia. Averianov, 2007
<i>Arambourgiania philadelphiae</i> cf. <i>Arambourgiania</i>	Cast of holotype 1966 XXV 501 1966 XXV 503 1966 XXV 506-508 1966 XXV 512 YUPC-RUSEIFA-001	In person analyses at Bayerische Staatsammlung für Paläontologie und Geologie in Munich, Germany and at the University of Michigan Museum of Paleontology in Ann Arbor, Michigan, USA. Arambourg, 1952; Martill and Moser, 2017
<i>Azhdarcho lancicollis</i>	CCMGE 8/12454 CCMGE 8/11915 CCMGE 10/11915 ZIN 8/44-10/44 ZIN 12/44 ZIN 15/44	In person analyses at the Zoological Institute of the Russian Academy of Sciences in St. Petersburg, Russia. Nesov 1984; Averianov 2010

---

	ZIN 24/44	
	ZIN 41/44	
	ZIN PH 16/44	
	ZIN PH 27/44	
	ZIN PH 30/44	
	ZIN PH 34/44	
	ZIN PH 36/44	
	ZIN PH 44/08	
	ZIN PH 44/65	
	ZIN PH 86/44	
	ZIN PH 94/44	
	ZIN PH 105/44	
	ZIN PH 108/44-109/44	
	ZIN PH 131/44-132/44	
	ZIN PH 137/44-139/44	
	ZIN PH 141/44	
	ZIN PH 144/44-145/44	
	ZIN PH 147/44-150/44	
	ZIN PH 170/44	
	ZIN PH 176/44-177/44	
	ZIN PH 199/44	
	ZIN PH 203/44-205/44	
	ZIN PH 207/44	
	ZIN PH 212/44-213/44	
	ZIN PH 215/44-216/44	
	ZIN PH 218/44	

---

	V 2001.051	
	V 2001.082	
<i>Bakonydraco galaczi</i>	V 2007.110.1	In person analyses at Magyar Természettudományi Múzeum in Budapest, Hungary Osi et al., 2005
	V 2010.074.4-.083.1	
	V 2010.100.1-.102.1	
	PAL 2019.244.1	

---

<i>Cryodrakon boreas</i>	TMP 1980.16.1367	Hone et al., 2019
	TMP 1980.16.1506	

---

	TMP 1981.16.0107 TMP 1989.36.0254 TMP 1992.83.0007 TMP 1993.40.0011 TMP 1996.12.0369 TMP 1998.68.0100 TMP 2005.39.0008	
<i>Eurazhdarcho lagendorfensis</i>	EME VP 312/1-7	In person analyses at the Transylvanian Museum Society in Cluj-Napoca, Romania Vremir et al., 2013; Vremir et al., 2015
<i>Hatzegopteryx thambema</i> cf. <i>Hatzegopteryx</i>	EME 315 EME 316 FGGUB R 1083 LBP R. 2347 MMIRS 688	In person analyses at the Transylvanian Museum Society in Cluj-Napoca, Romania and the Laboratory of Fossil Vertebrates, Faculty of Geology and Geophysics, at the University of Bucharest in Bucharest, Romania Buffetaut et al., 2002; Buffetaut et al., 2003; Vremir et al., 2017
<i>Inabtanin alarabia</i>	YUPC INAB6 001-012	In person analyses at the University of Michigan Museum of Paleontology in Ann Arbor, Michigan, USA
<i>Mistralazhdarcho magii</i>	MMS/VBN.09.C.001	Vullo et al., 2018; Pêgas et al., 2022
<i>Montanazhdarcho minor</i>	MOR 691	Padian et al., 1993; Padian et al., 1995; McGowen et al., 2002; Carroll et al., 2015
<i>Phosphatodraco mauritanicus</i>	OCP DEK/GE 111	Pereda Suberbiola et al., 2003
<i>Quetzalcoatlus lawsoni</i>	TMM 41544 TMM 41545 TMM 41546 TMM 41547 TMM 41954 TMM 41961 TMM 42138 TMM 42157 TMM 42161	In person analyses at the Vertebrate Paleontology Laboratory, University of Texas at Austin, Texas, USA Andres & Langston, 2021; Andres, 2021

	TMM 42180	
	TMM 42246	
	TMM 42272	
	TMM 42422	
<i>Quetzalcoatlus northropi</i>	TMM 41398 TMM 41450 TMM 44036	In person analyses at the Vertebrate Paleontology Laboratory, University of Texas at Austin, Texas, USA Andres & Langston, 2021; Andres, 2021
<i>Volgadraco bogolubovia</i>	SUG 46-48/104a	Personal communication, Averianov, 2018 Averianov et al., 2008
<i>Wellnhopterus brevirostris</i>	TMM 42489	In person analyses at the Vertebrate Paleontology Laboratory, University of Texas at Austin, Texas, USA Andres & Langston, 2021; Andres, 2021
<i>Zhejiangopterus linhaiensis</i>	M1324-1325 M1328-1330	Cai and Wei, 1994; Andres, 2021



Table 3.4 Phylogenetic nomenclature relevant to this analysis with original citations and definitions. The last column lists the species included when these definitions are applied to our analysis. Some contents list subgroups that are defined further in the table.

Group name	Citation	Definition	Contents
Pterosauria	Owen, 1842 sensu Andres and Padian 2020a	The most inclusive clade exhibiting fourth metacarpal and digit hypertrophied to support wing membrane synapomorphic with that in <i>Pterodactylus antiquus</i> (Sömmerring, 1812)	See Appendix B for full list
Ornithocheiroidea	Seeley, 1891a, sensu Kellner, 2003	The least inclusive clade containing <i>Anhanguera blittersdorffi</i> (Campos and Kellner, 1985), <i>Pteranodon longiceps</i> (Marsh, 1876), <i>Dsungaripterus weii</i> (Young, 1964), and <i>Quetzalcoatlus northropi</i> (Lawson, 1975)	Pteranodontoidea Dsungartipteridae Thalassodromidae Azhdarchoidea
Pteranodontoidea	Kellner, 2003	The least inclusive clade containing <i>Anhanguera blittersdorffi</i> (Campos and Kellner, 1985), and <i>Pteranodon longiceps</i> (Marsh, 1876)	Pteranodontia Nyctosauromorpha Ornithocheiromorpha
Pteranodontia	Marsh, 1876, sensu Unwin, 2003	The least inclusive clade containing <i>Pteranodon longiceps</i> (Marsh, 1876), and <i>Nyctosaurus gracilis</i> (Marsh, 1876)	<i>Tethydraco regalis</i> <i>Pteranodon sternbergi</i> <i>Pteranodon longiceps</i>
Nyctosauromorpha	Andres, 2021	The most inclusive clade containing <i>Nyctosaurus gracilis</i> (Marsh, 1876) but not <i>Pteranodon longiceps</i> Marsh, 1876	<i>Alamodactylus byrdi</i> <i>Cretornis hlavaci</i> <i>Simurghia robusta</i> <i>Alcione elainus</i> <i>Nyctosaurus lamegoi</i> <i>Nyctosaurus grandis</i>

			<i>Nyctosaurus nanus</i> <i>Nyctosaurus gracilis</i>
Ornithocheiromorpha	Andres et al., 2014	The most inclusive clade containing <i>Ornithocheirus simus</i> (Owen, 1861) but not <i>Pteranodon longiceps</i> (Marsh, 1876)	See Appendix B for full list of included species
Dsungaripteridae	Young, 1964, sensu Unwin, 2003	The least inclusive clade containing <i>Dsungaripterus weii</i> (Young, 1964), and <i>Noriopterus complicidens</i> (Young, 1973)	<i>Noriopterus parvus</i> <i>Noriopterus complicidens</i> <i>Domekodactylus ceciliae</i> <i>Dsungaripterus weii</i>
Thalassodromidae	Kellner and Campos, 2007	The least inclusive clade containing <i>Thalassodromeus sethi</i> (Kellner and Campos, 2002), and <i>Tupuxuara longicristatus</i> (Kellner and Campos, 1988)	<i>Tupuxuara sethi</i> <i>Tupuxuara longicristatus</i> <i>Thalassodromeus sethii</i>
Azhdarchoidea	Unwin, 1995, sensu Kellner, 2003 and Unwin, 2003	The least inclusive clade containing <i>Tapejara wellnhoferi</i> (Kellner, 1989), and <i>Quetzalcoatlus northropi</i> (Lawson, 1975).	<i>Lacusovagus magnificens</i> <i>Keresdrakon wilsoni</i> <i>Bennettazhia oregonensis</i> Tapejaridae Azhdarchimorpha
Tapejaridae	Kellner, 1989, sensu Lu et al., 2006b	The least inclusive clade containing <i>Tapejara wellnhoferi</i> (Kellner, 1989), and <i>Sinopterus dongi</i> (Wang and Zhou, 2003a)	Tapejarinae Sinopterinae
Azhdarchomorpha	Pêgas et al., 2022	The most inclusive clade containing <i>Azhdarcho lancicollis</i> (Nessov, 1984) but not <i>Thalassodromeus sethi</i> (Kellner and Campos, 2002) or <i>Tapejara wellnhoferi</i> (Kellner, 1989)	Chaoyangopteridae Azhdarchiformes

Chaoyangopteridae	Lü et al., 2008b, sensu Andres et al. 2014	The most inclusive clade containing <i>Chaoyangopterus zhang</i> (Wang and Zhou, 2003b) but not <i>Quetzalcoatlus northropi</i> (Lawson, 1975)	<i>Eoazhdarcho liaxiensis</i> <i>Microtuban altivolans</i> <i>Shenzhoupterus chaoyangensis</i> <i>Jidapterus edentus</i> <i>Chaoyangopterus zhang</i>
Azhdarchiformes	Andres, 2021	The most inclusive clade containing <i>Quetzalcoatlus northropi</i> (Lawson, 1975) but not <i>Chaoyangopterus zhang</i> (Wang and Zhou, 2003b)	Aerotitaninae Group 2
Aerotitaninae	New clade name	The most inclusive clade containing <i>Aerotitan</i> <i>sudamericanus</i> (Novas et al., 2012), but not <i>Quetzalcoatlus lawsoni</i> (Andres and Langston, 2021)	<i>Radiodactylus langstoni</i> <i>Aptorhamphus gyrostega</i> <i>Xericeps curvirostris</i> <i>Ornithostoma sedgwicki</i> <i>Argentinadraco barrealensis</i> <i>Mistralazhdarcho maggii</i> <i>Aerotitan sudamericanus</i>
Group 2	New clade name	The most inclusive clade containing <i>Quetzalcoatlus lawsoni</i> (Andres and Langston, 2021) but not <i>Aerotitan sudamericanus</i> (Novas et al., 2012)	<i>Zhejiangopterus linhaiensis</i> <i>Quetzalcoatlus lawsoni</i> <i>Wellnhopterus brevirostris</i> <i>Phosphatodraco mauritanus</i> <i>Eurazharcho lagendorfensis</i> <i>Aralazhdarcho bostobensis</i> <i>Cryodrakon boreas</i> Azhdarchidae

---

Azhdarchidae	Padian 1986, sensu Unwin, 2003	The least inclusive clade containing <i>Azhdarcho lancicollis</i> (Nessov, 1984) and <i>Quetzalcoatlus northropi</i> (Lawson, 1975)	<i>Quetzalcoatlus northropi</i> <i>Arambourgiania philadelphiae</i> <i>Montanazhdarcho minor</i> <i>Inabtanin alarabia</i> <i>Volgadraco bogolubovi</i> <i>Hatzegopteryx thambema</i> <i>Albadraco tharmisensis</i> <i>Alanya saharica</i> <i>Azhdarcho lancicollis</i>
--------------	-----------------------------------	---	---

---

### 3.7 Figures

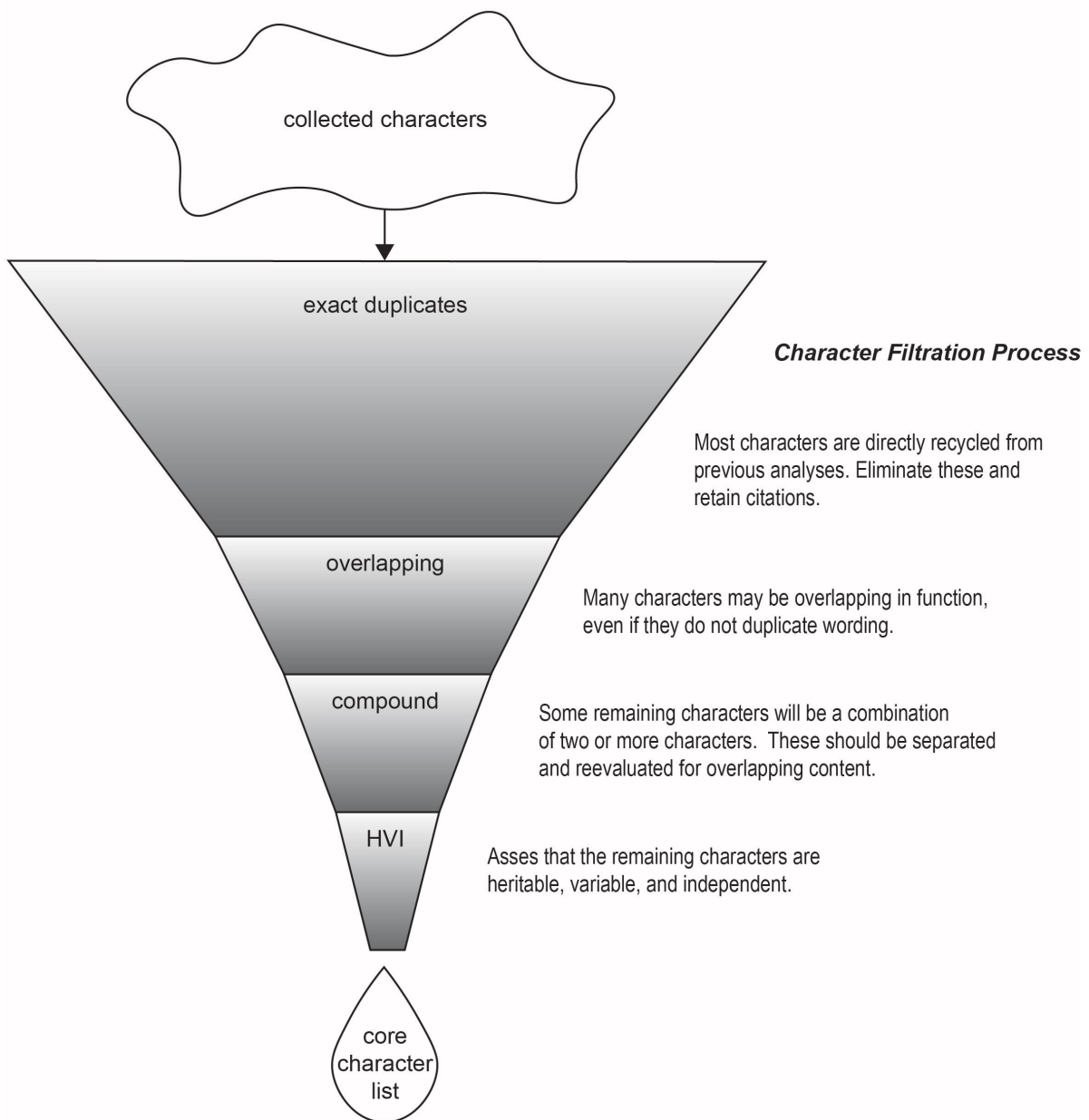
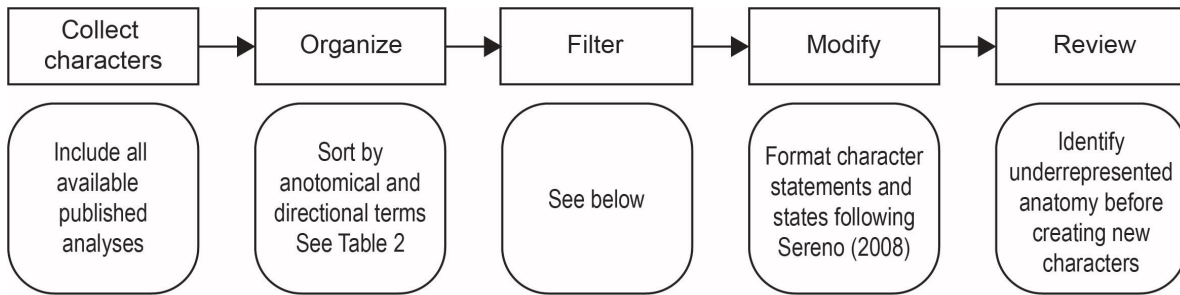


Figure 3.1 Workflow diagram summarizing the methods used to collect and filter through thousands of character statements and to organize and standardize characters prior to creating new characters and adding new OTUs or rescore existing taxa. Similar to a filtration process, we filtered the database to create a core group of characters that are heritable, variable, and independent.



Figure 3.2 Phylogenetic relationships of Late Cretaceous pterosaurs. Strict consensus tree highlighting relationships within Ornithocheiroidea. Temporal ranges are taken from published literature, uncertainty is represented by gradient bars. Solid bars represent documented ranges of groups collapsed for simplicity. Some of the temporal scaling is restricted by the constraints of the diagram and minimum spacing to visualize divergence. Wingspan estimates are taken from published literature (see Table 2). Pterosaurs with wingspans less than 3 m are represented by a single box; those with wingspan estimates from 3–7 m are represented by two boxes; and three boxes represent pterosaurs with estimated wingspans greater than 7 m. According to our phylogenetic results, Azhdarchiformes are characterized by a medium wingspan of 3–7 m, but some members of the group independently attained giant wingspans exceeding 7 m.



## **4 Analyzing Pneumatic Bones for Volumetric Airspace Proportion and Internal Trabecular Structures to Infer Flight Capacity and Style**

**Authors:** Kierstin L. Rosenbach, Danielle M. Goodvin, Ethan Shirley, and Jeffrey A. Wilson Mantilla

### **4.1 Introduction**

Pterosaurs, like other flying vertebrates, possessed a skeleton heavily modified for sustained powered flight. Pterosaurs evolved powered flight approximately 50 million years before flight feathers appeared in the fossil record, and some achieved wingspans twice that of the largest volant birds (10 m vs. 6 m). They are notable for their patagium-based wings supported by elongated, pneumatic forelimbs, and their skeletons are characterized by a high degree of skeletal pneumaticity that exceeds that of all other archosaurs (Martin and Palmer, 2014a).

Skeletal pneumaticity causes the hollowing of bone and accommodates the respiratory system in the form of air sacs. Many living and extinct vertebrates possess cranial pneumaticity associated with the sinuses, including birds, reptiles, and mammals. In contrast, postcranial skeletal pneumaticity (PSP) is only common among reptiles. Archosaurs possess variable and extensive forms of both cranial and postcranial skeletal pneumaticity. PSP is present in modern birds and is inferred to have been present in pterosaurs and some dinosaurs (sauropods, theropods). Given this distribution of the trait, it is possible that these archosaurian lineages developed PSP either independently or inherited it from a common ancestor on the

avemetatarsalian line. Regardless of origin, PSP imparts certain benefits to an organism and is linked to the evolution of flight as well as large body size. This adaptation aids in unidirectional airflow and reduces skeletal strength to weight ratio. These features are particularly advantageous to flying vertebrates.

Previous research has confirmed the presence of PSP in pterosaurs based on the structure of their bones (Britt, 1993; Bonde & Christiansen, 2003; Claessens et al., 2009; Butler et al., 2009). This includes the presence of pneumatic foramina and preserved hollow spaces that can be observed on the macroscopic level, as well as with more destructive techniques like thin-sectioning. Modern research on the topic depends largely on the use of micro-computed tomography scanning (micro-CT), which can also provide a macroscopic view of internal structure without damage to the specimen. The results of micro-CT scanned pterosaur bones were previously studied in a slice-wise manner (Martin and Palmer 2014a; Martin and Palmer 2014b). Here we sought to take a volumetric approach to reconstructing both fossils and modern bones in three-dimensional (3D) models that can be used to observe, compare, and analyze PSP.

Postcranial skeletal pneumaticity actively remodels bone in a living organism. Analysis of the internal bone structure of modern birds suggests that this remodeling of bone is a response to the stresses of flight and indicates that these distinct structures correlate with different flight behavior (Novitskaya et al., 2017). Because these structures are diagnostic for flight behavior in birds, we sought to infer flight behavior in pterosaurs by identifying these patterns of pneumaticity in their limb bones using the methods described in this paper.

## **4.2 Methods**

We developed this method with the intention of exploring internal bone structure in birds and pterosaurs, but it is designed to be applicable to any pneumatic bone tissue regardless of age

(fossil or recent) or group. Still, not all specimens will be suitable for this method. Important factors to consider when choosing elements for analysis include quality of three-dimensional preservation with minimal crushing or wear as well as an absence of any crystallization that may interfere with the results of a scan or damage delicate internal structures. Additionally, for fossil elements, the surrounding or infilled matrix should be different enough in density or composition to produce distinguishable grayscale values. Here we demonstrate this method on a sample of pterosaur, dinosaur, and avian specimens.

#### ***4.2.1 Micro-computed tomography scanning***

We scanned individual skeletal elements in a micro-computed tomography (microCT) scanner at the Computed Tomography Laboratory at the Department of Earth and Environmental Sciences, which is equipped with a Nikon XT H 225 ST. We mounted specimens vertically along their longest axis, supported by floral foam inside a cardboard tube affixed to a 15 cm-thick cardboard base. We autoconditioned the scanner to maximum capacity at 225 kV in order to accommodate long scans of fossils with a matrix that has a similar density to bone. The scanner is equipped with a tungsten target. For each scan, voltage ranged from 175 to 205 kV and current ranged from 200 to 255  $\mu\text{A}$ . We set exposure times between 1.42 and 2.83 seconds. In order to maintain the grayscale histogram values at a minimum near 10,000 and maximum near 60,000, we used copper filters ranging in width from 1.5–2.5 mm. Each scan had a resolution between 50–60 microns. For elements that were too large to scan at this resolution, we completed multiple overlapping scans of smaller regions. For each scan, we chose to enable flux normalization, capture 2 frames per projection, and minimize ring artifacts. With these settings, scans typically took 12 hours to complete. We reconstructed the resulting scans using CT Pro 3D and saved the reconstructions as volume files.

#### **4.2.2 Reconstructing three-dimensional models**

We processed the volume files using Mimics image processing software (Materialize NV) to visualize the CT slices for segmentation. We then proceeded through the CT slices in intervals from the proximal to distal end of each humerus to capture internal structures using the segmenting tools *Lasso*, *LiveWire*, *Mask*, and *Interpolate*. For each CT slice, one of us (DMG) selected all trabecular bone to add to the *Mask*, which differentiated the trabecular bone from the matrix. A completely segmented slice displays black air space, gray matrix, and highlighted bone. After each slice was segmented, we scrolled distally and repeated the process on a subsequent slice. In regions where the struts had a dense distribution or complex internal structure, we segmented slice-wise to minimize interpolation. In regions where the trabecular bone was sparse or simple and elongate, we segmented approximately every 10 slices. Once a bone was completely segmented, we used the *Interpolate* tool, which connects consecutive segmented structures to produce a 3D model that accurately reconstructs the true anatomy.

#### **4.2.3 Analyzing 3D models and measuring volumetric airspace proportion**

The resulting 3D model allows us to explore the image and categorize the internal bone structure according to structures present (struts, ridges, or combination). Where relevant, we oriented these models vertically along their long axes and used the *Angles* tool to measure the angles of individual struts or ridges in relation to the long axis of the wing bone and in relation to intersecting trabecular bone.

The resulting models can also be analyzed for airspace proportion in Mimics. Before an accurate interpretation of ASP is made using these 3D models we must first ensure that the

model is air-tight and the cortical bone is complete. For the model to be air-tight, the pixels representing the airspace within a bone cannot be in contact with the ambient air. This is unlikely to occur with fossils that are infilled with matrix but is highly likely to occur in modern bones at the sight of pneumatic foramen. To ensure a model is airtight, we used the *Gap Closing* tool to create a virtual plug over all pneumatic foramina with a *gap closing distance* set to 0.01.

The most appropriate fossils for the measurement of vASP will be those that preserve cortical bone entirely and without deformation. This type of preservation is rare, especially for the extreme hollow appendicular bones of pterosaurs. Elements that partially preserve cortical bone can be virtually repaired by interpolation. For the purpose of this study, we were also interested in specimens that preserved delicate internal structure but preserved no cortical bone (humerii of *Inabtanin alarabia*). In order to approximate the presence of cortical bone on an element that was encased in matrix only, we use the *Wrap* tool, which creates a customizable sheath over the model. We designed the virtual cortical bone to have a thickness of 2 mm, which is both the average cortical thickness of other elements in this individual, as well as for the humerus of *Arambourgiania* used in this analysis.

We then use the *Measure* to acquire the total volume (in mm<sup>3</sup>) enclosed in the model. The next step is to create an inversion of the model, thus capturing all internal air space in a new mask. We record this volume (mm<sup>3</sup>) and divide by the total volume to calculate the air space proportion.

$$vASP = \frac{\text{volume of internal airspace}}{\text{total volume of a bone}}$$

## 4.3 Results and Discussion

### 4.3.1 *Inferring air space proportion*

The airspace proportion (ASP) of a bone is defined as the volume of air contained in the total volume of the bone; this inverse of this measurement is the volume of bone tissue. Both values are informative about the structure of a bone and are used to measure the degree of pneumaticity in an element. The ASP of pterosaur wing bones ranges from 70-90% which is extremely high compared to the ASP of extant bird bones which fall between 30-70% (Martin and Palmer, 2014b: Table 2).

The precursor to our method also uses micro-CT scans but analyses these two-dimensionally using *imageJ* to manually highlight the bone tissue visible in a single image from the resulting scan (Martin and Palmer, 2014a, 2014b). This produces a representative sample of highlighted sections across the length of the bone. Samples can be taken more or less frequently at the discretion of the researcher. This is similar to the segmenting process in *Mimics* or a similar program, but *Mimics* has the capability to interpolate 3D shape from a series of highlighted slices. The 2D method produces ASP values based on an average of two-dimensional data compared to the new method that produces volumes. For this reason, we refer to these results as volumetric airspace proportions (vASPs). The 2D method uses free software and provides slices across a bone that can be informative about variation in ASP within a skeletal element. The 3D method requires expensive software licenses with the benefit of automating some aspects of the process and produces visually compelling results that can be 3D printed, shared on online repositories, and used for further research like investigating internal structure.

Both methods share sources of error that are inherent with micro-CT data. Fossils infilled with matrix require long scans with precise settings that allow for the machine to process the

density difference between the bone and the matrix. This is particularly difficult for fossils that are preserved in carbonate sediments with a very similar density and composition to bone. This is often the case for pterosaur fossils. With both methods, we find that highly irregular pneumatic structure is slow to process, often needing to go slice-wise with minimal interpolation. This introduces room for human error in interpretation of grayscale values that differentiate bone from surrounding material.

The vASP method can be accomplished with the use of any 3D imaging software, including *Mimics*, *Amira/Avizo*, and *VG Studios*. We performed the process on the same scan with multiple users across multiple platforms and found the variation in the resulting vASP values to be within 1%. Additional benefits of the vASP method include the use of certain tools that can correct for damage to the specimen. The loss of cortical bone can be addressed with the “wrap” tool, which can be customized to assign cortical thickness to missing areas. We applied this to the humeral material of *Inabtanin* to recreate a 2 mm thick cortical structure that was consistent with the other bones in the individual.

A sample of the results of vASP measurements are in Figure 1 and the full table is available in Appendix C. The pterosaur humeri had the largest vASP values, averaging 79%. This average vASP of hummingbird bones sampled including cranial and postcranial bones was 45% compared to the feather-bearing wing bones (humerus, ulna) that had an average vASP of 58%. The sauropod vertebra had a vASP of 47%. These results are consistent with those of the studies using two-dimensional methods (Martin and Palmer 2014a, 2014b). The most notable feature of these and past results is that pterosaurs of extremely long wingspan have the highest ASP and vASP ratios. With the secondary loss of flight, we would expect to see a decrease in airspace proportion as bones become denser to support the weight of the body on the ground.

### 4.3.2 *Inferring flight performance*

The wings of *Inabtanin* outstretch those of the largest wandering albatrosses by at least a meter (5 m versus 3.5 m). Many of the pterosaurs of the latest Cretaceous represent the upper wingspan limits of vertebrate flight capacity. This has led to the suggestion that organisms of such extreme wingspans cannot maintain powered flight, based on scaling calculations that the upper limit of body mass for a dynamic soaring individual is only 41 kg (Sato et al., 2009). Some body mass estimates indicate that giant pterosaurs like *Quetzalcoatlus northropi* weighed almost 550 kg (Henderson, 2010), although consensus around body mass estimates for giant azhdarchids has settled at an upper limit of 200–250 kg (Witton, 2008; Martin and Palmer, 2014b).

The opposing view that pterosaurs were capable of powered flight at high body masses is supported across many studies citing retention of flight anatomy in the form of highly pneumatic bones, thin cortical bone, well-developed deltopectoral crests, no reduction of wing bones, as well as modeling flight capacity based on body mass estimates and wing aspect ratio (Alexander, 1998; Buffetaut et al., 2002; Chatterjee and Templin, 2004; Habib, 2008; Witton, 2008; Witton and Naish, 2008; Claessens et al., 2009; Witton and Habib, 2010; Geist et al., 2014; Middleton and English, 2015; Naish et al., 2021). Additionally, whereas some studies assert the morphology and depositional environments of giant azhdarchids indicate terrestrial locomotion and foraging, they do not claim that these adaptations preclude flight (Witton, 2007; Witton and Naish, 2008; Naish and Witton, 2017). The internal trabecular bone structure preserved in the two specimens described here corroborates the hypothesis that flight was possible in the largest pterosaurs.

Here, we rely on avian bone structure as an extant analog because they possess pneumatic bones and share a common archosaurian ancestor, allowing for direct osteological comparison.



The spectrum for flight behavior in living birds ranges from continuous flapping to extended periods of soaring (Pennycuick, 1982). The internal structure of wing bones from modern birds has been explored in model-based materials science research, establishing three categories for the internal trabecular structures that occur in pneumatized wing bones: struts, ridges, or no structures (Novitskaya et al., 2017; Sullivan et al., 2017). Formation of internal support structures is the result of adaptive reformation of bone in response to the stresses of flight, Birds that exhibit a flapping flight behavior have wing bones that contain networks of perpendicular struts in the shaft supporting the cortical bone. The structure and arrangement of these struts have been shown to resist the forces of compression more than those of torsion (Novitskaya et al., 2017). Most birds are categorized with flapping flight behavior, and so this structural pattern is found across a wide range of wingspans and wing morphologies. Birds that exhibit a soaring flight behavior develop helical ridges in their humeri. Birds with soaring flight behavior are generally large and have long wingspans and high wing aerodynamic aspect ratios. Examples include pelagic sea birds and vultures, which rely on thermal currents to support flight by minimizing flapping and the associated mechanical stress. Soaring flight behavior confers greater torsional forces on wing bones than does flapping flight. In stress tests of idealized models, these helical ridges have been shown to withstand torsion (Novitskaya et al., 2017). Additionally, a case study examined the wing bone structure of an individual of a volant species that was not permitted to fly (Kiang, 2013). This individual developed densely packed spongy trabecular bone instead of thin cortical bone with supportive trabeculae. Therefore, we can conclude that the presence of characteristic internal trabecular bone structure is indicative of flight behavior, and that the presence of either struts or ridges suggests that individual was volant.

#### 4.3.2.1 *Inabtanin*

Three-dimensional models of the trabecular bone in the humeri of *Inabtanin* reveal a network of hollow struts with circular cross sections. The struts are thicker and more densely packed at the epiphyses compared to the thinner, more sparsely distributed struts in the diaphysis (Fig. 4.2). The diaphyseal struts range in diameter from 1–3 mm and intersect each other at an average angle of 83 degrees. Epiphyseal struts range in diameter from 2–4 mm and intersect each other at an average angle of 87 degrees (Table 3). For the humerus of *Inabtanin* the average angle of strut intersection is nearly a right angle. For irregular lattices, it is the average angle of the struts that signifies optimal resistance to compressional forces (Bakhvalov et al., 2009). The arrangement and structure of the struts in the humeri of *Inabtanin* match those found in the wing bones of modern flapping birds (Fig. 4.2). The presence of these adaptive structures indicates that this individual experienced the compressional forces associated with continuous flapping flight and so it is most likely that *Inabtanin* flew mostly by flapping and was not soaring specialized.

#### 4.3.2.2 *Arambourgiania*

The humeral shaft of *Arambourgiania* does not possess struts. Instead, a three-dimensional model of the trabecular bone in the humeral shaft of *Arambourgiania* reveals a series of thin ridges lining the cortical bone of the diaphysis. These diaphyseal ridges line the shaft in two opposing helical sets forming a crosshatch pattern that can be seen both on the surface of the bone and within the three-dimensional model (Fig. 4.2). A sample of these ridges measured in relation to the long axis of the shaft gives an average angle of 45 degrees. One set of helical ridges occurs with greater frequency; these ridges are each 1 mm across and have a left-

handed or clockwise chirality. The clockwise ridges are oriented at an average of 43 degrees from the long axis of the humerus. Another, less frequent set of helical ridges are thicker (2 mm) and have a right-handed or counterclockwise chirality. The counterclockwise ridges are angled at an average of 54 degrees from the long axis of the humerus. The clockwise and counterclockwise ridges intersect each other at an average angle of 92 degrees (Table 3).

The presence of diapophyseal ridges in the humerus of *Arambourgiania* suggests that this individual experienced the torsional forces associated with soaring flight. These ridges are similar to those found in the humeri of vultures (Fig. 4.2). The optimal ridge angle for torsional resistance is 45 degrees if forces are acting equally in both planes. However, we would expect variation in ridge angles if there were asymmetry in the torsional forces associated the upstroke and downstroke. This likely explains the different average ridge angle between the primary and secondary diapophyseal ridges in *Arambourgiania*, this suggests that this individual was not solely gliding (non-powered flight where gravity is the energy source) but was soaring (flight sustained partially by external sources of lift, but which is still powered flight that requires launch and maintenance flapping). This evidence combined with the stratigraphic evidence that *Arambourgiania* existed in a marine environment highlights an interesting dichotomy for giant pterosaurs, which are otherwise known from terrestrial deposits. Our findings suggest that some giant azhdarchids were volant, perhaps supported by marine thermal soaring given the geological context of their fossils.

The correlations presented here are supported by comparing the anatomy of individual birds and pterosaurs to materials science analyses (Kiang, 2013; Novitskaya et al., 2017; Sullivan et al., 2017). We seek to establish a more thorough understanding of the link between internal structure and flight behavior in modern and extinct Aves as well as pterosaur fossils. This

research supports the pursuit of questions about the links of body mass, and wing morphology (wingspan, aspect ratio, wing loading) with flight capacity and flight behavior.

#### **4.4 Conclusion**

With this, we are able to provide evidence for sustained powered flight in giant pterosaurs and to draw conclusions about their flight behavior after launch. Additionally, this study provides framework for further investigation of the correlation between internal bone structure and flight capacity and behavior, which has been observed on a case study basis but remains to be established as a biological principle associated with the mechanics of vertebrate flight. Variation in structure and ASP in bird bones has been known for some time but never quantified or studied on a larger scale, we hope that further research can utilize these methods to explore questions of individual variation, phylogenetic variation, and correlations with flight behavior and flight capacity.

## 4.5 Figures

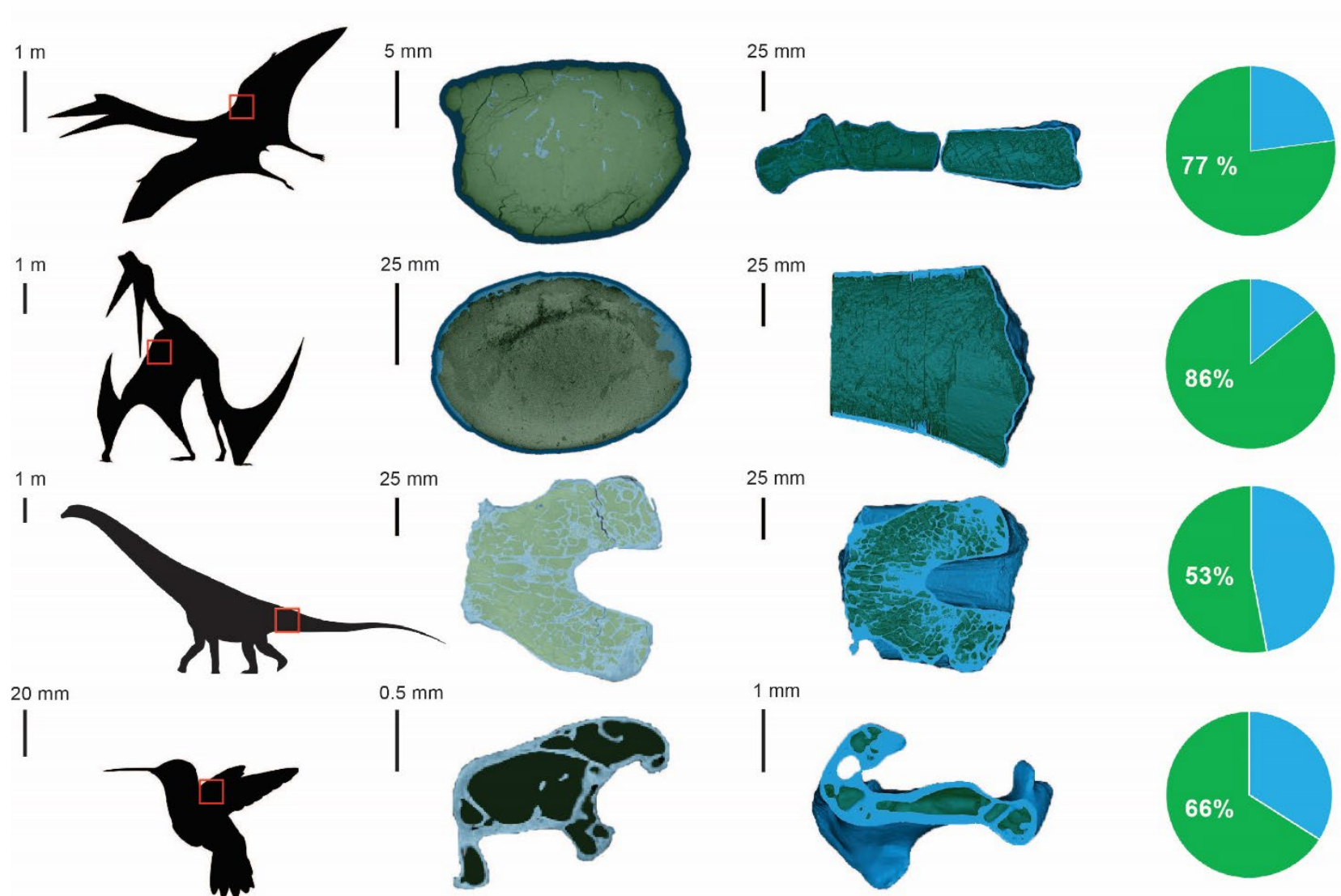


Figure 4.1 Summary of workflow to produce and analyze 3D models of pneumatic bone structure along with examples of results. Column 1 represents the following organisms, represented by silhouettes with a red box indicating the location of the bone analyzed: row 1, the humeri of *Inabtanin*; row 2, the humeral shaft of *Arambourgiania*; row 3, a caudal vertebra from a titanosaur; row 4, a humerus of a hummingbird. Column 2 contains a sample of micro-CT slices from each bone with airspace highlighted in green and bone tissue highlighted in blue. Column 3 shows a complete 3D model sliced medially to show highlighted air and bone tissue. Column 4 shows the calculated vASPs in a pie charts.

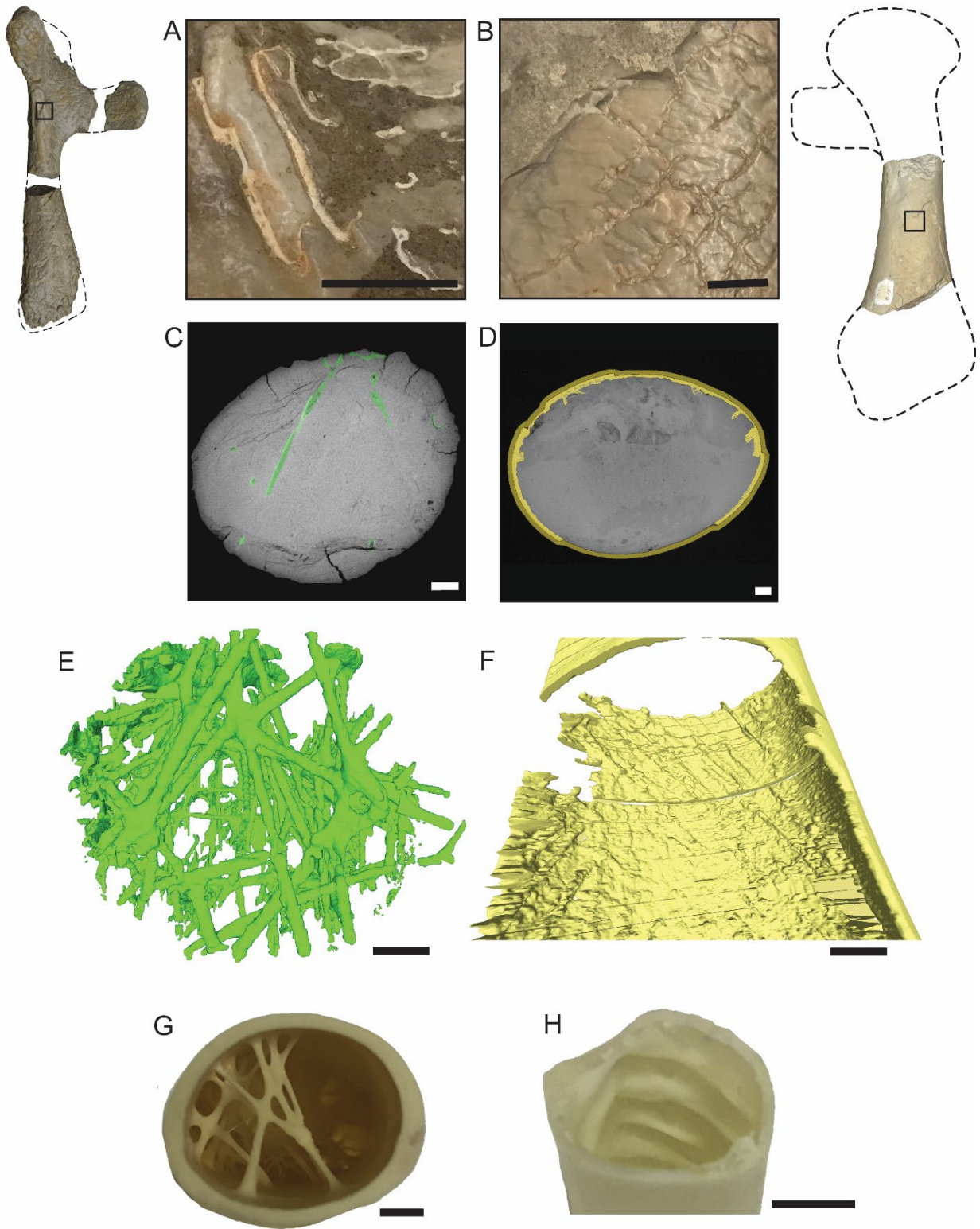


Figure 4.2 Comparison of the internal structure of pterosaur and bird wing bones. **A**, photograph of the bone structure visible on the surface of the left humerus of *Inabtanin alarabia*. **B**, photograph of the bone structure visible on the exposed surface of the humerus of *Arambourgiania philadelphiae*. **C**, micro-CT slice from the mid-shaft of the humerus of *Inabtanin alarabia*. **D**, micro-CT slice from the mid-shaft of the humerus of *Arambourgiania philadelphiae*. **E**, 3D reconstruction of the humerus of *Inabtanin alarabia* displaying struts. **F**, 3D reconstruction of the humerus of *Arambourgiania philadelphiae* displaying helical ridges. **G**, photograph of the distal cross-sectional anatomy of the humerus of a flapping bird. The humeral midshaft contains struts hypothesized to resist bending forces during flight (modified from Sullivan et al., 2017). **H**, photograph of the cross-sectional anatomy of the ulna of a soaring bird. The humeral midshaft contains helical ridges hypothesized to resist torsional forces during soaring (modified from Sullivan et al., 2017). Scale bars equal 5 mm.



## 5 Conclusion

Pterosaur researchers often describe this group as “enigmatic,” meaning difficult to interpret or mysterious. This is reflected in our ever-changing interpretations of pterosaur relationships and physiology across the centuries since their discovery in the late 1700s. The group is often overlooked because of preservation biases in the fossil record, fragmentary information for morphological phylogenetic analysis, and the lack of extant analogs for biomechanical interpretation. Despite these challenges, there are more paleontologists actively studying pterosaurs now than ever before. The chapters presented in this dissertation provide a foundation to build further research on pterosaurs of the Late Cretaceous.

Here I explore the evolutionary relationships and flight behavior of large pterosaurs through the lens of new pterosaur remains from the latest Cretaceous of Jordan. I begin with Chapter 1 as an overview of the history of pterosaur research and broad taxonomic divisions of pterosaur groups. I review the differences between more basal rhamphorhynchoids and more derived pterodactyloids that include the group Azhdarchiformes, which is the focus of this dissertation. I also summarize each chapter and the inspirations that lead to the development of each project.

Chapter 2 provides a detailed anatomical description of new pterosaur remains from the Late Cretaceous of Afro-Arabia. Here we described a new genus and species of azhdarchoid pterosaur named *Inabtanin alarabia* and additional material of the contemporaneous *Arambourgiania philadelphiae*. These remains are remarkable for their 3D preservation

providing us with valuable morphological information and rarely seen internal bone structure. The quality of these remains warrants continued field work in Jordan and the Arabia peninsula since these localities are productive locations for marine organisms and pterosaur fossils with 3D preservation. This chapter also includes descriptions of the geological settings, stratigraphy, and paleoenvironment relevant to these organisms. We named *Inabtanin alarabia* for the locality and is described this fairly complete individual as a new genus and species with a 5 m wingspan, unique lower jaw anatomy, short cervical vertebrae, and characteristic azhdarchid-type humeral structure. We identified new material of *Arambourgiania philadelphiae* based on comparisons of size and shape with other giant Azhdarchiformes and spatiotemporal context. The results of this field work and description also support the notion that regions where single species of azhdarchiform pterosaurs have been uncovered are good candidates for discovering additional species coexisting in the same environment.

As part of this descriptive study, we have worked with the University of Michigan Museum of Paleontology to create 3D photogrammetric models of all the material, which will be returned to Jordan after publication. These models will be publicly available via the University of Michigan Online Repository of Fossils. This tool is free to access for the purpose of education and research thus allowing these specimens to be available to students and professionals worldwide. This is particularly important for the future of paleontological research as international travel is costly and inaccessible to many of our colleagues. The description of these specimens inspired the work in the following chapters and will provide accessible data to paleontologists studying pterosaurs.

In Chapter 3 I review the history of pterosaur research to provide context for the unique filtration method developed here. The literature on pterosaurs is limited in comparison to similar

groups and my review of the published data prompted an analysis of all existing morphological characters. This consisted of collecting, organizing, filtering, and formatting existing characters to ensure that they function as independent variables. This is an iterative process that should take place before the addition of new characters and highlights the importance of careful consideration in recycling character matrices.

This character list guided in-person collections work in the US and internationally as I studied and rescored most of the putative azhdarchid pterosaurs from the latest Cretaceous. The results of a parsimony analysis in TNT found new topology including a monophyletic group that contained all putative azhdarchids. This node was previously defined as Azhdarchomorpha, so I have proposed that we discontinue using the term Azhdarchidae to refer to the assemblage of large, toothless, Late Cretaceous pterosaurs. Within the group Azhdarchomorpha, I found an independent acquisition of extremely long wingspans (7–10 m); most members have a ca. 5 m wingspan. Additionally, I found that there is a potential pattern of increasing elongation of cervical vertebrae, and a subsequent loss of the trait among the azhdarchomorphs.

Future work on Late Cretaceous pterosaur relationships should include careful consideration of cervical vertebrae and forelimb bones, especially the humerus. In a broader context, this filtration process can be used to systematically evaluate matrices of any group that primarily depends on morphological data.

In Chapter 4, I explore the connection between the structure of pneumatic bones and flight behavior in pterosaurs and modern birds. Pneumaticity is a valuable trait for both of these groups of flying organisms since it improves the strength to weight ratio of a bone and allows for the development of internal support structures. I used micro-CT scans and 3D imaging software

to create virtual models of the bones of pterosaurs, dinosaurs, and birds. I found that pterosaurs and birds have similar internal structures in their humeri, and that larger individuals had the highest airspace proportion. Previous work on this topic suggests that the presence of internal trabecular bone structures are an adaptive remodeling of bone in response to the stresses of flight. Modern birds are known to have a correlation between flight behavior and these structures, where struts correlate with continuous flapping flight, ridges correlate with the torsional forces of soaring flight, and flightless birds have thick cortical bone and do not produce structures. We used this information to infer that the pterosaurs studied in this dissertation do not show any osteological correlates with secondary loss of flight, but rather *Inabtanin* (5 m wingspan) likely flew by continuous flapping and *Arambourgiania* (10 m wingspan) likely exhibited soaring behavior.

## Appendices

### Appendix A

TNT code used to obtain the results of the phylogenetic analysis in Chapter 3.

```
nstates cont ;
mxram 300;
xread
303 176
&[continuous]
'Euparkeria_capensis'          0.0526 0.5543 1.044 ? 6.87 0.1084 0.4076 3.65
1.683 0.2561 0.679 0.0563 0.053 ? 1.018 1.94 0.1542 0.9572 1.67 1.461 2.0 0.942 ?
2.338 0.183 0.767 ? ? 0.871 0.892 ? 0.243 1.922 ? ? ? ? 1.476 0.0 2.483 0.857 1.0
0.4014 1.434 0.2291 0.6328 0.476
'Ornithosuchus_longidens'      0.0586 0.5628 0.913 ? 3.92 0.4762 ? 2.67 1.633
0.3331 ? 0.1885 ? ? 1.188 ? 0.1205 ? 2.444 1.0 3.0 1.0 ? 1.806 0.262 0.704 ? ? 1.171
0.842 ? 0.132 1.64 ? ? ? ? 1.526 ? ? 0.839 1.0 0.4795 2.787 0.4288 0.605 0.357
'Herrerasaurus_ischigualastensis' 0.0302 0.6 0.962 ? 8.6 0.5 0.4229 3.1 1.892
0.2333 2.315 0.0799 ? ? 0.955 ? 0.2038 0.8308 1.947 0.961 2.0 1.133 ? ? 0.453 0.613 ?
? 1.0 0.897 ? 0.189 2.329 0.057 ? ? ? 1.971 ? ? 0.913 1.005 0.5238 2.265 0.2226
0.7135 ?
'Scleromochlus_taylori'       0.1607 0.4472 1.052 ? 12.4 0.098 0.4016 ?
2.535 0.2124 ? 0.0835 ? ? 1.826 1.813 0.2348 0.678 1.696 1.913 4.0 1.227 ? 2.75 1.007
0.323 ? ? 0.788 0.923 ? 0.128 3.28 0.067 ? ? ? 1.641 ? ? 1.078 1.0 0.4783 2.825
0.2718 0.4693 0.262
'Eudimorphodon_ranzii'        0.264 0.6667 0.863 ? 13.81 0.079 0.6897 3.45
0.884 0.1122 4.324 0.1897 ? ? 1.492 ? ? ? 1.168 1.956 4.0 ? ? 1.374 ? ? 3.114 ? 0.743
1.448 0.3081 0.618 2.237 ? ? ? ? 0.96 2.091 ? ? ? ? ? ? ?
'Eudimorphodon_rosenfeldi'    0.264 0.5525 0.792 ? 10.98 0.2139 0.7281 2.49 1.562
0.1432 5.71 0.2248 ? ? 1.833 ? 0.1164 0.3964 1.194 2.02 ? 6.073 ? 1.243 0.64 ? ? ?
0.726 1.339 0.2785 0.455 2.053 1.466 0.937 0.991 0.864 0.787 ? ? 1.428 0.935 0.3875
5.184 0.2728 0.6995 0.632
'Eudimorphodon_cromptonellus' ? ? ? ? ? ? ? ? ? ? ? ? ? ? ? ? ? ? ? ? ? ?
2.0 ? ? ? ? 0.851 1.107 ? 0.463 2.088 0.992 1.139 1.139 ? 1.085 0.925 2.269 1.041
0.732 0.5537 ? ? ? ?
'Peteinosaurus_zambellii'     ? ? ? ? ? ? ? ? ? ? ? ? ? ? ? ? ? ? ? ? ? ?
0.747 ? ? ? ? ? ? ? 2.252 ? 0.868 ? 0.815 ? ? ? ? 0.89 0.3273 ? ? ? ?
'Caviramus_schesaplanensis'  ? ? ? ? 6.92 0.1263 ? ? ? ? ? ? ? ? ? ? ? ?
? ? ? ? ? ? ? ? ? ? ? ? ? ? ? ? ? ? ? ? ? ?
'Raeticodactylus_filisurensis' 0.2692 0.5381 0.884 ? 8.84 0.1976 0.5594 3.06
1.727 0.2 3.111 0.1474 ? ? 1.106 ? 0.1499 ? 1.429 2.181 ? ? ? ? ? ? ? 1.293
0.1971 ? ? 1.378 0.965 1.035 ? 0.683 ? ? 1.482 0.522 0.3855 ? ? ? ?
'Austriadactylus_cristatus'    0.1659 0.5653 0.808 ? 13.27 0.1242 0.617 3.88
1.423 0.1626 3.042 0.2122 ? ? 1.105 2.346 0.0889 0.5657 1.241 ? ? 3.5 ? 1.415 ? ? ? ?
0.79 1.361 ? 0.436 ? 1.212 1.025 1.051 0.868 0.777 ? ? 1.272 ? 0.223 ? ? ? ?
'Preondactylus_buffarinii'     0.1179 0.6525 0.875 ? 17.69 0.075 0.5691 3.41 1.484
0.2129 5.235 0.2812 ? ? 1.094 ? ? ? 1.377 1.554 4.0 7.188 ? ? 0.855 ? 4.559 ? 0.766
```

1.358 0.1786 0.445 2.371 1.103 1.143 1.159 0.779 1.038 ? ? 1.359 0.674 0.369 4.696  
0.4051 0.4467 ?  
'Dimorphodon\_macronyx' 0.1965 0.6049 0.895 0.0858 11.87 0.1255  
0.6596 3.56 1.024 0.2117 1.938 0.3906 ? ? 0.716 ? ? ? 1.279 1.889 4.0 2.029 ? 1.387  
0.95 1.969 1.671 ? 0.696 1.291 0.18 0.44 2.555 1.135 1.088 1.248 1.0 0.943 0.754  
2.477 1.449 0.521 0.2902 3.934 0.3631 0.6658 0.526  
'Dimorphodon\_koi' ? ? ? ? ? ? ? ? ? ? ? ? ? ? ? ? ? ? 0.225 2.839 ? ? ?  
?  
'Dimorphodon\_hanseni' ? ? ? 0.1653 14.83 0.2561 0.7363 ? ? ? ? ? ?  
?  
'Dimorphodon\_jenkinsi' ?  
?  
'Dimorphodon\_weintraubi' ? ? ? ? ? ? ? ? ? ? ? ? ? ? ? ? ? ? 0.1861 1.779 ? ? ?  
? 1.034 ? ? ? ? 0.87 1.203 0.2393 0.51 2.171 1.212 0.938 0.938 0.778 ? ? ? ? ? ? 3.0  
0.2586 0.5667 0.4  
'Parapsicephalus\_purdoni' 0.2716 0.4393 ? ? ? ? ? 3.72 1.819 0.2288 2.958  
0.2344 ? ? 0.963 2.039 0.0811 0.7652 ?  
? ? ? ? ? ?  
'Campylognathoides\_liasicus' 0.2336 0.6156 0.846 ? 12.37 0.1202 0.6794  
3.31 1.685 0.1259 2.863 0.2731 ? ? 1.443 1.144 0.1137 0.5895 1.578 2.333 5.0 2.612 ?  
1.203 2.319 1.586 0.775 ? 0.669 1.241 0.2943 0.461 2.063 1.839 1.068 0.94 0.742 0.763  
2.008 2.391 1.239 0.632 0.4267 3.594 0.264 0.6222 0.605  
'Campylognathoides\_zitteli' 0.3134 0.599 0.937 ? 8.38 0.164 0.6424 2.63  
1.745 0.145 4.087 0.212 ? ? 1.343 ? ? ? 1.5 1.923 5.0 1.92 ? 1.595 2.439 1.592 ? ?  
0.766 1.06 0.2427 0.418 2.215 2.925 1.046 0.818 0.606 ? 1.834 2.352 1.314 0.955  
0.4179 2.966 0.232 0.6033 0.622  
'Sericipterus\_wucaiwanensis' 0.301 ? ? ? ? ? ? 4.08 ? ? ? ? ? ? ? ? 0.1279  
? 1.866 2.019 ? ? ? 1.013 ? ? ? ? 0.94 ? ? ? ? ? 1.271 0.922 ? 0.924 ? ? ? ? ? ? ? ? ?  
?  
'Angustinaripterus\_longicephalus' 0.3114 0.5174 0.871 ? 15.78 0.1425 ? 4.02  
2.646 0.3159 9.444 0.2114 ? ? 1.143 ?  
? ? ? ? ? ? ?  
'Harpactognathus\_gentryii' ? ? ? ? ? ? ? 3.67 ? ? ? ? ? ? ? ? ? ? ? ? ? ? ? ? ? ?  
?  
'Cacibupteryx\_caribensis' ? ? ? ? ? ? ? 3.15 2.167 ? 2.833 ? ? ? 0.867 1.624 ?  
0.7241 ?  
'Rhamphorhynchus\_muensteri' 0.3463 0.579 0.763 ? 13.91 0.4102 0.6816 3.64  
2.099 0.0933 4.276 0.1375 ? ? 1.311 1.31 0.0935 0.2298 1.498 1.987 4.0 2.144 ? 1.139  
2.193 2.365 1.323 0.753 0.762 1.633 0.2033 0.56 2.198 2.531 0.942 0.857 0.867 0.859  
1.657 1.955 1.451 0.501 0.4781 4.73 0.1875 0.5448 0.085  
'Qinglongopterus\_guoi' 0.3333 0.64 1.002 ? 11.29 0.3807 0.6387 ? ?  
0.2376 ? 0.2376 ? ? ? ? ? 0.6455 1.215 1.685 4.0 2.454 ? 0.936 ? ? 1.798 ? 0.941 1.59  
0.1413 0.511 2.328 1.781 1.009 0.937 0.584 0.685 ? ? 1.254 0.654 0.4641 4.57 0.3521  
0.4 0.24  
'Nesodactylus\_hesperius' ? ? ? ? ? ? ? ? ? ? ? ? ? ? ? ? ? 1.287 2.143 4.0  
1.123 ? 0.941 ? ? 1.379 0.717 0.653 1.72 ? 0.574 2.604 2.946 ? ? ? ? ? ? ? ? ? ? ? ?  
?  
'Orientognathus\_chaoyangensis' ? ? ? ? 11.73 0.2671 0.4432 2.14 ? ? ? ? ? ?  
? ? ? ? 1.342 2.0 4.0 1.657 ? 1.101 1.976 3.453 ? ? 0.618 0.843 0.2442 0.38 ? 1.11  
1.38 ? ? 0.885 ? ? 1.012 0.57 0.5065 2.213 0.2224 0.4513 0.453  
'Dorygnathus\_banthensis' 0.3733 0.6338 0.906 ? 12.0 0.3144 0.6066 3.59 1.428  
0.1895 5.358 0.2783 ? ? 1.055 2.482 0.0857 0.503 1.515 2.11 4.0 2.167 ? 1.333 2.039  
2.161 1.41 ? 0.876 1.62 0.1721 0.506 2.068 1.231 1.205 1.204 0.992 0.837 1.722 2.368  
1.359 0.581 0.3767 2.475 0.4096 0.3956 0.286

'Klobiodon\_rochei' ? ? ? 0.1906 11.62 0.244 0.7155 ? ? ? ? ? ? ? ? ? ?  
 ?  
 'Fenghuangopterus\_lii' ? 0.7214 0.996 ? 12.87 0.1334 ? 2.57 ? 0.1612  
 ? ? ? ? ? 3.962 ? ? 1.375 1.951 3.0 2.669 ? 0.8 ? 2.61 1.51 ? 1.0 1.349 0.1968 0.556  
 2.027 1.984 0.6 0.446 0.396 0.905 ? ? 1.754 0.435 0.2991 ? ? ? ?  
 'Scaphognathus\_crassirostris' 0.2649 0.5469 0.783 ? 9.07 0.2029 0.5444 2.78  
 1.416 0.1765 2.152 0.1713 ? ? 1.103 ? 0.1381 0.3554 1.208 2.296 4.0 1.324 ? 1.275  
 2.27 1.696 1.52 ? 0.843 1.7 0.1685 0.499 2.355 1.2 1.089 1.05 0.98 0.952 0.58 2.365  
 1.148 0.364 0.3402 1.925 0.2429 0.4521 0.24  
 'Sordes\_pilosus' 0.2 0.5034 0.736 ? 15.62 0.2935 0.4726 3.51 1.712  
 0.215 2.753 0.1931 ? ? 1.176 1.36 0.1601 0.6188 1.011 2.2 5.0 1.933 ? 1.109 2.589  
 1.559 3.32 ? 0.867 1.639 0.1855 0.403 2.338 1.068 1.081 1.038 0.755 0.79 0.484 ?  
 1.411 0.39 0.3293 1.574 0.255 0.3269 0.359  
 'Darwinopterus\_modularis' 0.3455 0.4846 0.834 ? 24.88 0.2167 0.5475 4.65 ? ? ?  
 ? 4.284 0.4432 1.169 ? 0.0852 ? 2.02 1.639 5.0 3.747 ? 1.038 2.462 2.364 1.118 ?  
 0.918 1.465 0.4063 0.601 2.627 1.181 1.146 1.229 1.104 0.909 1.125 2.302 1.35 ? 0.352  
 1.841 0.336 0.2808 1.217  
 'Darwinopterus\_zhengi' ? ? ? ? ? ? ? ? ? ? ? ? ? ? ? ? ? ? 3.55  
 2.467 6.0 1.495 ? 1.439 3.236 ? ? ? 0.83 1.227 0.5161 0.656 ? 1.098 1.054 0.999 0.848  
 0.83 ? ? 1.744 0.448 0.3185 1.905 ? ? ?  
 'Darwinopterus\_linglongtaensis' 0.413 0.4833 0.842 ? 20.72 0.2197 ? 3.78 ? ?  
 ? ? 2.927 0.3275 0.976 ? ? ? 1.61 1.81 5.0 1.921 ? 1.215 2.846 2.963 0.769 ? 0.834  
 1.484 0.4849 0.574 2.027 1.497 1.135 1.18 1.184 0.99 ? ? 1.25 0.46 0.322 1.345 0.3493  
 0.2304 0.368  
 'Darwinopterus\_robustodens' 0.3486 0.3441 0.863 ? 23.18 0.2661 0.396 5.0  
 ? ? ? ? 3.8 0.4343 0.841 ? 0.0662 ? 2.839 1.546 ? 2.514 ? 1.129 2.873 0.947 1.07 ?  
 0.571 1.6 0.4375 0.6 2.167 1.3 1.154 1.154 1.031 0.86 ? ? 1.395 ? 0.35 1.0 0.3333  
 0.1429 0.143  
 'Kunpengopterus\_sinensis' 0.3789 ? 0.842 ? 11.69 0.2444 ? 2.93 ? ? ? ? 4.025  
 0.6632 1.1 ? ? ? 2.598 1.236 ? 1.792 ? 1.21 ? ? ? ? 0.823 1.635 0.4358 0.635 2.416  
 1.128 1.07 1.092 0.9 1.11 ? ? 1.356 0.355 0.382 1.035 0.2718 0.2393 0.22  
 'Archaeoistiodactylus\_linglongtaensis' ? ? ? ? ? ? 4.2 ? ? ? ? 3.577 ? ? ? ? ?  
 2.493 ? ? ? ? 2.636 2.597 ? ? 1.0 1.489 0.51 0.596 ? ? ? ? ? 0.936 ? ? 1.409 0.251  
 0.3335 ? ? ? ?  
 'Cuspicephalus\_scarfi' 0.3659 0.6204 ? ? ? ? ? 5.93 ? ? ? ? 5.167  
 0.4755 0.906 ? 0.045 ?  
 'Wukongopterus\_lii' 0.2722 0.4952 0.86 ? 13.02 0.1938 ? 4.15 ? ? ? ? ?  
 0.5072 ? ? ? ? 2.039 ? 5.0 ? ? 1.324 2.655 ? ? ? 1.602 0.1176 0.591 2.342 1.179  
 1.243 1.287 1.127 0.889 0.648 2.283 1.533 0.356 0.3367 1.79 0.4357 0.2307 0.199  
 'Pterorhynchus\_wellnhoferi' 0.3215 0.5125 0.922 ? 14.2 0.1834 0.4878 2.95  
 ? ? ? ? 5.471 0.5318 1.204 ? ? 0.3315 1.544 1.505 5.0 2.893 ? ? 2.384 2.206 ? ? 0.722  
 1.75 0.2453 0.548 ? 1.106 1.252 1.148 0.8 0.808 ? ? 1.167 0.347 ? ? ? ? ?  
 'Changchengopterus\_pani' ? ? ? ? ? ? ? ? ? ? ? ? ? ? ? ? 1.167 1.333 3.0  
 1.133 ? 1.222 ? ? ? ? 1.0 1.421 0.462 0.602 ? 1.158 1.067 1.0 ? 0.811 ? ? 1.19 0.471  
 0.4091 ? ? ? ?  
 'Batrachognathus\_volans' 0.0208 0.6351 0.977 ? 11.53 0.0644 ? ? ? ? ? ? 0.859  
 0.1816 1.398 2.923 0.1406 ? 1.17 1.737 ? ? ? 1.033 ? ? ? ? 0.823 1.609 ? 0.326 2.594  
 ? ? ? ? 0.628 ? ? 1.616 0.292 0.3833 1.545 0.1477 0.5742 0.62  
 'Jeholopterus\_ningchengensis' 0.0877 0.6883 1.065 ? 13.01 0.0926 0.6377  
 2.76 ? ? ? ? 0.92 0.2596 1.095 2.399 ? ? 1.126 1.507 5.0 0.403 ? 1.532 3.055 ? 1.416  
 ? 0.819 1.275 0.1529 0.326 2.562 1.48 0.891 0.633 0.178 0.702 0.078 2.238 1.149 0.457  
 0.4517 1.494 0.159 0.6528 0.494  
 'Luopterus\_mutoudengensis' 0.1272 ? 0.801 ? 12.87 0.0989 ? ? ? ? ? ? 1.46  
 0.1917 2.136 3.218 0.1127 ? 1.181 ? 5.0 ? ? 1.889 2.528 1.871 ? ? 1.0 1.556 0.1215  
 0.323 2.404 1.852 0.82 0.5 0.1 0.778 ? ? 1.286 0.556 0.4444 1.506 0.1667 0.75 0.5

'Anurognathus\_ammonii' 0.0419 0.4894 0.891 ? 12.88 0.1651 0.3678  
1.66 ? ? ? ? 1.175 0.183 1.211 2.546 0.1655 ? 1.384 1.321 5.0 0.556 ? 1.22 3.139  
1.622 ? ? 0.839 1.433 0.1389 0.285 2.279 1.686 0.798 0.462 ? 0.796 1.485 2.068 1.463  
0.475 0.4649 2.469 0.1857 0.524 0.487

'Dendrorhynchoides\_curvidentatus' 0.1068 ? 1.083 ? 18.21 0.0517 ? ? ? ? ? ? ?  
? 2.466 ? ? ? 1.516 ? 0.935 ? 1.182 ? ? ? ? 0.908 1.298 0.1114 0.308 2.614 1.623  
0.822 0.628 ? 0.723 0.643 2.358 1.344 0.518 0.4523 1.211 0.2417 0.4524 0.3

'Herbstosaurus\_pigmaeus' ? ? ? ? ? ? ? ? ? ? ? ? ? ? ? ? ? ? ? 5.0 ? ? ? ?  
? 1.428 ? ? ? ? ? ? ? ? ? ? ? ? ? ? ? ? ? ? ?

'Kryptodrakon\_progenitor' ?  
? ? ? ? ? 1.027 2.547 ? ? ? ? ? ? ? ? ? ? ? ? ? ? ?

'Gnathosaurus\_subulatus' 0.5019 0.5704 ? ? ? ? ? 12.44 ? ? ? ? 5.179 0.2927  
1.461 3.233 0.0504 0.2884 ?

'Gnathosaurus\_macrurus' ? ? ? ? 43.47 0.3961 0.5584 ? ? ? ? ? ? ? ? ? ? ?  
? ? 8.216 ?

'Plataleorhynchus\_streptophorodon' ?  
? ?

'Huanhepterus\_quingyangensis' ? ? ? ? ? ? ? 9.55 ? ? ? ? ? ? ? ? ? ? 8.258  
0.758 5.0 ? ? ? ? ? 0.821 ? 0.861 1.648 ? 0.875 1.578 1.479 0.883 0.704 0.634 0.931 ?  
? 2.04 ? 0.2523 ? 0.2073 ? ?

'Moganopterus\_zhuiana' 0.888 0.3067 0.913 ? 34.25 0.3109 0.3796  
11.54 ? ? ? ? 9.706 0.22 1.0 ? ? 0.0899 7.25 ? ? ? ? ? ? ? ? ? ? ? ? ? ? ? ? ? ?  
? ? ? ? ? ? ? ?

'Elanodactylus\_prolatus' ? ? ? ? ? ? ? ? ? ? ? ? ? ? ? ? ? ? ? 3.638 1.37 ? ? ?  
1.321 2.13 2.13 1.029 ? 0.816 1.107 ? 0.848 1.59 1.4 1.142 1.049 0.701 ? ? ? ? ? ?  
1.132 0.2248 0.2058 ?

'Kepodactylus\_inspiratus' ? ? ? ? ? ? ? ? ? ? ? ? ? ? ? ? ? ? ? 2.712 ? ? ? ? ?  
? ? ? ? ? ? ? ? 1.25 ? ? ? 0.858 ? ? ? ? ? ? ? ? ? ?

'Aurorazhdarcho\_primordius' ? ? ? ? ? ? ? ? ? ? ? ? ? ? ? ? ? ? ? 1.165 ?  
0.48 ? 1.25 ? 3.235 1.094 ? 0.933 1.329 0.6538 1.511 ? 1.915 0.592 0.423 0.422 1.226  
? ? 1.51 0.346 0.1823 0.963 0.3278 0.1555 0.161

'Liaodactylus\_primus' 0.5 0.5515 0.88 ? 33.94 0.305 0.5888 6.69 ? ?  
? ? 3.322 0.3113 1.087 2.327 0.0685 0.3762 ? ? ? ? ? ? ? ? ? ? ? ? ? ? ? ? ? ?  
? ? ? ? ? ? ? ?

'Ctenochasma\_elegans' 0.6119 0.6095 0.806 ? 24.33 0.5873 0.7242  
8.11 ? ? ? ? 3.214 0.1265 1.719 3.561 0.0878 0.1758 4.21 ? 5.0 0.479 ? 1.236 3.389  
2.452 1.255 ? 0.765 1.235 0.5138 1.047 1.366 1.4 0.919 0.718 0.667 0.857 0.7 2.474  
1.442 0.327 0.373 1.054 0.3146 0.2332 0.152

'Pterodaustro\_guinazui' 0.6873 0.7238 0.961 ? 26.11 0.5955 0.8843  
10.77 ? ? ? ? 3.79 0.1419 1.262 ? 0.0377 ? 4.294 1.228 7.0 0.822 ? 1.039 ? 2.94 1.273  
? 0.757 1.435 ? 1.052 1.865 1.604 0.975 0.753 0.602 0.855 ? ? 1.556 0.53 0.5125 1.69  
0.3537 0.2212 0.168

'Beipiaopterus\_chenianus' ? ? ? ? ? ? ? ? ? ? ? ? ? ? ? ? ? ? ? 3.984 0.966 5.0  
0.404 0.4221 1.123 ? ? ? ? 0.819 1.349 0.2735 1.035 1.687 0.927 1.575 1.317 1.102  
0.706 0.649 ? 1.993 0.38 0.3428 0.927 0.3146 0.1107 0.119

'Gegepterus\_changae' 0.67 0.4224 0.861 ? 30.98 ? 0.4718 9.94 ? ? ?  
? 4.429 0.1879 1.212 ? 0.0667 ? 3.672 0.987 ? ? 0.3852 ? ? 2.171 ? ? ? ? ? ? ? ?  
1.015 ? ? ? ? ? ? ? ? ? ? ? ?

'Feilongus\_youngi' 0.5946 0.3009 0.893 ? 29.14 0.4476 0.3536 10.38 ? ?  
? ? 6.332 0.2261 ? ? 0.0414 0.0788 6.364 ? ? ? ? ? ? ? ? ? ? ? ? ? ? ? ? ? ?  
? ? ? ? ? ?

'Cycnorhamphus\_suevicus' 0.4032 0.0514 0.827 ? 15.23 0.3065 0.0928 4.42 ? ? ?  
? 3.569 0.3364 1.427 6.016 0.1623 ? 2.224 1.286 5.0 0.432 ? 1.057 2.645 1.666 1.19 ?  
0.81 1.305 0.7317 1.63 1.788 2.123 0.818 0.595 0.499 1.152 1.586 2.033 1.482 0.339  
0.228 ? ? ? ?



'Ardeadactylus\_longicollum' 0.4952 0.4803 0.837 ? 24.73 0.4087 0.4823 5.7  
? ? ? ? 3.404 0.3096 1.318 6.789 0.0891 ? 5.335 1.301 5.0 0.432 ? 1.157 2.307 2.117  
1.198 ? 0.754 1.29 0.6005 1.661 1.5 2.055 0.776 0.466 0.393 1.143 1.981 2.435 1.505  
0.226 0.2013 ? ? ? ?  
'Pterodactylus\_antiquus' 0.456 0.4625 0.802 ? 23.05 0.3878 0.5105 6.16 ? ? ?  
? 3.194 0.2467 1.474 ? 0.0766 ? 5.09 1.313 5.0 0.489 ? 1.359 3.154 2.127 1.154 ?  
0.855 1.339 0.5036 0.991 1.556 1.306 0.945 0.84 0.641 0.994 1.98 2.858 1.388 0.373  
0.3668 0.969 0.3336 0.1637 0.177  
'Pterodactylus\_micronyx' 0.5025 0.2631 0.777 ? 25.0 0.3878 0.3248 5.32 ? ? ?  
? 3.262 0.1885 2.138 3.253 0.062 0.6449 3.038 1.192 5.0 0.624 ? 1.099 2.731 2.443  
1.303 ? 0.764 1.102 0.5169 1.328 1.874 1.646 0.778 0.594 0.518 1.039 ? ? 1.379 0.301  
0.2585 0.997 0.341 0.1976 0.213  
'Normannognathus\_wellnhoferi' ? ? ? ? ? ? 4.9 ? ? ? ? ? ? ? ? ? ? ? ?  
?  
'Germanodactylus\_cristatus' 0.3921 0.5213 0.752 ? 16.9 0.4112 0.626 4.33  
? ? ? ? 2.404 0.3552 1.149 ? 0.068 ? 3.312 1.194 5.0 0.499 ? 1.266 3.408 1.966 1.528  
? 0.812 1.274 0.5467 1.093 1.783 1.381 0.943 0.825 0.718 0.958 1.185 1.98 1.434 0.383  
0.334 1.091 0.3395 0.1957 0.092  
'Germanodactylus\_rhamphastinus' 0.3118 0.5242 0.862 ? 17.43 0.4718 0.5016  
4.54 ? ? ? ? 3.043 0.4105 1.065 ? 0.0446 ? 2.693 1.074 5.0 ? ? 1.253 3.64 2.064 1.169  
? 0.875 1.448 ? 1.068 1.317 1.427 0.824 0.772 0.705 1.032 1.706 2.415 1.471 0.469  
0.3179 ? ? ? ?  
'Haopterus\_gracilis' 0.424 0.5405 0.82 ? 13.09 0.4719 0.6728 3.82  
? ? ? ? 7.616 0.3555 ? ? ? ? 1.395 1.017 ? ? ? 0.786 ? ? ? 0.888 1.438 0.3736 1.18  
? 2.095 0.799 0.649 0.331 ? ? ? ? ? ? ? 0.316 0.1111 0.169  
'Aetodactylus\_halli' ? ? ? ? 29.6 0.4078 0.754 ? ? ? ? ? ? ? ? ? ?  
?  
'Anhanguera\_piscator' 0.4741 0.6452 0.845 0.2796 16.06 0.4833  
0.6671 5.43 ? ? ? ? 2.823 0.2921 1.828 ? 0.0572 0.3454 1.389 1.048 5.0 0.747 ? 0.772  
? 2.754 ? ? 0.464 1.529 ? 1.004 1.899 ? ? ? 0.918 2.22 2.09 1.218 ? 0.205 0.514  
0.4879 ? ?  
'Anhanguera\_blittersdorffi' 0.5019 0.6592 0.841 0.2683 17.3 ? 0.6732 6.0  
? ? ? ? 3.326 0.3022 0.989 2.096 0.058 0.4173 ? ? ? ? ? ? ? ? ? ? ? ? ? ? ? ?  
? ? ? ? ? ? ? ?  
'Hamipterus\_tianshanensis' 0.5684 0.6652 ? ? 15.91 0.4453 0.5725 4.85 ? ? ? ?  
2.522 0.2948 0.806 1.431 0.0695 0.1966 2.731 1.312 6.0 ? ? 0.905 1.622 2.629 ? ? 0.5  
? 0.4882 ? 1.834 1.836 0.758 ? 0.219 1.133 ? ? ? ? ? ? ? ?  
'Liaoningopterus\_gui' ? ? ? ? 12.09 0.3625 ? 6.73 ? ? ? ? ? ? ? ? ? ?  
? 2.207 ?  
'Siroccopteryx\_moroccensis' ?  
?  
'Tropeognathus\_mesembrinus' 0.4508 0.5589 0.85 0.2491 16.93 0.2994 0.6539  
5.1 ? ? ? ? 3.534 0.3721 0.808 1.879 0.0433 0.4809 ? ? ? ? ? ? ? ? ? ? ? ? ? ?  
? ? ? ? ? ? ? ? ? ? ?  
'Aerodraco\_sedgwickii' ? ? ? ? ? ? 5.62 ? ? ? ? ? ? ? ? ? ? ? ?  
?  
'Coloborhynchus\_capito' ?  
?  
'Coloborhynchus\_clavirostris' ?  
?  
'Coloborhynchus\_wadleighi' ?  
?  
'Ornithocheirus\_simus' ?  
? ?

'Ornithocheirus\_platystomus' ?  
?  
'Pterodactylus\_polyodon' ? ? ? ? ? ? 7.74 ? ? ? ? ? ? ? ? ? ? ? ? ? ? ? ? ?  
?  
'Brasileodactylus\_araripensis' ?  
?  
'Targaryendraco\_wiedenrothi' ?  
? ? ? ? ? ? 0.672 ? ? ? ? ? ? ? ? ? ? ? ? ? ? ? ? ? ?  
'Aussiedraco\_molnari' ?  
?  
'Barbosania\_gracilirostris' 0.5349 0.6733 0.844 ? 17.6 0.5128 0.7098 3.25  
? ? ? ? 4.545 0.2455 0.851 ? 0.0598 ? ? 0.927 ? 0.619 ? ? ? ? ? ? 0.528 1.407 0.5785  
0.981 ? ? ? ? ? 0.801 ? ? ? ? ? ? ? ? ?  
'Camposipterus\_nasutus' ? ? ? ? ? ? ? 4.97 ? ? ? ? ? ? ? ? ? ? ? ? ? ?  
?  
'Ludodactylus\_colorhinus' ?  
?  
'Ludodactylus\_sibbicki' 0.5049 0.6882 0.891 ? 14.69 0.3832 0.6982  
4.52 ? ? ? ? 2.668 0.3055 0.983 ? 0.0449 0.1919 ? ? ? ? ? ? ? ? ? ? ? ? ? ? ? ?  
? ? ? ? ? ? ? ? ? ?  
'Boreopterus\_cuiaie' 0.5534 0.6628 0.851 ? 20.13 0.65 0.7771 5.88 ? ? ? ?  
3.96 0.2261 1.094 ? ? 2.198 ? ? ? ? ? ? ? ? ? ? ? 1.392 0.4091 1.19 1.758 1.734 0.894  
0.715 0.635 1.038 1.119 1.892 1.0 ? 0.1585 ? ? ? ?  
'Boreopterus\_giganticus' 0.586 0.6872 0.876 ? 15.09 0.6353 0.7897 6.38 ? ? ?  
? 2.767 ? 0.2161 0.935 ?  
'Guidraco\_venator' 0.5395 0.6342 0.868 ? 13.63 0.5364 0.7322 4.42 ? ? ?  
? 3.167 0.25 0.948 ? 0.0423 ? 1.278 ?  
? ? ? ?  
'Zhenyuanopterus\_longiristris' 0.5505 0.8073 0.908 ? 21.16 0.5616 0.8671  
8.17 ? ? ? ? 3.998 0.2752 1.268 ? 0.0397 ? 2.664 ? 6.0 0.593 ? 1.333 ? ? ? ? 0.526  
1.248 0.4389 1.095 1.317 1.714 0.764 0.583 0.528 1.0 2.281 2.099 0.952 0.468 0.11 ? ?  
? ?  
'Cearadactylus\_atrox' 0.4259 0.4171 0.846 ? 13.94 0.2282 0.4542  
4.83 ? ? ? ? 2.206 0.3253 ? 3.238 ?  
? ? ? ? ?  
'Hongshanopterus\_lacustris' 0.4895 0.5 ? ? ? ? ? ? ? ? ? ? ? ? ? ? ? ? ? 0.2795 ?  
2.996 0.077 0.4516 1.325 ?  
'Piksi\_barbarulna' ?  
?  
'Ikranodraco\_avatar' 0.5002 0.6059 0.907 0.4588 20.24 0.5136 0.5815 7.07  
? ? ? ? 3.782 0.3366 1.5 4.07 0.0579 0.1988 2.648 ? ? ? ? ? ? ? ? ? 0.524 1.644  
0.7117 1.264 1.46 2.06 0.954 ? ? ? ? ? ? ? ? ? ? ? ?  
'Ikranodraco\_machaerorhynchus' ?  
?  
'Serradraco\_sagittirostris' ?  
?  
'Lonchodectes\_compressirostris' ? ? ? ? ? ? ? 6.9 ? ? ? ? ? ? ? ? ? ? ? ? ? ? ?  
?  
'Lonchodraco\_giganteus' ? ? ? ? ? ? ? 3.26 ? ? ? ? ? ? ? ? ? ? ? ? ? ? ?  
? ? ? ? ? ? ? 0.683 ? ? ? ? ? ? ? ? ? ? ? ? ? ? ? ? ? ?  
'Lonchodraco\_microdon' ? ? ? ? ? ? ? 9.46 ? ? ? ? ? ? ? ? ? ? ? ? ? ? ?  
?  
'Lonchodraco\_denticulatus' ? ? ? ? ? ? ? 1.66 ? ? ? ? ? ? ? ? ? ? ? ? ? ? ? ? ?  
? ?

'Cimoliopterus\_cuvieri' ? ? ? ? ? ? 5.08 ? ? ? ? ? ? ? ? ? ? ? ?  
?  
'Cimoliopterus\_dunni' ? ? ? ? ? ? 10.88 ? ? ? ? ? ? ? ? ? ? ? ? ? ?  
?  
'Nurhachius\_ignaciobritoi' 0.3779 0.3506 0.881 ? 21.68 0.3207 0.375 5.16 ? ? ?  
? 6.399 0.5968 1.402 5.966 0.0648 ? 2.311 1.407 ? ? ? 0.81 ? 1.889 ? ? 0.454 1.709  
0.3798 1.124 1.619 2.021 0.82 0.638 ? 1.104 ? ? 1.257 ? 0.1349 1.136 0.443 ? ?  
'Liaoxipterus\_brachyognathus' ? ? ? ? 22.39 0.2863 0.3418 ? ? ? ? ? ? ? ? ? ?  
?  
'Istiodactylus\_sinensis' 0.2097 0.2331 0.902 ? 17.07 0.1196 0.2314 5.21 ? ? ?  
? 4.61 0.6409 1.265 ? 0.0576 ? 2.073 1.212 ? ? ? 0.896 ? ? ? ? 0.483 1.751 ? 1.249  
1.716 2.046 0.892 0.715 ? 1.206 ? ? 1.134 ? ? ? ? ? ?  
'Istiodactylus\_latidens' 0.1748 0.1539 0.755 ? 18.42 0.1655 0.2279 6.29 ? ? ?  
? 3.707 0.4304 1.134 3.833 0.0509 ? ? 1.105 ? ? ? 0.796 ? ? ? ? 0.442 1.732 0.252 ? ?  
? ? ? ? 0.909 2.562 2.36 ? ? ? ? ? ? ?  
'Pteranodon\_longiceps' 0.6939 ? 0.87 ? 16.02 0.6367 ? 4.78 ? ? ? ?  
2.086 0.2257 0.761 3.475 0.0497 0.0336 2.07 ? 10.0 ? ? 0.903 2.04 2.423 1.132 ? 0.678  
1.369 0.3003 2.154 1.704 2.428 0.814 0.593 0.297 0.982 ? ? 1.408 0.316 0.3196 1.074  
0.413 0.0939 0.108  
'Pteranodon\_sternbergi' 0.7135 ? 0.914 ? 16.42 0.6883 ? 6.14 ? ? ? ?  
1.986 0.1789 0.716 ? 0.0325 0.0402 2.15 0.937 ? 0.832 ? 0.914 2.169 2.075 1.283 ?  
0.741 1.446 0.3726 2.367 1.542 2.684 0.798 0.582 0.324 1.003 0.743 2.015 1.397 0.315  
0.2479 ? ? ? ?  
'Tethydraco\_regalis' ?  
? ? ? ? ? 1.041 ?  
'Alamodactylus\_byrdi' ?  
? ? ? ? ? 0.975 ?  
'Nyctosaurus\_grandis' ? 2.345 ? ?  
? ? ? ? ? ? 0.716 0.678 1.3 ? 0.91 1.898 ? ? ? ? 0.878 ? ? ? ? ? ? ? ?  
'Alcione\_elainus' ? 0.999  
? ? ? 0.695 0.715 1.274 ? 1.504 ? ? ? ? ? 1.003 ? ? ? ? ? ? ? ? ?  
'Simurghia\_robusta' ?  
? 0.671 ?  
'Cretornis\_hlavaci' ?  
?  
'Nyctosaurus\_gracilis' 0.6637 ? 0.885 ? 21.58 0.5612 ? 5.83 ? ? ? ?  
2.759 0.269 1.109 1.935 0.0788 0.5217 2.173 1.088 9.0 0.462 ? 0.898 2.138 3.719 0.902  
0.626 0.697 1.837 0.7837 2.996 1.576 3.523 0.796 0.453 0.377 0.913 1.049 2.271 1.352  
0.292 0.2755 ? ? ? ?  
'Nyctosaurus\_nanus' ? 0.995 ? ? ? ?  
? ? ? 0.596 ?  
'Nyctosaurus\_lamegoi' ?  
? ? ? ? 0.74 ?  
'Muzquizopteryx\_coahuilensis' ? ? ? ? ? ? 4.08 ? ? ? ? 2.688 ? 1.714 ? ?  
? ? ? 8.0 ? ? ? ? 2.425 0.957 0.702 0.773 1.391 0.6011 ? ? ? ? ? ? 0.969 1.387 2.004  
1.397 ? 0.2018 ? ? ? ?  
'Tupandactylus\_navigans' 0.2531 ? ? ? ? ? ? 3.04 ? ? ? ? 2.071 0.4747 0.766  
1.75 0.102 0.1104 ?  
'Tupandactylus\_imperator' 0.1838 ? ? 0.51 12.86 0.51 ? 3.52 ? ? ? ? 2.68  
0.6803 0.772 ? 0.0257 ?  
'Bakonydraco\_galaczi' ? ? ? 0.4822 20.17 0.5 ? 5.68 ? ? ? ? ? ? ? ?  
?  
'Tapejara\_wellnhoferi' 0.224 ? 0.77 0.3967 7.04 0.4387 ? 2.46 ? ? ?  
? 1.913 0.477 0.894 1.12 0.13 0.0415 2.722 0.928 ? 0.57 0.47 1.226 2.495 2.13 ? ?

0.79 1.406 0.4906 1.316 1.365 1.966 0.835 0.646 0.435 1.154 1.511 0.0 1.26 0.486  
0.2908 ? ? ? ?  
'Europejara\_olcadesorum' ? ? ? 0.277 11.59 0.2505 ? ? ? ? ? ? ? ? ? ? ? ? ? ?  
?  
'Vectidraco\_daisymorrisae' ? ? ? ? ? ? ? ? ? ? ? ? ? ? ? ? ? ? ? 1.75 5.0 ? ? ?  
? 2.073 ?  
'Caiuajara\_dobruskii' ? ? ? 0.3116 9.78 0.3677 ? ? ? ? ? ? 1.542 ?  
0.807 ? ? 0.0338 1.712 1.053 6.0 0.497 0.4396 ? ? ? 1.489 ? 0.574 1.33 ? 1.673 2.027  
1.932 0.907 0.955 0.291 1.009 1.095 1.667 1.225 ? ? ? ? ? ?  
'Huaxiapterus\_benxiensis' 0.3346 ? 0.779 0.5468 15.83 0.5369 ? 3.36 ? ? ? ?  
3.003 0.4705 ? ? 0.1009 ? 2.889 ? ? ? ? ? ? ? ? ? 0.857 1.919 0.5042 2.145 1.267  
2.839 0.739 0.557 ? 1.806 ? ? 1.375 ? 0.2273 ? ? ? ?  
'Huaxiapterus\_corallatus' 0.3073 ? 0.854 0.6613 13.91 0.5515 ? 3.66 ? ? ? ?  
2.321 0.4417 ? ? ? ? 1.637 ? ? ? 0.5086 1.175 ? ? 0.999 ? 0.806 1.479 0.5408 1.941  
1.655 2.185 0.64 0.417 0.196 1.319 ? ? 1.513 0.285 0.1996 0.912 0.4092 0.1338 0.116  
'Eopteranodon\_lii' 0.3015 ? 0.949 ? ? 0.6131 ? 4.03 ? ? ? ? 2.14 0.4478  
? ? ? ? 2.555 1.259 ? ? ? ? 2.543 3.146 ? ? 0.898 1.495 0.5443 1.539 1.692 2.025  
0.773 0.522 0.347 1.182 ? ? ? ? ? ? ? ? ? ?  
'Huaxiapterus\_jii' 0.1096 ? 0.909 0.6576 14.72 0.4752 ? 3.83 ? ? ? ?  
2.201 0.5257 ? ? ? ? 3.399 1.171 ? ? 0.4123 ? ? ? 0.845 ? 0.844 1.481 0.5128 1.671  
1.727 2.044 0.786 0.567 0.279 1.266 0.968 ? 1.41 0.355 0.2411 ? ? ? ?  
'Sinopterus\_dongi' 0.1576 ? 0.721 0.5005 13.13 0.5184 ? 3.45 ? ? ? ?  
2.983 0.6829 0.867 ? ? ? 2.448 1.14 5.0 ? 0.5071 1.069 2.535 ? 1.366 ? 0.821 1.454  
0.4896 1.577 1.409 1.988 0.762 0.525 0.239 1.226 0.556 ? 1.415 0.208 0.2081 0.927  
0.2607 0.2571 0.285  
'Bennettazia\_oregonensis' ?  
?  
'Dsungaripterus\_weii' 0.3941 0.3685 0.787 ? 12.66 0.4175 0.6253  
4.24 ? ? ? ? 2.072 0.3218 1.18 1.312 0.098 0.3903 1.324 1.105 7.0 0.545 ? 1.429 ?  
1.322 ? ? 0.814 1.606 ? 1.85 1.777 2.398 0.77 0.798 0.582 1.44 ? ? 1.571 ? 0.16 ? ? ?  
?  
'Domeykodactylus\_ceciliae' ?  
?  
'Noripterus\_parvus' 0.4682 0.4819 0.852 ? 18.84 0.5363 0.3 3.66 ? ? ? ?  
2.002 0.3394 1.089 ? 0.0874 0.2628 1.481 1.63 ? ? ? ? ? 1.666 ? ? 0.823 1.412 0.5456  
1.917 1.773 2.044 0.857 0.666 0.5 1.262 0.5 ? 1.516 0.303 ? ? ? ? ?  
'Noripterus\_complicidens' ? ? ? ? ? ? ? ? ? ? ? ? ? ? ? ? ? ? ? 3.185 1.887 7.0  
0.607 ? ? 1.097 2.425 1.567 ? 0.902 1.368 ? 1.868 1.771 2.289 0.713 ? ? 1.145 2.535  
2.025 1.839 0.22 0.2 0.75 0.3808 0.372 0.389  
'Tupuxuara\_longicristatus' ? ? ? ? ? ? ? 3.16 ? ? ? ? ? ? ? ? ? ? ? ? ? ? ? ? ? ?  
?  
'Tupuxuara\_leonardii' 0.2439 ? 0.722 ? 18.49 0.6211 ? 6.25 ? ? ? ?  
2.752 0.4129 0.603 2.109 0.0316 0.3496 1.802 1.057 ? ? ? 1.187 ? ? ? ? 0.694 1.258  
0.5221 1.582 1.678 2.185 0.611 0.41 ? 1.271 ? ? 1.339 0.348 0.2232 ? 0.3765 0.1664  
0.129  
'Thalassodromeus\_sethi' 0.436 ? 0.927 ? 12.12 0.4776 ? 2.96 ? ? ? ?  
2.2 0.6088 0.44 ? 0.048 ?  
'Ornithostoma\_sedgwicki' ? ? ? ? ? ? ? 5.43 ? ? ? ? ? ? ? ? ? ? ? ? ? ? ? ? ? ?  
?  
'Keresdrakon\_vilsoni' ? ? ? ? ? ? ? 4.12 ? ? ? ? 1.482 ? ? ? ? ?  
2.519 ? ? ? ? ? ? 1.526 ? ? 0.637 1.32 ? ? ? 2.156 ? ? ? ? ? ? ? ? ? ? ? ? ? ?  
'Argentinadraco\_barrealensis' ?  
?  
'Lacusovagus\_magnificens' ? ? ? ? ? ? ? 8.51 ? ? ? ? ? ? ? ? ? ? ? ? ? ? ? ? ? ?  
? ?

'Chaoyangopterus\_zhangi' ? ? ? ? 26.36 0.4641 ? 4.09 ? ? ? ? ? ? ? ? ? ?  
3.733 1.099 ? ? 0.3052 1.133 1.385 1.695 ? ? 0.791 1.368 ? 1.965 1.459 2.171 0.658  
0.39 0.24 1.44 ? ? 1.559 0.399 0.242 ? 0.2353 ? ?  
'Jidapterus\_edentus' 0.5182 ? 0.895 ? 19.68 0.5684 ? 3.12 ? ? ? ?  
1.806 0.4312 ? ? ? ? 2.605 1.216 ? 0.325 ? 1.138 ? 2.38 ? ? 0.687 1.429 0.6166 1.91  
1.762 2.133 0.707 0.433 0.216 1.262 0.051 2.094 1.493 0.427 0.2416 0.961 0.3818  
0.1647 0.141  
'Eoazhdarcho\_liaoxiensis' ? ? ? ? 27.81 0.4444 ? ? ? ? ? ? ? ? ? ? ? ? 3.5  
1.143 ? ? 0.5505 1.136 ? ? ? ? 0.364 1.356 0.4473 1.5 1.641 1.978 0.781 0.522 0.281  
1.044 1.358 ? 1.702 ? ? ? ? ? ?  
'Shenzhopteris\_chaoyangensis' 0.5 ? 0.603 ? 12.97 0.5 ? 2.64 ? ? ? ? 2.109  
0.6027 0.429 ? ? ? 3.444 ? ? ? ? 1.0 ? ? ? ? ? 1.591 ? 2.121 1.634 2.227 0.68 0.463  
0.245 1.545 ? ? 1.363 ? 0.2806 ? ? ? ?  
'Radiodactylus\_langstoni' ?  
?  
'Microtuban\_altivolans' ?  
0.3672 1.282 ? ? ? ? 0.7 1.363 ? 1.807 1.409 2.0 0.848 0.47 0.026 ? ? ? ? ? ? ? ? ? ?  
'Volgadraco\_bogolubovi' ? 2.4 0.801  
?  
'Montanazhdarcho\_minor' ? 4.841 ? ?  
? 0.5791 ? ? ? ? ? 0.719 1.652 ? 1.452 2.375 ? ? ? ? ? ? ? ? ? ? ? ? ? ?  
'Mistralazhdarcho\_maggii' ? ? ? ? ? ? ? 11.43 ? ? ? ? ? ? ? ? ? ? ? ? ? ? ? ?  
? ? ? ? 0.606 1.521 0.5536 ? 1.238 ? ? ? ? ? ? ? ? ? ? ? ? ? ? ? ? ? ?  
'Alanqa\_saharica' ?  
?  
'Inabtanin\_alarabia' ? 1.787 ? ?  
? ? ? ? ? ? ? 0.771 1.523 ? 2.277 2.418 2.915 ? ? ? ? ? ? ? ? ? ? ? ? ? ?  
'Xericeps\_curvirostris' ?  
?  
'Leptostomia\_begaaensis' ? ? ? ? ? ? ? 22.9 ? ? ? ? ? ? ? ? ? ? ? ? ? ? ? ? ? ?  
?  
'Aptorhamphus\_gyrostega' ? ? ? ? ? ? ? 4.67 ? ? ? ? ? ? ? ? ? ? ? ? ? ? ? ? ? ?  
?  
'Azhdarcho\_lancicollis' ? ? ? ? ? ? ? 6.21 ? ? ? ? ? ? ? ? ? ? ? 5.248  
1.13 ?  
'Albadraco\_tharmisensis' ? ? ? ? ? ? ? 5.68 ? ? ? ? ? ? ? ? ? ? 4.828 ? ? ? ?  
?  
'Zhejiangopterus\_linhaiensis' 0.444 ? 0.877 ? 20.94 0.5649 ? 5.4 ? ? ? ?  
2.686 0.3814 0.993 ? 0.059 ? 9.124 1.407 7.0 ? ? 1.215 ? ? ? ? 0.778 1.525 0.6255  
2.074 1.411 1.941 0.781 ? ? 1.434 ? ? 1.582 0.156 0.2279 1.208 0.3341 0.1619 0.111  
'Aralazhdarcho\_bostobensis' ?  
?  
'Eurazhdarcho\_langendorffensis' ? 6.316 ? ?  
? ? ? ? ? ? ? ? ? ? 1.267 ?  
'Phosphatodraco\_mauritanicus' ? 6.25 ? ?  
?  
'Wellnhopteris\_brevirostris' ? ? ? ? ? ? ? 2.59 ? ? ? ? 1.376 ? ? ? ? ?  
8.457 ?  
'Quetzalcoatlus\_lawsoni' 0.5914 ? 0.947 ? 30.31 0.5846 ? 7.05 ? ? ? ? 3.319  
0.3123 1.015 2.012 ? ? 9.923 1.056 ? ? 0.5752 1.112 2.441 2.184 1.339 ? 0.635 1.521  
0.5835 2.041 1.736 2.474 0.519 0.303 0.067 1.619 ? ? 1.46 0.222 0.148 ? ? ? ?  
'Aerotitan\_sudamericanus' ? ? ? ? ? ? ? 7.7 ? ? ? ? ? ? ? ? ? ? ? ? ? ? ? ? ? ?  
?  
'Cryodrakon\_boreas' ? 7.821 ? ? ? ? ?  
? ? ? ? ? ? ? 2.48 1.527 ? ? ? ? ? ? ? ? ? ? 0.2154 ? ? ? ? ?

'Hatzegopteryx\_thambema' ? 2.609 ? ? ? ? ?  
?  
'Arambourgiana\_philadelphiae' ? 8.781 ? ?  
?  
'Quetzalcoatlus\_northropi' ?  
? ? 0.812 1.362 ? ? 3.596 ? ? ? ? ? ? ? ? ? ? ? ? ? ? ? ? ? ?  
&[numeric]  
'Euparkeria\_capensis'  
010?00000?00010000000?0000?0?00000100?0000000021[0  
2]00010011100?0000010000?00000000?0000000010000?0?000000?0?000?00000000000000  
00000?00000000000?010?0010000000?00000011?0000000001?0?0000000000000000010?0?0?0?  
?00?0?0?0?0?0?0?0?0?0?0?0?000001000000[0 1]110  
'Ornithosuchus\_longidens'  
010?00?00?00010000?00?000??0?0?00?100?00000000?1?0000011100?0000011?00?0?0?0?  
?0?000?0?0?0?0?000?010?0?002010?0?0?10?0000000000000000?0?0?000000000[0  
1]0?0?0?0?0?0100001?000000?0?00000000?0?0?0000000000?0001?0?0?0?0?0?0?0?0?0?  
?0?0?0?0?00100?0?0?0?0?0?  
'Herrerasaurus\_ischigualastensis'  
010?00?00?00010000?00?000??0?0000?200?00000000?1?0000011100?0000010000?0?0?0?  
?2?000?0?0?0000000000?0?100010?0?0?00?0000000000000000000?0?000000?000?0?0?0?0?0?  
?0?0?0000?0?0?00001000?0?0?001000001001000001?0?0?0?0?0?0?0?0?0?0?0?0?0?0?0?  
?0?  
?0?0?0?30  
'Scleromochlus\_taylori'  
0?1?00?10?0010?00?00?000??0?0000?120?00?0?0?0?21200?0?0?1?100?0?0?0?0?0?0?0?0?  
?00010?0?0?0?00000?0?0?1?000010?0?0?0?100?0?00?0?02?0?0?00?100?0?00?0?01000010?0?  
?0?0?00000?1?000000000?0?0000?000001?0?0?1?0?0?0?0?0?0?0?0?0?0?0?0?0?0?0?0?0?0?  
?0?0?014?  
'Eudimorphodon\_ranzii'  
011?00?10?00020000000?0000?1001000110?10101001[0 1]0[0  
2]1111001110200241?12000?  
?00?0?0?01?000?0?0?00?000?10010110?000200010?0000?0?0?0?0?0?0?0?0?0?0?0?0?0?0?  
100?0?1111010010021?0?0?1?00?000?0?0?0?0?0?  
'Eudimorphodon\_rosenfeldi'  
011?00?10?00010000?00?000??0100?110?10101001?0?0?110001110200241?12000?0?0?0?  
?3?010?0?0?0?0?0100000?00?1?000010?0?0?111?10?00000000200000?0?0001?0000?0?0?0?0?0100  
001?000?10?0?0?0?00000?  
?0?0?0?0?  
'Eudimorphodon\_cromptonellus'  
?????0?0?0?0001?0?0?00?000?000?000?000?001?02011000?020200220?0?0?0?0?0?0?0?0?  
1]01001202111000?110?0024?0?  
?0?  
0?  
?0?0?0?0?  
'Peteinosaurus\_zambellii'  
???????0?  
??  
?????????0?0?0?0?0?0?00000000[0  
2]?0?  
'caviramus\_schesaplanensis'  
?????0?0?0?00010100?00?0?11?0?0?110000?02?0?0?0[0  
1]0?00?0  
1]?21?100?0?010?0231?0?  
?0?  
?0?  
'Raeticodactylus\_filisurensis'  
011?00?10?00210100?01?0?11?0?110000?02?00100001?0?0?11001110120231?12001000010  
121010?0?0?0?0?00000000?1?1000?0?0?0?0?0?1?100000000000200?0?0?0001?00?0?0?0?0?0?0?0?0?0?

?????0????????????????????????????????0?001011?00?1??0?????000?0??0?????????????10000??  
??????0  
'Austriadactylus\_cristatus'  
011?0?10?00200?0?00?00??0?0000?12??0000001[0 2]0201110011102[0  
1]0110?11?0100001021?010??0??10100000?1?000010?0?00?00000?0?00100?00?000??  
0000??0?000000??00?1?0?0010???0000?0?0??0??0?01011?00?0??1?1??00?0??011  
?10??1?0011????1?????????  
'Preondactylus\_buffarinii'  
011?00?10?00010000?00?00??0?0000?11??00000001202011?001110200110?11000?????  
?1?010?????????01000?0??1?00?0?0??????10?000??00?10????0?00??0?0?????0000??  
?????0?0?1001?000000000?0000?????01011?00????1????0000?0201?010?000??0011?0001?0  
10100[1 3]20  
'Dimorphodon\_macronyx'  
011?00?10?00212000002000000?0?0020013??00000001[0  
2]0201410011112?1?0?02100??????11110????0??101000100?1?002010??300?1000000001001  
00????0??01?100?0010?0?0002??00??00002101??1100000100113101000002011100001?01????  
002001010110100?021000?10000?0010100120  
'Dimorphodon\_koi'  
?????????0?10?01?0??0?0?0?00200????000?01?0?1?????002????????1??????  
????????????10????????????[0  
1]?0?10????????????????0100???1?01?10????????????????????????????????????  
??  
'Dimorphodon\_hanseni'  
?????1????00?0011?02000?00?100120024??0000001?0??1?300?1102?1????21??????  
?1?1100??????00000?0?1?00?1?12010????1?10?0000????????????????????????  
??  
?????????  
'Dimorphodon\_jenkinsi'  
?????1??0000?0??????100?1?2????????????  
?????0??????10?????0?????0[0  
2]?????????10?10??01??01?00?0??  
??  
'Dimorphodon\_weintraubi'  
??1??????  
????????????10????????????[0  
1]????10????????????0??10000?0?1?010100????????????00????0021????????????  
???0?0022?1000?01?0?0????2?0?0???01???0?00?????????0????20  
'Parapsicephalus\_purdoni'  
0????101????????????????????????????0?00[0  
1]0?????????????11????002100????2111000?0000101000000?1?002010??0?300?100000  
00100100000??  
??  
'Campylognathoides\_liasicus'  
011?00?10?10221000000?0000?0?0?100130000001001[0 2]0[1  
2]00000010112?1??1012100?????2102000?0?0?0100000000?1?000010?0?211?000010000100200  
00000?0001?000000?1010?0002011001100000201000?000011??13100001001011100??1?110010?0  
200102011010010001010110011000101?0[0 1]21  
'Campylognathoides\_zitteli'  
011?00?10?10221000000?000?0?0?100130?00001001[0 2]0[1  
2]00000010112?1??1?12100?????2?0200????????0000000?1?000010?0????000010?0100?00  
??0?000??00?0010?0?000201?001??00020100011000011??131000?10010111????111100????  
2001?20110100110010101100110?0101?0[0 1]21  
'Sericipterus\_wucaiwansensis'  
013111?1101??0010001??1000??0?000?31?001111?0?2100221100222?1??11?101011000  
?2??10?0?????0000??0?1?11??0?0?????1?00?0111?020000?0?0001000??0?0??????????

?????002011?????1????20?00003011101?011?00?????????????010201?????  
?????  
'Angustinaripterus\_longicephalus'  
013111?11010210011?01??10?0?0?0?0?13??1011110002100221100221?1??112?01011000  
?21010????0??00000?00?1?110010????211?10000001110020????0?????????????????  
??  
????????  
'Harpactognathus\_gentryii' 21301101101?????????????????????????????0[0  
1]1??0?2??0???022????11?01011000?21?0000??0???0?00????1?1????????????????  
??  
??  
'Cacibuptyx\_caribensis' 01???111??1?????????????????????????????00[0  
1]0?0?2??0???022????11?100??????2100000?0000100000000?0?110000?0?200?000000  
01100100000??  
01????????????????????????????????00????????????????  
'Rhamphorhynchus\_muensteri'  
012?00110?10200000001??1000?0?1?01013102020110002100221000222?1??1112100?????  
?2100000?0000100000001?0?110000?0?211?1000001?1100200000000000101000000101000002101  
0010[0 1 2]00002001??110001011021[1  
2]2010000060111000010000110012011100110100110100101100111001101012[1 2]  
'Qinglongopterus\_guoi'  
013??0?0?102100??00??1??????0??13?00111100?2??0201100?22?1??11?2????????  
?2?0?0??0?010000?0??1?1100?????2?1?000?0????020?0????01?000?0??0?0?0?2???  
00??000020?????101??11?01??03011100?1?0?0???301?1????01?????00?1?011?0?  
1????21  
'Nesodactylus\_hesperius'  
?????1??  
??  
001??0020????10001????00??0?006011100??1?0101?0?01????01????0?0100??1????  
????????  
'Orientognathus\_chaoyangensis'  
111?00?0?10210000?01??1?????1?00?13?0?0101100?2??0?0001012211??1?2[1  
2]??0??????2??10????????????????011?10?[0  
2]?????????10?00??1??0?????????01?000??????0?0?1??00??000020????010001?1?????  
20?????0?001?????0??????5?1??????1????0??0??10211?0??1????21  
'Dorygnathus\_banthenensis' 011?00010?10210000001??1020?100?000131?00101100[0  
2]2100201010122?1??1112100?????2100000?0000100000000?1?110010?0?211?100000011002  
00000000001?0000001[0 1]01000002101001?100002001??110001011021[1  
3]20100100301110000100001000030111001101001100110011001100110011001122  
'Klobiodon\_rochei'  
?????????10210000?02011????101?01?12??010?101?2??0?000?32221??1?????????  
??  
??  
????????  
'Fenghuangopterus\_lii'  
112?00?0?10110000?0??1?????0?1?00?13?10010?100?2??0?0111012211??11??0?????  
?2??0???0?001??????0?1?10?[0  
2]?????????1?000??110002?00????01?000????0?0?0?210?0?1?000020????1??101????13  
201?00003001?00?1????????2?1?0????01????0??0??1?111?0????????  
'Scaphognathus\_crassirostris'  
011?00?10?10210000?01??10??0?0?0?13?0000110002100200010122?1??0312100?????  
?21010??0?0?100000000?1?100010?0?211?10000001100200?000?000?0?000001101010002??1  
001?2000020????0[0  
1]000101??112?0000003011000?1?01011000201110110111000?100011001110011121222



'Sordes\_pilosus'  
011?00110?1001100000?100100?0?100130?10001000?2??0300010122?1??0112100?????  
?2101000?0?00101000001?1?000010?0?211?1000011?1100200000?0?0001?100000?0?0?0?201?  
001?000020??01000101??11201001000011100?1?0100?0?01?1??01??0?000010011?0?  
?1????22

'Darwinopterus\_modularis'  
011?00?10?10011000?00?10??0?0?10?10??1000100002100300120322?1??011?101020011  
2??1?001000??101001001?0?00010?0?41101000111?1100200?101?100??10?0?1100010002???  
0011100002011?000001110?013201?0?012011000??1?1?00?04011000110?1111??1?0011?011100  
11011322

'Darwinopterus\_zhengi'  
??  
??0??0??0??0??2???  
00??000020??01000?1????3??009001?00?1??????4?1?0??01?????????1?211???  
?1????21

'Darwinopterus\_linglongtaensis'  
111?00?0?10010000?00?1??0?1?10?10?010001000?2??0?0012032231??01??101020011  
2??0?0??010000011?0?00010?0?411010?011??1100020?01??1?01?10?0?0?0?0?2011?  
001??0020??00001?1??132011?1009?11100?1??0??4?1?0??01??0??0??1?211?0?  
?1????22

'Darwinopterus\_robustodens'  
111?00?0?10010000?00?1??0?1?10?10?010001000?2??0?0012032231??01??101020011  
2??0?0??0100?0011?0?00010?0?41101000111?1100020?1?1?1?01?0?01?0?0?0?0?201?  
001?000020??00000?11??13201?00019011?00?1??1??4?1?1??01??0?0?0?1?211?0?  
?1????22

'Kunpengopterus\_sinensis'  
111?00?0?10010000?00?1??0?1?10?10?010001000?2??0?0012032231??01??10101?001  
2??0?0??010000011?0?00010?0?411010?001??1101020?1?1?1?0?010100?0?0?0?0?201?  
001??0020??00000?11??13201?00019011?00?1??1??4?1?1??01??0?0?0?1?111???  
?1????21

'Archaeoistiodactylus\_linglongtaensis'  
1??0?0??110?0??1?0??1??0?00010?0?2??0?001??32?31??01??0?????  
????0??0??????1?0??0??1??1??1??1??1??1??1??1??1??1??1??1??1??1??1??1??1??1??  
??????10000111????20??0190?1100?1?????0?4?1?????????????????1?211???  
?????22

'Cuspicephalus\_scarfi'  
112?00?0?1????????????????????????????????02000?00?2??0??10121????11?101030001  
2??0?010?00??01?1??11?0?000?0?0?41101000011?1120030011????????????????????  
??  
???????

'Wukongopterus\_lii' 011?00?10?10011000?00?10??0?0?10?10??000100002[0  
2]00300120322?1??011?0????????1?0??0??0????????0????????????01????????2??  
?????100?0?0100110?010002??00??00002011?0?00010??????10?0??110????1101?????  
4011000100111000?1?011?0111?110?0322

'Pterorhynchus\_wellnhoferi'  
011?00110?10011000?00?10??0?0?10?10??20001000?2??0300110122?1??011??01010001  
1??0?0????0101000?0??0?000?0?0?4110100001??1100200?00?1??0?00??0??0?0?2???  
????0?0?????10000101????2010??02011000?1??1????001?????01????0??0001????0?  
?????2?

'Changchengopterus\_pani'  
??  
??100?0001??100010001???  
00????0020?1??0?0?1010??20?0?000011100??1?1?0?0?04011?[0  
2]010011?11?21000?1?1111?0110?1321

'Batrachognathus\_volans'  
111?000?0?1101120000?0000?1?0220?0000100001100300010122?1?030?110?????  
??0?0?1?1?0??0??0?00010?0?0110?00011??00010??0??0??01?0?0?0??000  
001??00020??10000??0?1??00000011000?1?10??0111101101??0??0??1?01??0  
0??12??  
'Jeholopterus\_ningchengensis'  
111?000?0?1101120000?0000?0?0?0?1?22?00001000?1100300010122?1?030?110?????  
??0?0?1?1?0??0??0?00010?0?0110?0001??00010??0??10??0??110?0011?0?0??  
00??0000201010?10000010??11??0?00040111000?11?100??050111??011??0?100011?0111?0  
10121220  
'Luopterus\_mutoudengensis' ??1?00?0?11?10200?0?????0?0?????00[0  
1]?000??0?000?12?31?0?2?1?????????0??1?101?????10?0?0001?????0?0??  
????????????0??01?????1?0?0?????0?0020??01000001????201??0000?1100??1?  
0?00?0?5?1?1??01?????3?1?11?0?0??20  
'Anurognathus\_ammoni'  
111?00010?11011200000?0000?0??1?0220?0000100001100300010122?1?030?110?????  
??0?0??1?1?0??000??0?00010?0?01?0?00011??000100?01?????1?00?011?0010??  
??000020?1??10000011??1010?0004011100?1101?1?05011100110111000?1?0110011100  
10120220  
'Dendrorhynchoides\_curvidentatus'  
111?000?0?1011200000?000?0?0?1?0?0?000010?011003000?122?1?030?10?????  
??0?0??1?101?????????0????????????????1?0??0?10??0??1??00?110?0??  
00??0000201??0?00??1??00000111000?1101?1?050111001101111?1?0011??0100  
10??1221  
'Herbstosaurus\_pigmaeus'  
??  
??  
????????????????00?00??13?10??10011?0?  
??????  
'Kryptodrakon\_progenitor'  
?????1??  
??  
????????2????????????????00?00??1?????01??00?0?????00??0?000?????  
??????  
'Gnathosaurus\_subulatus'  
211?00?111120110?0?00?10??0??1?????2021?10022100200110321?1??1?101030001  
1?1?0?0?0011001000001?0?10010?0?41101000011?1111300?121????????????????  
??  
?????????  
'Gnathosaurus\_macrurus'  
???001?1?2011?000??1000?0?0?101?2??021?00?2?0????321??01?????????  
??2200?111????????  
??1????????????????????00?????  
????????  
'Plataleorhynchus\_streptophorodon'  
211?00?10??1????????????????????????011?00?21?????10321??01?????????  
?????10?0????????1????????????????????1????????????????????????????  
??  
?????????  
'Huanhepterus\_quingyangensis'  
011?00?1101001?000?00?10??0?0?????0101100[0  
2]2100200110321?1?01??01030001????????????????????????????????????  
????????220????1100?0?????0????1?0?2????001010??13?1??00501?1??11?1???  
??0?1????1?1?????011?01?1?????????

'Moganopterus\_zhuiana'  
011?00?10??0210000?00??10??0?0?00?02??2010110002100201110121?1??0?2?10101?001  
0???0?0?????1001010?0??1?00000??13411??00?0???1111300??20??22??1?????????????  
??  
?????????

'Elanodactylus\_prolatus'  
??  
??  
001?000020100010010101??1330??1005011100?011010000?0401?02??0101?00001?000?0011??  
?1????33

'Kepodactylus\_inspersatus'  
??  
??  
????????????????????0????????01005011100?01?0????????????????????10??0??0?1?????  
?????????

'Aurorazhdarcho\_primordius'  
??  
??  
??1?000020????????1????13?01?0?008011100??1??0????2?1?0????10????00?1??1?0?  
?1????33

'Liaodactylus\_primus'  
011?00?0?10210000?00??1?0?0?1?00?02?020211100?1?0?0011011111?021??01030001  
??1?01??0?010?????11?0?10010?0?41101000011?1111300?12?0????????????????????  
??  
?????????

'Ctenochasma\_elegans'  
011?00100?1001000000??1000?0?0?00112?02021110021000200110111?1??012?10[0  
1]030001????010?00??001020101??0?00010?0?41101000011?1111300??20?21000??10100?10??  
101?000?00??00002001??00101010??13301?00005011100??110100??14?11??0001011110?10??  
100111001110??33

'Pterodaustro\_guinazui'  
001?00110?10002000000??100??0?0?20102??1000210021200200100002?1??012?100?????  
?????010?0??001020101??0?00010?0?411?1000001?1111300??21??1000011?10?11??0101?0001  
001?000020??1001010?0??133?11000050?11?0?110100?00?4?101??10000021000110?11110  
11100333

'Beipiaopterus\_chenianus'  
??  
??  
00??000220010????????????1?0?005011????1?0?0?0??4?10????101??00?0??1??????  
11??1133

'Gegepterus\_changae'  
00??0?1?1?00?0000?00????0?00?02??102011?011002001?001??1??12?1010300??  
0???010?0???01020101?0?00010?0??110100001?11?1300??200?1000?110?????0??????  
00??[0  
2]????220000????0?0??3??100?00011????100??  
?????

'Feilongus\_youngi'  
011?00?10?10210000?00??10??0?0?00?0200?010110002100201110121?1??0?2?101010001  
0???010?0??1001000101??1?0?000??1041101000011?1111300??2??220??11?????????????  
??  
?????????

'Cycnorhamphus\_suevicus'  
201?10?10?12000010?01??10?0?0?1?01?110?200011??0?10?20001?1?1?1??012?10[0  
1]0200212?1??010?0011?01010101??0?00010??1121101000011?1111300?1200?0000001?0??1???

?01?001?001120?002011??0000010111?13301?00008011100??1001000??0401?000101011010210001  
1001110111????33  
'Ardeadactylus\_longicollum'  
011?00111010011?00000??1?0100?0?101120?2010110002000500110321?1??012?100?????  
??1??010??001?0010?0100??0?10010??0?411010000101111300?12000220001111001100??0??010?  
00??0000020????1001010101?13301?1?0050011000?1101000??0401??????101?100?10?0110011100  
?1??????  
'Pterodactylus\_antiquus'  
011?00?10?1001000000??10?0?0?00013??2000100002100300010121?1??011?100??????  
?????010??0???01010101??0?00010??0?41101000011?111300??20001000?001100010?110010100  
0010100002011??1001010111?133010000050111000011010010004011121111011??0?1000110011100  
11001133  
'Pterodactylus\_micronyx'  
011?00??0?10010000?00??1?00?0?1?00002?020101000?2??0?0011012111??021?100??????  
??1??010??00010010201011?0?00010??0?41101000011?1111030?12?0?1?00?111100??0?1?0??0??1  
001??000020????11010101????13201000005011100??1?0?00??4?1?0????10??0?0?00??10111?0?  
?1????33  
'Normannognathus\_wellnhoferi'  
?01?00110?120??00000??1?0??0????1?????0?01100?2??0200011111?1??0?2??1020021  
?????10??  
??00????????  
?????????  
'Germanodactylus\_cristatus'  
012?00?10?1011100000??10??0?0?10013??2000100002200300001121?1??111?101030001  
2??0?01??????01010101??0?00010??0?41101000011?1102300??110??0??011000100??0??????  
00??000020001010000101??133010000050111?0?110000??4?11120101001??0?10?0?10011100  
1101133  
'Germanodactylus\_rhamphastinus'  
012?00?10?1011100000??0??0?0?10013??2000100002100300011121?1??011?101030001  
2??0?01??????01010101??0?00010??0?41101000011?1102300??100?100??01????100?1??000  
00?1200002?01??0000?01?00133010??0??111????10010?1?004?1?1????011100210?0110011100  
1100????  
'Haopterus\_gracilis'  
011?00?10?102110??00??1????0?0?10?10??3000100002200300010122?1??011??00??????  
?????00????????00100001??0?00?0?0??1?1?0??1????0200????????0??01?0??0??????100  
??112100020?010????????????????00007101100??1?1?????40101?011?011??0210001??????  
1100????  
'Aetodactylus\_halli'  
2??0?0?1??012011200001??1000?0??1?1101?0101?00?1??05101??321?1??00??0??????  
??????100??  
??00????????  
?????????  
'Anhanguera\_piscator'  
011?01011010010000?020110?0?0?0?0?1011301011110210151111032121??001?101041101  
0?1??00?????1001101111??0?11011201021111001011?100020011101101001111010110?111010010  
11012?011201011110101?1001??2110010071001100121000?011041??100?110111111100010111001  
1?00?4?  
'Anhanguera\_blittersdorffi'  
011?0101101001?0??0201100??0?0?011?1130101111?210151111032121??001?101041101  
0?1??00100011101????111?0?11011201021111001011?10002001110????????????????????  
??  
?????????  
'Hamipterus\_tianshanensis'  
111?01??1010011000?00??1?0100?1?00110?120101100?2??1?1011032121??020?101030021  
3?1??00100000101????1111?0?01010??0021101000101?1000020111?1?0?00?111?1?????????0?1

??1??111120??11010111????101111007100?10??2?0??1?1??4??????10??0??1?211?0?  
??????  
'Liaoningopterus\_gui'  
011?01?110100100?0?02??0??0?0?00?10113010111102[1  
2]0151011032121??0?1??010411010??0?100????????11??0?11?????211?1001011?100020?  
??????00?111??  
??  
'Siroccopteryx\_moroccensis'  
010?0?1?111????????????????????????????????010?00??2??5?012?32121??0????104?100  
??????101??  
??1????????????????????00??????  
????????  
'Trapeognathus\_mesembrinus'  
011?01111010010000002011000?0?0?001131130101?01?2??151011032121??001??01041100  
0?1??00100011101????111??0?11011201021111001011?1000200111????????????????  
??1????????????????00??????  
????????  
'Aerodraco\_sedgwickii'  
111?0??121????0????????????????????????????010?01?2??????1?3?121??1????????  
??????100??  
??  
????????  
'Coloborhynchus\_capito'  
?10?0??121????0????????????????????????????010?01?1??????2?3?121??????1041100  
??  
??  
????????  
'Coloborhynchus\_clavirostris'  
010?0?1?121????????????????????????????????010?01?2??5??2?32121????????1041100  
??????101??  
??1????????????????00??????  
????????  
'Coloborhynchus\_wadleighi'  
010?0?11121????????????????????????????????010?01?2??5??12?32121??0????1041100  
??????101??  
??1????????????????00??????  
????????  
'Ornithocheirus\_simus'  
010?0?1?101????????????????????????????????000????2??5??1?3?12????????1041100  
??????101??  
??1????????????????00??????  
????????  
'Ornithocheirus\_platystomus'  
11?0????1????????????????????????????????000???1?2??????1?3?2????????1?41100  
??????101??  
??  
????????  
'Pterodactylus\_polyodon'  
111?0??0?1????0????????????????????????????010?00?2??????1?311?????1????0????  
??????100??  
??  
????????  
'Brasileodactylus\_araripensis'  
????????01001?000101??100?0??1????010?0102[1  
2]015001??32121?00??

????????????????11????????????????????????1010?????????1????????????????????????  
????????????????1????????????????????????  
'Targaryendraco\_wiedenrothi'  
?????????1001000?01??1?0?0?0??110?1?010?00?1?0?0?0?0?32231?0?0?????????  
??  
?????????2??  
?????????  
'Aussiedraco\_molnari'  
?????????1001000?01??1?0?0?0??1????010?00?2?????0?322?1?0?0?????????  
??  
??  
?????????  
'Barbosania\_gracilirostris'  
111?01??1010001000?01??1????0?1?00110??30101101?2??1?1011032121??010?100?????  
?????0010?0??001?1?111?0??010?0??110?0?01????00?201?0????????????????????1?1??0???  
10??1???20?????????01????211??007100?10?2?????????4????????10??1??0?1?211?0?  
?????????  
'Camposipterus\_nasutus'  
111?0??101????0????????????????????????010?00?2??????103?1?????2????0?????  
??????100??  
??  
?????????  
'Ludodactylus\_colorhinus'  
111?0??101????0????????????????????????010?01?2??????1?3?0?????????????????  
??????100??  
??  
?????????  
'Ludodactylus\_sibbicki'  
011?01?110100110010000?100?0?0?101101?2010110102[1  
2]0151011032121??0?1?100????????1?0010100?1001101111??0?1101111221111001001?1000200  
?110??  
??  
'Boreopterus\_cuiaie'  
011?11?10?10210011?0??10??0?0?0?10??2010110000100200010122?1??0?1?100?????  
?????0?????????????1?1?0?110112010?11?1000011?1?0020??10??010??11??????1??0???  
?????????0?????????????????????????1????0?????1?????????11010011?1?????1?0011?111??  
?10??4?  
'Boreopterus\_giganticus'  
111?11?0?10010011?00??1??0?1?10?12?120201100?0??1?111012211??01??100?????  
?????0????0??1????1111?0?11010?0?21101000011?1000020?11?1????????????????????  
??  
?????????  
'Guidraco\_venator'  
011?01?11010?11001?00??10??0?0?10?101?20101101021015011012121??0?1?100?????  
?????0??0??0????111?0?110112122111100001?1000200??10??00?111????????????????  
??  
?????????  
'Zhenyuanopterus\_longiristris'  
011?01?10?10?10001?0??10??0?0?0?10??2000110000100200010122?1??0?1?10103??21  
1??0?0??0??01100101?0?11011201041101000011?1100200??10?0010?111?11?11011?010??  
??21111201000????0?????1??007100110??21?1?????4?1010??101100??1?011?1111?0  
110014?  
'Cearadactylus\_atrox'  
011?01?11010011000101??1000?0?0?101101?301011010210150011032121??001??0101110?  
0?1?00100011?01100?1?0?110?0????11010?1011?100?20????????????????????????

```

????????????????????????????????????????????????????????????????????????????????????????????????????
?????????
'Hongshanopterus_lacustris'
  012?111?0?1????????????????????????????????????????????????????????????????????????????????????
?1?0?01000?11000100??1?0?1?0?????????11?1?0011?????0?0?11?1?0100?111????????????????????
????????????????????????????????????????????????????????????????????????????????????????????????????
?????????
'Piksi_barbarulna'
  ??????1????????????????????????????????????????????????????????????????????????????????????
????????????????????????????????????????????????????????????????????????????????????????????????
????????????????????????????????????????????????????????????????????????????????????????????????
?????????
'Ikandraco_avatar'
  111?11?0?10010011?02111?????0?1?10?10?130001000?2?0?0011032131??01??100????????
?1?0?010000110011011011?0?01010?0?21101000001?1000030?11?1?0?00?111????????????????????
????????????????????????????????????????????????????????????????????????????????????????????????
?1???????
'Ikandraco_machaerorhynchus'
  ??????????10?001?021?1?0?0?0?1?????000?000?2????????????321????????????????????????
????????????????????????????????????????????????????????????????????????????????????????????
????????????????????????????????????????????????????????????????????????????????????????????
?????????
'Serradraco_sagittirostris'
  ??????????1??????1??????????1?10????1?020?0???2???200?42?1????????????????????
????????????????????????????????????????????????????????????????????????????????????????
????????????????????????????????????????????????????????????????????????????????????????
?????????
'Lonchodectes_compressirostris'
  31??121?13?1?????0?1?????0????????????????????????000?0000100????031?????011???0????????
??????0100?????????????????????0????????????????????????????????????????????????????????????
????????????????????????????????????????????????????????????????????????????????????????
?????????
'Lonchodraco_giganteus'
  011?0?110?1001?00?1020010?0??0??1?????0001000?0??150011031221??011??01051101
??????1000??????????????????0????????????????????????????????????????????????????????????
?????1???2?????????????????????????????????0071?1?1???2???1????????????????????????00????????
?????????
'Lonchodraco_microdon'
  1???1?????1?????????????????????????????????????????????????????????000???0?2????????32?????1????0?????
??????101????????????????????????????????????????????????????????????????????????????????????
????????????????????????????????????????????????????????????????????????????????????????
?????????
'Lonchodraco_denticulatus'
  111?1??0?1001001?02011?????0?1?????0001000?2?0?0011032131??011??01051101
??????1010?????????????1?0?0????????????????????????????????????????????????????????????
?????1???2?????????????????????????????0071?1?1???2????????????????????????????????????????
?????????
'Cimoliopterus_cuvieri'
  011?0?11101?????????????????????????????????????????????????????????010?000?2??0510112321?1????1???1041101
??????100????????????????????????????????????????????????????????????????????????????????????
????????????????????????????????????????????????????????????????????????????????????00?????????
?????????
'Cimoliopterus_dunni'
  011?0?11101?????????????????????????????????????????????????????????010?000?2??05?0112321?1????1???1041101
??????100????????????????????????????????????????????????????????????????????????????????????

```





????????????????????????????????????6000?0?1????????????????????????0?1?????  
?????????  
'Cretornis\_hlavaci'  
?????1??  
??  
????????????????????????????????1001?100110003?01?1?????2?????????0?1?0?000?1?????  
?????????  
'Nyctosaurus\_gracilis'  
012?11?10?10110011001?110100?1?010101131?????????????????????01?100?????  
??1?000?0?1101?1?101?0?10011021121111000011?1000200?1101?03001011011?1101?1?0110  
10000100120100011010100[0  
1]1220111001600111000310100111?121?????1011000?11010111110111?11??  
'Nyctosaurus\_nanus'  
?????1??1??0??1?????????????0??10????????????????????????????????????  
??1?????????  
10??????20????????????????????????10016001?1000???1????????????????????00????????  
?????????  
'Nyctosaurus\_lamegoi'  
?????1??  
??  
????????????????????????????????16001????????1????????????????????00????????  
?????????  
'Muzquizopteryx\_coahuilensis'  
?????1?1?1??0?1?????????????1?01?03??21????????????????????????????100?????  
?????0?1?????????1?0101?0?10010??11211?1000011?1?00200?101?030?1??1011?1??01??  
?0001001?0?000?101?0?0??12?1??016000110??1?1?????012??????1?1?????????1?1111?1  
?11??4?  
'Tupandactylus\_navigans'  
022?10110????????????????????????????31?????????????????????????0?101100111  
1???00?1??1?001010101?0?0120??041101000111?110020?1????????????????????  
??1????????????????  
?????????  
'Tupandactylus\_imperator'  
022?10?10?10220??0?210101??100?0001????31?????????????????????????0?101100111  
1???00?1?????????1??01?0??1201211331101000111?1?00201?11????????????????  
??  
?????????  
'Bakonydraco\_galaczi'  
012?11?10?1112001101201101??111?0101011?1????????????????????????????  
??  
????????????????????????????????0????????????????????????????????  
?????????  
'Tapejara\_wellnhoferi'  
022?10210?10120011012101011010?000100031?????????????????????00?101001111  
1?1?010?0011001010101?0?01201211341101000111?1100201111?00000111010110??0??011  
0011011002201??1111001001??31?1100800111100101011000?4?1011011011100?1100?11011010  
1102??4?  
'Europejara\_olcadesorum'  
?????01??1012?11?1210101??110?00100?1????????????????????????????  
??1?01??00?????????1????????????4110100?????0020????????????????  
??1????????????????????  
?????????  
'Vectidraco\_daisymorrisae'  
?????1??  
??

????????????111110?1?????3110????????????????1????????????????????????00????????  
?????????  
'Caiuajara\_dobruskii'  
022?10?10?1022001100210101??110?000100??1????????????????????????00?01101111  
1????000?0??10??????1?0?012?1211341101000111??0?01??1??000?111????11001?0?00??  
0?1121100220000?1111?????122?1?11?08001?11?1110??00?4??????1011000?1100?1101101?  
?????????  
'Huaxiapterus\_benxiensis'  
022?10110?1012201101201101??100?20012??31????????????????????????0?101061121  
1????0????????01?0?01?0?0?012113??101000111?1?0?30??1????00?111????0?????????  
????????????????????????????????????08001????????1?0??21?1????10????????10001??????  
??????4?  
'Huaxiapterus\_corallatus'  
022?10110?10122011??20110????100?20??2??1????????????????????????0?101061121  
1????0????????????????????0??20??10????01????????????1????????00?111????0?????01?  
00????0022??????111??????13????08001?1????1111??421?1????10????????100011??1???  
1????4?  
'Eopteranodon\_lii'  
022?10110??012????1??100??10??01?11?1????????????????????????00?01041101  
1????0????????????????1?0?0????????01?0111?????0??1?000??11?????????????????  
00?????0?22????11111101???1320??008001?1??1?1?1??4????????????0??0001?011?1?  
?????????  
'Huaxiapterus\_jii'  
022?1?10?101220????201100??100?20012??1????????????????????????0?01041?01  
1????0?0?0????0?010??1?0?0??????0411?1?0111?1??30????????0??1????001????01?  
00??[0  
2]????22????????????????13????1?008001?11?1?1????0411?1?0111011????110001?011110??  
?????  
'Sinopterus\_dongi'  
022?10?10?10122011??20110????100?20?12??31????????????????????????0?101041101  
1????0????????010101?1?0?002012113?1?01?0111?11?03?1??1??000??11????10?1????001?  
001101?0?221010111111??1??13?0?11?008001111??111111?0004211110111011??01110001????110  
0100124?  
'Bennettazhia\_oregonensis'  
??  
??0??1?????????  
??11008000111001????????????????????????  
?????????  
'Dsungaripterus\_wei'  
003010110?10100010001??100100?0?00110112000100002000100102422?1??101?101030121  
3?1??10100001101????001?0?00101211221101100111?1102201111120000111011111?100010011  
001??110021????1111??1????3?11??0800?011?1?1?11?0??0?1????10?101011120100012011  
?????????  
'Domeykodactylus\_ceciliae' ?????????10?1??0?01??10?10?0??0????000?00?2[0  
2]001????422??1????01?012??  
??  
??  
'Noripterus\_parvus'  
013010110?10110010001??100110?0?001101?20001000?2?0100101322?1??101?101030111  
3?1??1010000?101????001?0?001012112201?1100111?1102201?11?1?00001111011??1?????????  
00????0021????????????1????????00008001111001?1111?00?4?1?????10????0?020000012?1?  
?????????  
'Noripterus\_complicidens' ??????[1  
2]??10?00?0001?100110??0?1????0?0??00210010?1??322?1??0????????????????????



??????0022????????????????????????????????08001?????1??1??0?0?2111?001?01?00?21?0011?01?1?1  
1102??4?  
'Radiodactylus\_langstoni'  
??  
??  
????????????????000????????????????????10008001?110111?1?????0?1?1?????1????????01?????1??  
?????????  
'Microtuban\_altivolans'  
??  
??  
?????1?00221????????????????????00080011110??111?????4211?1001101100?21?001?10121??  
1???????  
'Volgadraco\_bogolubovi'  
??????????00110111001??1????0????????????1??  
??00101111?0????1????????  
??  
?????????  
'Montanazhdarcho\_minor'  
??1????????????????????????????????  
??1????????????????  
??????0011????????????????01007000010110110????????????????1?????11????????????  
?????????  
'Mistralazhdarcho\_maggii'  
112?1??0?0?????1????????????????????????????1?????????????????????????????2????0?????  
??????111??11201?1????????????  
????????????????????????????????0?08011?11?111?1??4????????????????????1????????  
?????????  
'Alanqa\_saharica'  
0?1?01?10?0011010010??1?2?0?10????????1????????????????????????????????????  
??  
??  
?????????  
'Inabtanin\_alarabia'  
01?01?10?10?10011001??110?0?1?10?????1????????????????????????????????00????  
?????0??1?1?101111????????  
??????01?2????????????????????00018001?????01011????????????????110?110111????????  
?????????  
'Xericeps\_curvirostris'  
??????????13?00011100??1?01?0?????1?????1????????????????????????????????  
??  
??  
?????????  
'Leptostomia\_begaaensis'  
0??10?0??2?0001??0??1?0?0?????1?????1????????????????????????????????1????????  
??????100??  
??  
?????????  
'Aptorhamphus\_gyrostega'  
112?1??0?1011001??1??1?0?0?????0?????1????????????????????????????????2????0????  
?????00??  
??  
?????????  
'Azhdarcho\_lancicollis'  
012?0?10?0????????????????????0?1?1????????????????????????????????01????  
????????????????????1????????????????????????????????0?????1022101011?01?110?????111

101?????120????????????????????01018001?1110001011?000??????0?1?00101?11???111111?  
????0??  
'Albadraco\_tharmisensis'  
3???00?1??00???20000???1???0?0????????1????????????????????????????????????  
??22101011????????????  
??  
????????  
'Zhejiangopterus\_linhaiensis'  
112?10?0?10110010001??1????0?1?00?10??31????????????????????????????0??100?????  
?????0?0??0??1?1????01?0?012?0?0?41101001011?1?01021??2?1?2?1?1??10?1?1?1?0??001?  
??????0022?????11111?1??131011??18001????1??11??4??1??10??????3??1?112?1?  
??????4?  
'Aralazhdarcho\_bostobensis'  
????0????????????????????????????1?1????????????????????????????????????  
??1??????11????????????11?1?0??????0?????  
?????1100????????????????????????10????????1????0????????????????????3??1?12??  
????????  
'Eurazhdarcho\_langendorffensis'  
??  
??121??11????????  
??111110??3????  
????????  
'Phosphatodraco\_mauritanicus'  
??  
??2210001100????  
??  
????????  
'Wellnhopterus\_brevirostris'  
112?101?0?10110010001??1????0?0????1????????????????????????00??01011?01  
0?1?01????????????1?0?1????????01????????11????????2210?011????????  
??  
????????  
'Quetzalcoatlus\_lawsoni'  
11??10?0?12?10001001??1?0100?1?01010?131????????????????00?1010[4  
6]10[0  
1]11?1?010??011?01????001??0?1120000???1101001011?11?03?????1?2?101011011?1????  
011001??110022????11111121??1320??10118000011011?1?11?00?4??0??10????0??13?01112  
?1??1????4?  
'Aerotitan\_sudamericanus'  
????11?10?0011?111101??1????0?0??1????1????????????????????????????  
??  
??  
????????  
'Cryodrakon\_boreas'  
??  
??22101011????  
????????????????????????????010180001111?2????????5????????  
????????  
'Hatzegopteryx\_thambema'  
????????????????0000????????????1????????????????????????????  
??121011?1????  
????????????????????????0180????????????10????????  
????????  
'Arambourgia philadelphiae'  
??

```
????????????????????????????????????????????????????????????????????????????????221010?1?????????????????
????????????????????????????????????????????????????????????????????????????????1?????????????????????
?????????
'Quetzalcoatlus_northropi'
      ?????????????????????????????????????????????????????????????????????????????????????????????????
????????????????????????????????????????????????????????????????????????????????????????????????????
????????????????????????????????????????????????????????????????????????????????????????????????????
????????????????????????????????????????????????????????????????????????????????????????????????????
?????????
;

nstates stand;
ccode + 48 60 79 82 86 88 90 95 106 110.111 113 115 123 125 133 143 170 177 182 186
219 238 266 291 301.302;
ccode - 0.47 49.59 61.78 80.81 83.85 87 89 91.94 96.105 107.109 112 114 116.122 124
126.132 134.142 144.169 171.176 178.181 183.185 187.218 220.237 239.265 267.290
292.300;
;

nstates stand ;
log KLRrun11_log.txt;
hold 130000;
rseed 0;
rseed [;
collapse auto;
mult= replic 2000 keepall ratchet;
bbreak=tbr;
best;
taxname= ;
procedure/;
end;
;
```

## Appendix B

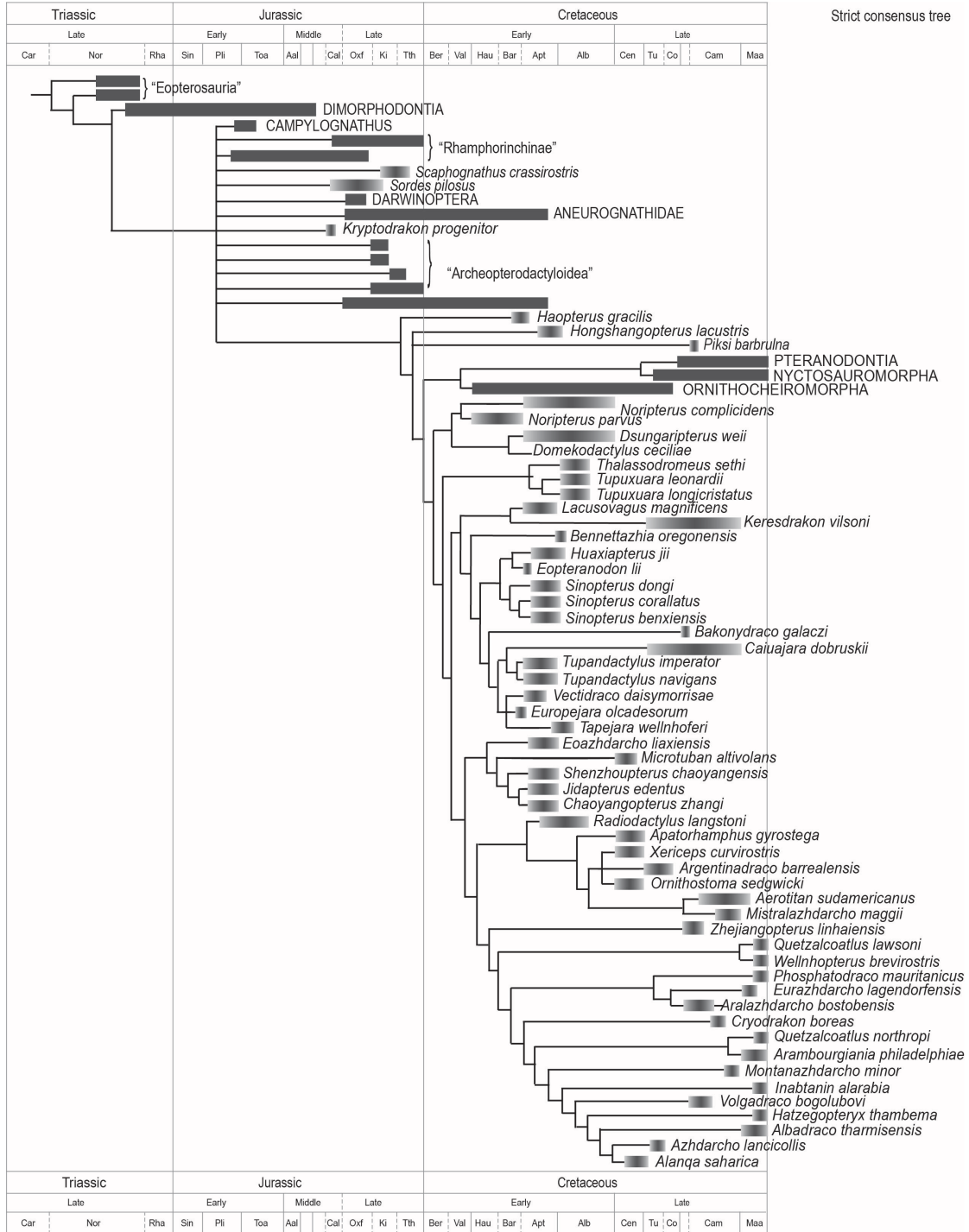


Figure B1. Phylogenetic relationships of Late Cretaceous pterosaurs. Strict consensus tree. Temporal ranges are taken from published literature, uncertainty is represented by gradient bars. Solid bars represent documented ranges of groups collapsed for simplicity. Some of the temporal scaling is restricted by the constraints of the diagram and minimum spacing to visualize divergence.

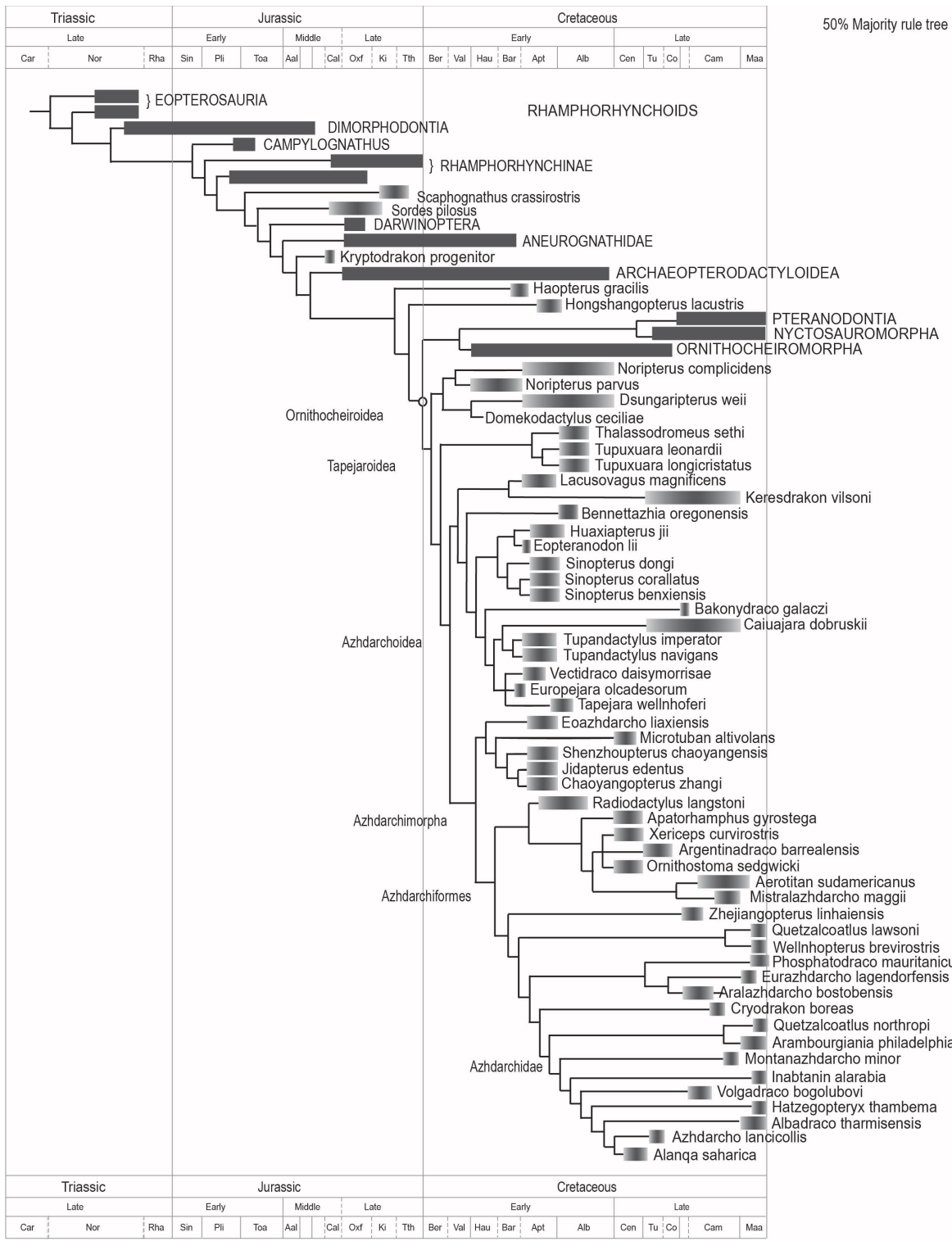


Figure B2. Phylogenetic relationships of Late Cretaceous pterosaurs. Majority rule 50% tree. Temporal ranges are taken from published literature, uncertainty is represented by gradient bars. Solid bars represent documented ranges of groups collapsed for simplicity. Some of the temporal scaling is restricted by the constraints of the diagram and minimum spacing to visualize divergence.



### Appendix C

Table C. Volumetric airspace proportion database organized taxonomically and anatomically. Results include the volume of air, bone, and total volume in millimeters cubed. vASP is calculated by dividing air volume by total volume and represented as a percentage.

Repository	Spec num	Taxon	ID	Element	Notes	Total vol (mm <sup>3</sup> )	Bone vol (mm <sup>3</sup> )	Air vol (mm <sup>3</sup> )	vASP	Scan location	file type
UMMP	n/a	Pterosaur	<i>Inabtanin alarabia</i>	humerus, left, distal	without virtual cortical bone	103758	1398	102360	99%	UM CTEES	vol
					with virtual cortical bone	127180	24820	102360	80%		
UMMP	n/a	Pterosaur	<i>Inabtanin alarabia</i>	humerus, left, proximal	without virtual cortical bone	98126	3359	94768	97%	UM CTEES	vol
					with virtual cortical bone	126504	32912	93592	74%		
UMMP	n/a	Pterosaur	<i>Inabtanin alarabia</i>	humerus, right, proximal	without virtual cortical bone	83439	2293	81145	97%	UM CTEES	vol
					with virtual cortical bone	107139	26523	80617	75%		
UMMP	n/a	Pterosaur	<i>Arambourgiana</i>	humerus, right, shaft	without virtual cortical bone	538141	23640	514501	96%	UM CTEES	vol
					with virtual cortical bone	600193	85622	514571	86%		
UMMP	n/a	Dinosaur	Titanosauria indet.	caudal vertebra		287177	151480	135697	47%	UM CTEES	vol
FLMNH	40378	aves	<i>Archilochus colubris</i>	coracoid		2.37	1.36	1.01	43%	UF	tiff
FLMNH	40378	aves	<i>Archilochus colubris</i>	coracoid		2.45	1.42	1.03	42%	UF	tiff
FLMNH	19832	aves	<i>Mellisuga</i> sp.	coracoid		1.92	1.22	0.70	36%	UF	tiff
FLMNH	38157	aves	<i>Mellisuga minima</i>	coracoid		1.27	0.73	0.54	43%	UF	tiff
FLMNH	201093	aves	Hummingbird indet.	coracoid, partial	subfossil	1.44	0.98	0.46	32%	UF	tiff
FLMNH	38157	aves	<i>Mellisuga minima</i>	coracoid, partial		1.01	0.64	0.37	37%	UF	tiff
FLMNH	19832	aves	<i>Mellisuga</i> sp.	coracoid, partial		1.95	1.24	0.71	36%	UF	tiff
FLMNH	219338	aves	Hummingbird indet.	coracoid, partial	subfossil	1.97	1.40	0.57	29%	UF	tiff
FLMNH	40378	aves	<i>Archilocus collubris</i>	humerus		3.98	1.37	2.61	66%	UF	tiff

FLMNH	40378	aves	<i>Archilocus collubris</i>	humerus		4.03	1.32	2.71	67%	UF	tiff
FLMNH	44177	aves	<i>Calliphlox evelynae</i>	humerus		3.46	1.46	2.00	58%	UF	tiff
FLMNH	201092	aves	Hummingbird indet.	humerus, partial		4.41	1.86	2.55	58%	UF	tiff
FLMNH	42475	aves	<i>Calliphlox evelynae</i>	humerus, partial		2.74	1.00	1.74	64%	UF	tiff
FLMNH	44177	aves	<i>Calliphlox evelynae</i>	humerus, partial		3.35	1.32	2.03	61%	UF	tiff
FLMNH	201092	aves	Hummingbird indet.	humerus, partial	subfossil	4.26	1.87	2.39	56%	UF	tiff
FLMNH	40378	aves	<i>Archilochus colubris</i>	ulna		3.99	1.40	2.59	65%	UF	tiff
FLMNH	19832	aves	<i>Mellisuga</i> sp.	ulna		1.37	0.64	0.73	53%	UF	tiff
FLMNH	201057	aves	Hummingbird indet.	ulna	subfossil	2.64	1.25	1.40	53%	UF	tiff
FLMNH	40378	aves	<i>Archilochus colubris</i>	ulna		2.81	1.09	1.72	61%	UF	tiff
FLMNH	218658	aves	Hummingbird indet.	ulna	subfossil	5.38	2.51	2.87	53%	UF	tiff
FLMNH	218662-3	aves	Hummingbird indet.	ulna		3.95	2.29	1.66	42%	UF	tiff
FLMNH	218644-5	aves	Hummingbird indet.	ulna, partial		4.38	1.74	2.64	60%	UF	tiff
FLMNH	201058	aves	Hummingbird indet.	carpometacarpus	subfossil	4.35	2.41	1.94	45%	UF	tiff
FLMNH	40378	aves	<i>Archilochus colubris</i>	carpometacarpus with allula		1.81	0.98	0.83	46%	UF	tiff
FLMNH	40378	aves	<i>Archilochus colubris</i>	carpometatarsus		1.65	0.94	0.71	43%	UF	tiff
FLMNH	201051	aves	Hummingbird indet.	carpometacarpus	subfossil	2.66	1.86	0.80	30%	UF	tiff
FLMNH	uncat	aves	<i>Chlorostilbon ricordii</i>	carpometacarpus	subfossil	2.57	1.51	1.06	41%	UF	tiff
FLMNH	218642	aves	Hummingbird indet.	carpometacarpus	subfossil	4.82	3.05	1.77	37%	UF	tiff
FLMNH	218654	aves	Hummingbird indet.	carpometacarpus	subfossil	3.74	2.64	1.10	29%	UF	tiff
FLMNH	218643	aves	Hummingbird indet.	carpometacarpus	subfossil	5.00	3.24	1.76	35%	UF	tiff
FLMNH	218644-5	aves	Hummingbird indet.	carpometacarpus, partial	subfossil	3.85	2.61	1.24	32%	UF	tiff
FLMNH	219188	aves	Hummingbird indet.	carpometacarpus, partial	subfossil	1.71	1.20	0.51	30%	UF	tiff

FLMNH	219334	aves	Hummingbird indet.	carpometacarpus, partial	subfossil	2.67	1.92	0.75	28%	UF	tiff
FLMNH	219103	aves	Hummingbird indet.	carpometacarpus, partial	subfossil	3.90	2.58	1.32	34%	UF	tiff
FLMNH	219288	aves	Hummingbird indet.	carpometacarpus, partial	subfossil	3.14	2.06	1.08	34%	UF	tiff
FLMNH	40378	aves	<i>Archilochus colubris</i>	digit II and allula		1.23	0.50	0.73	59%	UF	tiff
FLMNH	218662-3	aves	Hummingbird indet.	digit II		2.91	1.61	1.30	45%	UF	tiff
FLMNH	201062	aves	Hummingbird indet.	digit II	subfossil	2.22	1.15	1.07	48%	UF	tiff
FLMNH	40378	aves	<i>Archilochus colubris</i>	digit II		1.31	0.55	0.76	58%	UF	tiff
FLMNH	40378	aves	<i>Archilochus colubris</i>	digit II		0.97	0.50	0.47	48%	UF	tiff
FLMNH	201062	aves	Hummingbird indet.	tarsometatarsus	subfossil	0.97	0.60	0.37	38%	UF	tiff
FLMNH	42475	aves	<i>Calliphlox evelynae</i>	tarsometatarsus		0.64	0.31	0.33	51%	UF	tiff
FLMNH	uncat	aves	<i>Calliphlox evelynae</i>	tarsometatarsus	subfossil	1.01	0.52	0.49	49%	UF	tiff
FLMNH	40378	aves	<i>Archilochus colubris</i>	tarsometatarsus, partial		0.56	0.27	0.29	52%	UF	tiff
FLMNH	40378	aves	<i>Archilochus colubris</i>	tarsometatarsus, partial		0.78	0.36	0.42	53%	UF	tiff
FLMNH	219318	aves	Hummingbird indet.	tibiotarsus, partial	subfossil	0.96	0.64	0.32	34%	UF	tiff
FLMNH	19832	aves	<i>Mellisuga sp.</i>	dentary		5.27	2.99	2.28	43%	UF	tiff
FLMNH	uncat	aves	<i>Chlorostilbon ricordii</i>	dentary	subfossil	6.02	4.32	1.70	28%	UF	tiff
FLMNH	uncat	aves	<i>Chlorostilbon ricordii</i>	dentary	subfossil	1.89	1.15	0.74	39%	UF	tiff
FLMNH	uncat	aves	<i>Calliphlox evelynae</i>	dentary	subfossil	2.72	1.79	0.93	34%	UF	tiff
FLMNH	uncat	aves	<i>Chlorostilbon ricordii</i>	dentary	subfossil	4.89	3.43	1.46	30%	UF	tiff
FLMNH	uncat	aves	<i>Calliphlox evelynae</i>	dentary	subfossil	1.44	1.06	0.38	27%	UF	tiff

## Bibliography

- Alexander, R. M. 1998. All-time giants: the largest animals and their problems. *Palaeontology* 41:1231-1245.
- Andres, B. 2010. Systematics of the Pterosauria. Ph.D. dissertation, Department of Geology and Geophysics, Yale University, New Haven, Connecticut, 347 pp.
- Andres, B. 2012. The early evolutionary history and adaptive radiation of the Pterosauria. *Acta Geologica Sinica (English Edition)* 86:1356–1365.
- Andres, B. 2021. Phylogenetic systematics of *Quetzalcoatlus* Lawson 1975 (Pterodactyloidea: Azhdarchoidea). *Journal of Vertebrate Paleontology*, 41(S1), 203–217.
- Andres, B., J. M. Clark, and X. Xu. 2010. A new rhamphorhynchid pterosaur from the Upper Jurassic of Xinjiang, China, and the phylogenetic relationships of basal pterosaurs. *Journal of Vertebrate Paleontology* 30:163–187.
- Andres, B., J. M. Clark, and X. Xu. 2014. The earliest pterodactyloid and the origin of the group. *Current Biology* 24:1011–1016.
- Andres, B., and Q. Ji. 2008. A new pterosaur from the Liaoning Province of China, the phylogeny of the Pterodactyloidea, and convergence in their cervical vertebrae. *Palaeontology* 51:453–470
- Andres, B., and T. S. Myers. 2013. Lone star pterosaurs. *Earth and Environmental Science Transactions of the Royal Society of Edinburgh* 103:383–398.

- Andres, B., and W. Langston. 2021. Morphology and taxonomy of *Quetzalcoatlus* Lawson 1975 (Pterodactyloidea: Azhdarchoidea); pp. 46–202 in K. Padian and M. A. Brown (eds.), The Late Cretaceous pterosaur *Quetzalcoatlus* Lawson 1975 (Pterodactyloidea: Azhdarchoidea). Society of Vertebrate Paleontology Memoir 19. Journal of Vertebrate Paleontology 41(2, Supplement):46–202.
- Arambourg, C. 1959. Titanopteryx philadelphiae nov. gen., nov. sp., pterosaurien geant. Annual Review of Population Law 15:229–234.
- Averianov, A. 2007. New records of azhdarchids (Pterosauria, Azhdarchidae) from the Late Cretaceous of Russia, Kazakhstan, and central asia. Paleontological Journal, 41(2):189-197.
- Averianov, A. 2010. The osteology of Azhdarcho lancicollis Nesso, 1984 (Pterosauria, Azhdarchidae) from the late Cretaceous of Uzbekistan. Proceedings of the Zoological Institute RAS, 314(3):264-317.
- Averianov, A. 2014. Review of taxonomy, geographic distribution, and paleoenvironments of Azhdarchidae (Pterosauria). ZooKeys 432:1–107.
- Averianov, A., Arkhangelsky, M. S., & Pervushov, E. M. 2008. A new late Cretaceous azhdarchid (Pterosauria, Azhdarchidae) from the Volga Region. Paleontological Journal, 42(6):634-642.
- Bakhvalov, Y. O., Petrokovskiy, S. A., Polynovskiy, V. P., and , A. F. Razin. 2009. Composite irregular lattice shells designing for space applications. 17th International Conference on Composite Materials, Edinburgh, Scotland.
- Bardet, N., and X. Pereda Suberbiola. 2002. Marine reptiles from the Late Cretaceous Phosphates of Jordan: Palaeobiogeographical implications. Geodiversitas 24:831–839.

- Barrett, P. M., Butler, R. J., Edwards, N. P., & Milner, A. R. 2008. Pterosaur distribution in time and space: an atlas. *Zitteliana*:61-107.
- Bennett, S. C. 1989. A pteranodontoid pterosaur from the Early Cretaceous of Peru, with comments on the relationships of Cretaceous pterosaurs. *Journal of Paleontology* 63:669–677.
- Bennett, S. C. 1991. Morphology of the late Cretaceous pterosaur Pteranodon and the systematics of the Pterodactyloidea. Ph.D. dissertation, University of Kansas, Lawrence, Kansas, 680 pp.
- Bennett, S. C. 1993. The Ontogeny of Pteranodon and Other Pterosaurs. *Paleobiology* 19:92–106.
- Bennett, S. C. 1994. Taxonomy and systematics of the Late Cretaceous pterosaur Pteranodon (Pterosauria, Pterodactyloidea). *Occasional Papers of the Natural History Museum, University of Kansas* 169:1–70.
- Bonde, N., and Christiansen, P. 2003. The detailed anatomy of Rhamphorhynchus: axial pneumaticity and its implications. *Geological Society of London Special Publication* 217: 217–232.
- Britt, B. B. 1993. Pneumatic postcranial bones in dinosaurs and other archosaurs. Ph.D. dissertation, University of Chicago, Chicago, Illinois.
- Broom, R. 1913. Note on *Mesosuchus browni*, Watson, and on a new South African Triassic pseudosuchian (*Euparkeria capensis*). *Records of the Albany Museum* 2:394–396.
- Buffetaut, E., D. Grigorescu, and Z. Csiki. 2002. A new giant pterosaur with a robust skull from the latest Cretaceous of Romania. *Naturwissenschaften* 89:180–184.
- Buffetaut, E., D. Grigorescu, and Z. Csiki. 2003. Giant azhdarchid pterosaurs from the terminal

- Cretaceous of Transylvania (western Romania). *Geological Society Special Publication* 217:91–104.
- Butler, R. J., P. M. Barrett, and D. J. Gower. 2009. Postcranial skeletal pneumaticity and air-sacs in the earliest pterosaurs. *Biology Letters* 5:557–60.
- Butler, R. J., R. B. J. Benson, and P. M. Barrett. 2013. Pterosaur diversity: untangling the influence of sampling biases, Lagerstätten, and genuine biodiversity signals. *Palaeogeography, Palaeoclimatology, Palaeoecology* 372:78–87.
- Chatterjee, S., & Templin, R. J. (2004). Posture, locomotion, and paleoecology of pterosaurs. *Geological Society of America* 376:1-64
- Claessens, L. P. A. M., P. M. O’Connor, and D. M. Unwin. 2009. Respiratory evolution facilitated the origin of pterosaur flight and aerial gigantism. *PLoS ONE* 4.
- Collini, C. A. 1784. Sur quelques Zoolithes du Cabinet d’Histoire naturelle de SASE Palatine & de Bavière, à Mannheim. *Acta Academiae Theodoro Palatinae, Mannheim, Pars Physica* 5: 58-103.
- Dalla Vecchia, F. M. 2017. A wing metacarpal from Italy and its implications for latest Cretaceous pterosaur diversity. *Geological Society of London, Special Publications*, 455(1):209-219.
- Frey, E., and D. M. Martill. 1996. A reappraisal of *Arambourgiania* (Pterosauria, Pterodactyloidea): One of the world’s largest flying animals. *Neues Jahrbuch Fur Geologie Und Palaontologie - Abhandlungen* 199:221–247.
- Geist, N. R., W. J. Hillenius, E. Frey, T. D. Jones, and R. A. Elgin. 2014. Breathing in a box: Constraints on lung ventilation in giant pterosaurs. *Anatomical Record* 297:2233–2253.
- Goloboff, P. A., and S. A. Catalano. 2016. TNT version 1.5, including a full implementation of

- phylogenetic morphometrics. *Cladistics* 32:221–238.
- Henderson, D. M. 2010. Pterosaur body mass estimates from three-dimensional mathematical slicing. *Journal of Vertebrate Paleontology* 30:768–785.
- Howse, S. C. B. 1986. On the cervical vertebrae of the Pterodactyloidea (Reptilia: Archosauria). *Zoological Journal of the Linnean Society* 88:307–328.
- Huxley, T. H. 1877. The crocodilian remains found in the Elgin sandstones, with remarks on ichnites of Cummingstone. *Memoirs of the Geological Survey of the United Kingdom Monograph III*:1–51.
- Kaddumi, H. F. 2009. Fossils of the Harrana Fauna and the Adjacent Areas. Contributions from the Eternal River Museum of Natural History, Amman.
- Kellner, A. W. A. 2003. Pterosaur phylogeny and comments on the evolutionary history of the group; pp. 105–137 in E. Buffetaut and J.-M. Mazin (eds.), *Evolution and Palaeobiology of Pterosaurs*. Geological Society, Special Publications 217, London.
- Kiang, J. 2013. *Avian Wing Bones*. University of California, San Diego, 112 pp.
- Lawson, D. A. 1975. Could pterosaurs fly? *Science* 188:676–678.
- Longrich, N. R., D. M. Martill, and B. Andres. 2018. Late Maastrichtian pterosaurs from North Africa and mass extinction of Pterosauria at the Cretaceous-Paleogene boundary. *PLoS Biology* 16:e2001663.
- Martill, D. M., E. Frey, and R. M. Sadaqah. 1996. The first dinosaur from the Hashemite Kingdom of Jordan. *Neues Jahrbuch Fur Geologie Und Palaontologie - Monatshefte* 147–154.
- Martill, D. M., M. Green, R. Smith, M. Jacobs, J. Winch. 2020. First tapejarid pterosaur from the Wessex Formation (Wealden Group: Lower Cretaceous, Barremian) of the United



- Kingdom. *Cretaceous Research*. 113:104487.
- Martill, D. M., and M. Moser. 2017. Topotype specimens probably attributable to the giant azhdarchid pterosaur *Arambourgiania philadelphiae* (Arambourg 1959). *Geological Society Special Publication* 455:159–169.
- Martin, E. G., and C. Palmer. 2014a. Air Space Proportion in pterosaur limb bones using computed tomography and its implications for previous estimates of pneumaticity. *PLoS ONE* 9:1–7.
- Martin, E. G., and C. Palmer. 2014b. A novel method of estimating pterosaur skeletal mass using computed tomography scans. *Journal of Vertebrate Paleontology* 34:1466–1469.
- Middleton, K. M., and L. T. English. 2015. Challenges and advances in the study of pterosaur flight. *Canadian Journal of Zoology* 93:945–959.
- Naish, D., and M. P. Witton. 2017. Neck biomechanics indicate that giant Transylvanian azhdarchid pterosaurs were short-necked arch predators. *PeerJ* 5:e2908.
- Naish, D., M.P. Witton, and E. Martin-Silverstone. 2021. Powered flight in hatchling pterosaurs: evidence from wing form and bone strength. *Scientific Reports* 11:13130.
- Nesov, L. A. 1984. Upper Cretaceous pterosaurs and birds from Central Asia. *Paleontological Journal* 18:38–49.
- Novas, F. E., M. Kundrat, F. L. Agnolín, M. D. Ezcurra, P. E. Ahlberg, M. P. Isasi, A. Arriagada, and P. Chafraat. 2012. A new large pterosaur from the Late Cretaceous of Patagonia. *Journal of Vertebrate Paleontology* 32:1447–1452.
- Novitskaya, E., C. J. Ruestes, M. M. Porter, V. A. Lubarda, M. A. Meyers, and J. McKittrick. 2017. Reinforcements in avian wing bones: Experiments, analysis, and modeling. *Journal of the Mechanical Behavior of Biomedical Materials* 76:85–96.

- Pennycuik, C.J. 1982. The Flight of Petrels and Albatrosses (Procellariiformes), Observed in South Georgia and its Vicinity. *Philosophical Transactions of the Royal Society of London. Series B, Biological Sciences* 300:75–106.
- Pêgas, R. V., B. Holgado, L. D. Ortiz David, M. A. Baiano, F. R. Costa. 2022. On the pterosaur *Aerotitan sudamericanus* (Neuquen Basin, Upper Cretaceous of Argentina), with comments on azhdarchoid phylogeny and jaw anatomy. *Cretaceous Research* 129(2022):104998.
- Pereda-Suberbiola, X., N. Bardet, S. Jouve, M. Iarochène, B. Bouya, and M. Amaghazaz. 2003. A new azdarchid pterosaur from the Late Cretaceous phosphates of Morocco. *Geological Society, London, Special Publications* 217:79–90.
- Plieninger, F. 1901. Beiträge zur Kenntnis der Flugsaurier. *Palaeontographica* 48:65–90.
- Reig, O. A. 1963. La presencia de dinosaurios saurisquios en los “Estratos de Ischigualasto” (Mesotriásico superior) de las provincias de San Juan y La Rioja (República Argentina). *Ameghiniana* 3:3–20.
- Sato, K., K. Q. Sakamoto, Y. Watanuki, A. Takahashi, N. Katsumata, C. A. Bost, and H. Weimerskirch. 2009. Scaling of soaring seabirds and implications for flight abilities of giant pterosaurs. *PLoS ONE* 4:1–6.
- Seeley, H. G. 1901. *Dragons of the Air: An Account of Extinct Flying reptiles*. Methuen and Co., London, U.K., 239 pp.
- Sereno, P. C. 1991. Basal archosaurs: phylogenetic relationships and functional implications. *Journal of Vertebrate Paleontology*, 11(S4): 1-53.
- Sereno, P. C. 2007. Logical basis for morphological characters in phylogenetics. *Cladistics* 23:565–587.

- Scotese, C. R. 2016. PALEOMAP PaleoAtlas for Gplates and the PaleoData plotter program. PALEOMAP Project. <https://www.earthbyte.org/paleomap-paleoatlas-for-gplates/>.
- Sullivan, T. N., B. Wang, H. D. Espinosa, and M. A. Meyers. 2017. Extreme lightweight structures: avian feathers and bones. *Materials Today* 20:377–391.
- Tschopp, E. 2016. Nomenclature of vertebral laminae in lizards, with comments on ontogenetic and serial variation in lacertini (Squamata, Lacertidae). *PLoS ONE* 11:1–21.
- Unwin, D. M. 2003. On the phylogeny and evolutionary history of pterosaurs; pp. 139–190 in E. Buffetaut and J.-M. Mazin (eds.), *Evolution and Palaeobiology of Pterosaurs*. Geological Society, London.
- Vidovic, S. U., & Martill, D. M. (2014). *Pterodactylus scolopaceps* Meyer, 1860 (Pterosauria, Pterodactyloidea) from the Upper Jurassic of Bavaria, Germany: The problem of cryptic pterosaur taxa in early ontogeny. *PLoS ONE*, 9(10).
- Vidovic, S. U., & Martill, D. M. (2017). The taxonomy and phylogeny of *Diopecephalus kochi* (Wagner, 1837) and “*Germanodactylus rhamphastinus*” (Wagner, 1851). *Geological Society Special Publication*, 455(1), 125–147.
- Vremir, M., A. W. A. Kellner, D. Naish, and G. J. Dyke. 2013. A new azhdarchid pterosaur from the Late Cretaceous of the Transylvanian Basin, Romania: implications for azhdarchid diversity and distribution. *PLoS ONE* 8:e54268.
- Wellnhofer, P. 1978. Pterosauria. *Handbuch der Palaeoherpetologie*. Gustav Fischer Verlag, Stuttgart, Germany, 19:1–82.
- Wellnhofer, P. 1991. *The illustrated encyclopedia of pterosaurs*. Crescent books.
- Wellnhofer, P. 2008. A short history of pterosaur research. *Zitteliana* 28:7–19.

- Wilson, J. A. 2006. Anatomical nomenclature of fossil vertebrates: standardized terms or lingua franca? *Journal of Vertebrate Paleontology* 26:511–518.
- Witton, M. P. 2007. Titans of the skies: azhdarchid pterosaurs. *Geology Today* 23:33–38.
- Witton, M. P. 2008. A new approach to determining pterosaur body mass and its implications for pterosaur flight. *Zitteliana* B28:143–158.
- Witton, M. P., and M. B. Habib. 2010. On the size and flight diversity of giant pterosaurs, the use of birds as pterosaur analogues and comments on pterosaur flightlessness. *PLoS ONE*, 5(11).
- Witton, M. P., and D. Naish. 2008. A Reappraisal of Azhdarchid Pterosaur Functional Morphology and Paleoecology. *PLoS ONE* 3:17–32.
- Woodward, A. S. 1907. On a new dinosaurian reptile (*Scleromochlus taylori* gen. et sp. nov.) from the Trias of Lossiemouth, Elgin. *Quarterly Journal of the Geological Society London* 63:140–146.
- Zalmout, I. S., and H. Mustafa. 2001. A selachian fauna from the Late Cretaceous of Jordan. *Abhath Al-Yarmouk: Basic Sciences and Engineering* 10:377–434.